The Dissertation Committee for Brianna Rose White Certifies that this is the approved version of the following dissertation:

FRET Peptidyl Sensors for the Detection of Metal Ions

Committee:

James A. Holcombe, Supervisor

Jennifer S. Brodbelt

David A. Vandenbout

Dean R. Appling

Howard M. Liljestrand

FRET Peptidyl Sensors for the Detection of Metal Ions

by

Brianna Rose White, B.S.

Dissertation

Presented to the Faculty of the Graduate School of

The University of Texas at Austin

in Partial Fulfillment

of the Requirements

for the Degree of

Doctor of Philosophy

The University of Texas at Austin

August 2007

Dedication

To my parents for their unconditional love and support through all my endeavors, to my sister Alicia for being my best friend and always looking out for me and to Mark for his love and patience.

Acknowledgements

First, thanks to Dr. James A. Holcombe for his guidance and patience over the last four years. You gave me the room to breathe, but at the same time, I knew your door was always open. Also, thanks to my undergraduate advisor Dr. Deborah Huntley for getting me excited about research in the first place.

I would also like to thank past and present Holcombe group members. First and foremost, thanks to Dr. Gülay Ertaş for bringing her excitement, energy and fresh ideas into our lab and also for being a wonderful friend. Your love for chemistry and organization was very contagious. Thanks to Dr. Lisa Malachowski for her inspirational work ethic and for making me feel welcome in the lab so quickly, to Dr. Bill Balsanek for his crazy Navy/single male stories and for being my travel buddy to Augusta and Dr. John Molloy for his friendship and for being a patient listener when I needed to vent. A special thanks goes to Dr. Jacqueline Stair for being my research buddy as well as being a great friend. Thanks also to Adam for all his help with the ICP, Carina for her friendship, and Brandon for being such a hardworking undergraduate student.

Finally, I would like to gratefully acknowledge my family. Thanks to Mom, Dad and Alicia for their unwavering support through all of my undertakings. You guys are amazing!

FRET Peptidyl Sensors for the Detection of Metal Ions

Publication No._____

Brianna Rose White, Ph.D.

The University of Texas at Austin, 2007

Supervisor: James A. Holcombe

This research focuses on developing selective FRET peptidyl metal ion sensors as a portable and less costly alterative to traditional atomic spectrometric techniques. Initially, a selective sensor for Cu^{2+} was developed that consisted of glycine and aspartic acid residues and the FRET pair tryptophan (donor) and dansyl (acceptor). Aspartic acid's affinity for hard acid metals and Cu^{2+}'s preference for square planar coordination was used as the basis of design. Although the sensor was designed to utilize the signal enhancement capabilities of FRET, quenching of both fluorophores occurred and proved to be the most sensitive means of quantifying Cu^{2+} binding. Nonetheless, the sensor provided a selective and sensitive response to Cu^{2+} at pH 7.0.

Another FRET peptide metal ion sensor was designed with the help of a biological starting point, the mercury binding protein MerP. A sensitive FRET enhancement or "turn on" response was observed for Hg^{2+}, as well as Zn^{2+}, Cd^{2+} and Ag^{2+} in pH 7.0 solution. While a selective response for only Hg^{2+} was the ultimate goal

of this study, this sensor is still an improvement over current systems which utilize a quenching mechanism for Hg^{2+} detection.

While the previous studies investigated these sensors in aqueous solutions, the end goal was to devise a sensor based on an immobilized peptide chelator with FRET capabilities. To this end, immobilized, fluorophore labeled peptide studies were then conducted on Tentagel resin using a visible region FRET pair. A flow injection fluorescence analysis system using the immobilized fluorophore labeled peptide as the ion exchange material was also designed, allowing for the efficient analysis of fluorescence solutions.

In addition to the work conducted with FRET sensors, studies were also conducted using magnetic γ-Fe_2O_3 nanoparticles with PLCys immobilized onto the surface. The γ-Fe_2O_3 nanoparticles are ideal supports since they can be magnetically collected and have a very large surface area to mass ratio.

Finally, a method was developed to quantitatively screen metals bound to single Tentagel beads with immobilized peptides using ETV-ICP-MS. This method is an improvement over existing methods because it is nondestructive and simultaneously provides the absolute content of all metals bound.

Table of Contents

List of Tables

List of Figures

Chapter 1: Introduction

1.1 HEAVY METALS IN THE ENVIRONMENT

Humans and biological organisms require trace amounts of some heavy metals for nutritional purposes, such as iron, copper, manganese and zinc, but excessive levels can be detrimental. Other heavy metals, such as cadmium, lead and mercury, are not vital or beneficial and their accumulation over time can be harmful to humans and have a negative impact on the environment (Table 1.1).[1]

Table 1.1 Maximum Contaminant Level (MCL) of Various Metal Contaminants in Water[2]

Metal	MCL (mg/L)	Potential Health Effects from Ingestion of Water	Source of Contamination (man-made)
As	0.01	Skin damage Problems with circulatory systems Increased risk of getting cancer	Erosion of natural deposits; runoff from glass & electronics production wastes
Cd	0.005	Kidney damage	Corrosion of galvanized pipes; erosion of natural deposits; batteries and paints
Cr	0.1	Allergic dermatitis	Discharge from steel and pulp mills; erosion of natural deposits
Cu	1.3	Short term exposure: Gastrointestinal distress Long term exposure: Liver or kidney damage	Corrosion of household plumbing systems; erosion of natural deposits
Hg Inorganic	0.002	Kidney damage	Erosion of natural deposits; discharge from refineries and factories; runoff from landfills and cropland
Pb	0.015	Infants and children: Delays in physical or mental development Adults: Kidney problems; high blood pressure	Corrosion of household plumbing systems; erosion of natural deposits
Se	0.05	Hair or fingernail loss; numbness in fingers or toes; circulatory problems	Discharge from petroleum refineries; erosion of natural deposits; discharge from mines

Heavy metals are introduced into the environment through a number of industrial products and processes.[3] Beginning in the 1980's, heavy metal remediation became a significant area of research in response to their apparent increasing presence in the environment.[4] This is due, in part, to the fact that metals are a *recirculating environmental contaminant* and cannot be metabolized or decomposed like organic contaminants. As a result, it is necessary to remediate heavily contaminated sites. Currently, 757 of the 1237 sites on the EPA's National Priorities List[5] have metals listed as a contaminant of concern, illustrating the magnitude of this problem.

Certainly, much of the metal removal from highly contaminated sources can be done through bulk techniques such as precipitation and filtration.[6, 7] However, the low levels ordered by current EPA regulations for many of the metals often dictate the need for final solution "polishing" which may involve chemical extraction in an attempt to lower specific metals below regulatory limits. Because metals cannot be metabolized or decomposed, extraction and reclamation have to be used in order to prevent recirculation from one site to another.

1.2 CURRENT TECHNOLOGY FOR METAL REMEDIATION

Ion exchangers are commonly used for metal removal from wastewaters, and have even been proposed as a means of treating sludge leachates.[8] The ideal exchange media should exhibit selectivity, strong binding, fast binding kinetics, large capacity, on demand metal release (reclamation), environmental innocuity and low cost. Many of the materials that are commercially available or are being pursued in research laboratories provide *some* of the aforementioned characteristics, but are lacking in several areas. Crown ethers offer selectivity and strong binding. However, slow release kinetics and/or

unfavorable thermodynamics often prohibit efficient reclamation of the extracted material. (e.g.,[9]) In addition, many crown ethers are also very toxic, adding to the problem of contamination. Some of the more commonly used ion exchangers include Chelex-100, weakly acidic resins (e.g., Amberlite IRC 50 and resin 122 with salicylic functional groups) and 8-quinolinol. (e.g.,[10, 11]) However, the effective exchange capacity for most is still often limited when salty matrices are of interest.[12] In addition, many exchangers offer little selectivity and/or exhibit slow kinetics of uptake. Research activity in ion exchange materials for metals is a clear testament to the absence of obvious solutions to the problem of waste treatment.

1.3 THE USE OF AMINO ACIDS, SHORT PEPTIDES AND POLYAMINOACIDS IN METALS REMEDIATION

Using a few key building blocks (i.e., the amino acids), a host of very selective chelators are fabricated in nature. Malachowski et al. recently wrote a review article noting the increased interest in utilization of immobilized amino acids, short peptides, and proteins for metal binding.[13] In proteins, tertiary structure is responsible for the formation of size-selective cavities and the proper location of complexing or binding functionalities that result in selective, fast binding. Likewise, the polymeric character of synthetic peptides can permit polydentate chelation which can provide strong binding and fast kinetics[14, 15] and, as a result, very efficient extraction. A major advantage of these synthetic (linear) biopolymers over natural systems is durability due to the absence of a preformed structure. While natural proteins must sustain their tertiary structure to maintain their activity, synthetic peptides do not have preformed tertiary structure dependence. Rather, the flexibility of the biopolymer's peptide backbone allows it to "wrap" around a metal as it binds (Figure 1.1a), finally reaching a free energy minimum, which results in its *optimal tertiary conformation for binding that particular metal*.

This enhanced binding is further augmented for use in remediation by the ease with which the metal can be released – on demand! Simply lowering the pH alters the biopolymer's structure (Figure 1.1b) which assists proton exchange for easy, rapid release of the bound metal, i.e., quantitative recovery for reclamation.

Figure 1.1 a) Metal binding scheme of, for example, poly –L-cysteine (PLCys), and b) effect of pH in protonation of thiol which increases the hydrophobicity and promotes a conformation change to a random coil that assists rapid metal release. Similar behavior is available with other cation exchangers composed of linear chains with weak acid functionalities.

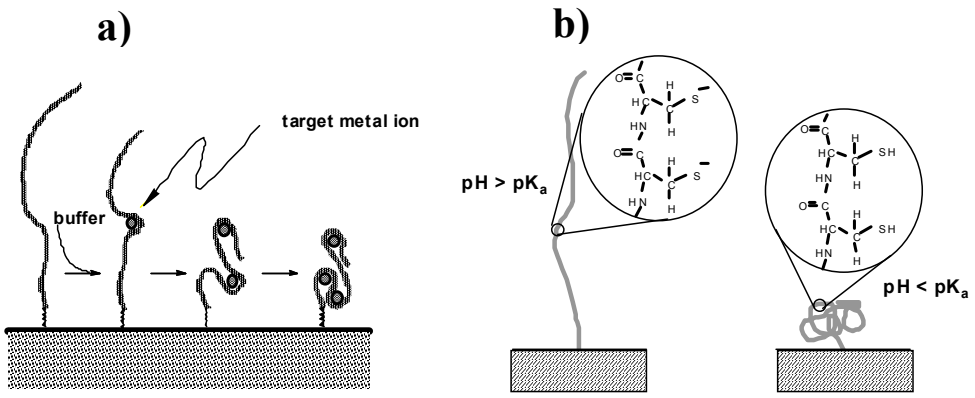

Research in the area of immobilized amino acids, short peptides and commercially available poly-amino acids as metal chelators has shown that high capacities as well as metal selectivity can be achieved. These selectivities are based primarily on the side group(s) functionality. Figure 1.2 shows the side groups of the various amino acids that have been shown to bind metals.

Figure 1.2 Amino acids utilized in metal binding studies

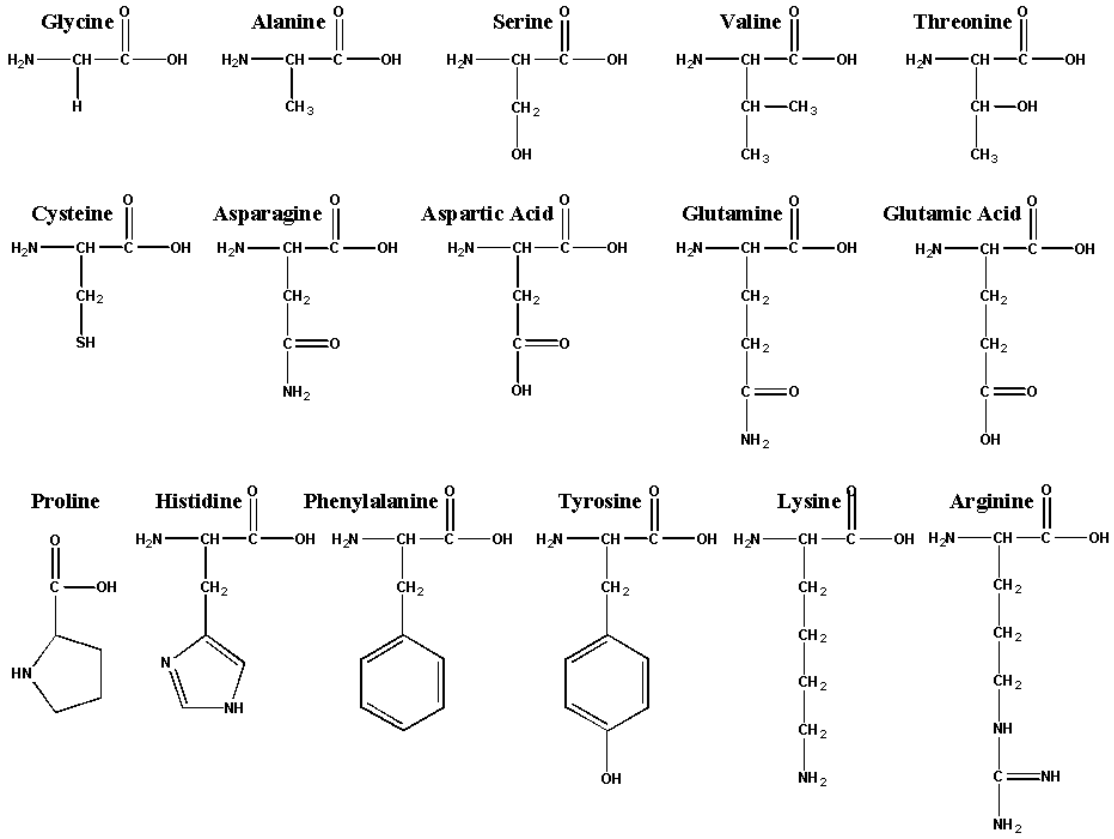

For example, Cys[16] and poly- L-cysteine (PLCys)[17-19] preferentially binds soft metal acids such as Cd^{2+} and Pb^{2+} through its soft donor ligand thiol side groups.[20] Poly-L aspartic acid (PLAsp)[21, 22] binds hard acid metals such as Ni^{2+} and Co^{2+} to a greater extent than soft acid metals. Poly-L-histidine (PLHis) shows a preference for anionic species, such as chromates and arsenates, in acidic solutions where its imidazole side chain is protonated.[23] Metal selectivity is further fine tuned by using short peptides consisting of mixed amino acids[24, 25] as well as peptides based on metal binding proteins such as MerP[26] and ACTUN.[27]

1.4 METAL ANALYSIS AND CURRENT DETECTION TECHNIQUES

Typically, amino acid/peptide metal remediation research is performed using a flow injection analysis (FIA) system with an online ion exchange column.[21] Columns are packed with immobilized amino acid/peptide, and a flow injection manifold is used to provide flow of acid, buffer and metal solution into the column. All remediation processes require a means of evaluating the success of the system. In column-type remediation techniques breakthrough (i.e. the point where the column capacity is depleted) is typically sensed using atomic spectrometric techniques. Because of low levels ordered by EPA regulations in waters and soils, very sensitive and selective monitoring techniques are required. Although continuous monitoring of column effluents for breakthrough can be conducted using flame atomic absorption spectroscopy or inductively coupled plasma emission or mass spectrometry, a more portable and less costly alternative is desired. The use of a continuous monitoring, inexpensive *in situ* sensor to monitor metal concentrations in the effluent stream and determine when the column is at capacity and needs to be regenerated would be ideal. A key requirement of the desired detection technique is the sensitivity to detect the metal concentrations leaving the column once breakthrough is reached. Such a sensor may also find applications in other areas of remote sensing and continuous monitoring.

1.5 FLUORESCENCE CHEMOSENSORS FOR METAL DETECTION

The design of sensors for the sensitive and selective recognition of metal ions has been fueled by decreasing regulatory limits for metal levels. The properties of an "ideal" sensor include high sensitivity, high selectivity for one metal ion only, fast and reversible (real time) response, real-space response down to the micrometer level and easy handling.[28] Fluorescence is an ideal detector for analyte sensing due to its high sensitivity compared to other available signaling types. Additionally, fluorescence

measurements are usually low cost, easily performed and versatile. Because of this, it has been widely used for the detection of a number of metal ions.[28-34]

Fluorescence chemosensors are typically composed of two structural subunits intramolecularly connected through a linking bridge: a fluorophore (for signal transduction) and an ionophore (for selective recognition of the metal ion). When designing these sensors, intense effort is put into maximizing the selectivity of the metal chelating unit. Early fluorescent chemosensors focused on using chelating units composed of organic molecules, but synthesis was rigorous, binding was not always reversible and organic solvents or mixed organic-aqueous solutions were required.[28, 35-45] Peptide motifs prove to be a viable alternative since they exhibit metal selectivity, can be easily synthesized via fluorenylmethoxycarbonyl (Fmoc)-solid phase peptide synthesis (SPPS)[46, 47] and are usable in aqueous solutions. Additionally, the biocompatibility of peptides allows conjugation to appropriate systems of biological interest such as proteins or nucleic acids. One of the first examples of a fluorescent peptidyl chemosensor was the use of a small peptide sequence (25 residues) based on the zinc finger protein by Walkup et al.[48] Other motifs, such as the Cu^{2+} binding tripeptide growth factor[49] and the Cu^{2+} and Ni^{2+} binding ACTUN[50-53] have also been used successfully. Peptide combinatorial libraries have also been used generate new selective fluorescent chemosensors for metal analytes such as Cu^{2+}.[54]

Typically, metal binding is detected by the quenching of a single fluorophore such as dansyl[35, 39, 42, 50-52, 54, 55] lucifer yellow[56] or anthracence[36, 57-59]Although concentration dependent quenching mechanisms have proven successful, it is inherently less sensitive than methods that *produce* fluorescence as a result of binding.[60] Also, it is often difficult to distinguish analyte response from sensor degradation when quenching is relied upon for quantitation.

1.6 FLUORESCENCE RESONANCE ENERGY TRANSFER

Fluorescence resonance energy transfer (FRET) is a distance dependent energy transfer mechanism that occurs between two molecules, a donor chromophore and an acceptor chromophore. The donor chromophore has to be fluorescent, but the acceptor fluorophore can be either fluorescent or non-fluorescent. In FRET, a donor fluorophore is excited by incident light and promoted to an excited state. If an acceptor chromophore is in close proximity, excited state energy from the donor can be transferred to it. This results in a decrease in the donor's emission intensity and an increase in the acceptor's emission intensity, providing that the acceptor is a fluorescent molecule.[61] Figure 1.3a and b show a Jablonski diagram for fluorescence and a modified diagram for FRET.

Figure 1.3 a) Jablonski diagram of standard fluorescence and b) modified Jablonski diagram of FRET

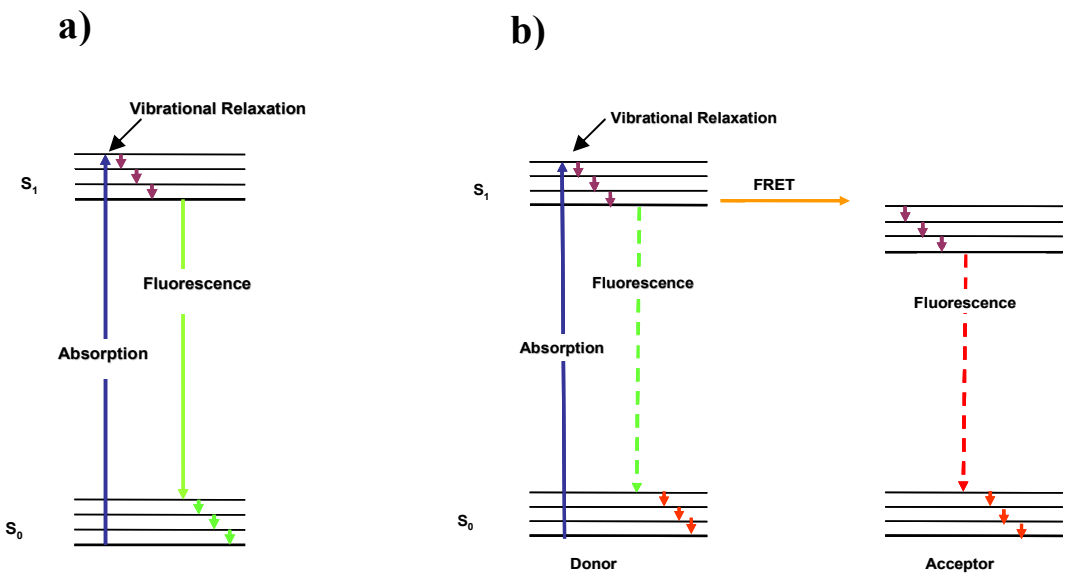

FRET was first observed in 1922 by Cario and Franck with a sample of mercury and thallium vapors.[62] The sample was illuminated at a frequency of light only absorbed

by mercury but peaks for both elements were observed in the emission spectrum, indicating that some energy transfer must have occurred. The theory of FRET was not formulated until 1948 by Förster, who found that the efficiency of energy transfer (*E*) is dependent upon the distance between the donor and acceptor (*r*) as well as the Förster critical distance (R_0).[63] This is shown in equation 1:

$$E = \frac{R_0^{\,6}}{R_0^{\,6} + r^6} \tag{1}$$

The Förster critical distance is the distance at which the efficiency of energy transfer between the donor and acceptor is 50%. It is a constant value for each FRET pair and is typically between 15 Å and 60 Å. Therefore, distances on this order can be measured. Equation 2 shows that the Förster critical distance (R_0) is dependent upon the donor and acceptor orientation (κ), the refractive index of the solvent (*n*), the donor quantum yield (*Q*), and the amount of overlap between the donor and the acceptor *(J)*:

$$R_0 = 9876(\kappa^2 n^{-4} Q_D J)^{1/6} \tag{2}$$

Conventionally, FRET efficiency is determined by comparing the donor intensity of the donor-acceptor sample (I_{DA}) to that of a donor only sample (I_D). This is shown in equation 3[63] :

$$E = 1 - \frac{I_{DA}}{I_D} \tag{3}$$

FRET has had a large impact on the biological world. Styrer and Haugland used FRET in 1967 to determine distances in poly-L-proline peptides of varying lengths.[64] Since then it has found widespread use as a spectroscopic ruler for measuring distances in

DNA, RNA, and proteins.[65] It is also a key phenomenon observed in natural light-harvesting complexes, accounting for energy transfer between chlorophyll molecules in photosynthesis.[66-68]

1.6.1 FRET Based Peptidyl Metal Ion Sensors

Because of the "wrapping" and "folding" of the peptide chelating unit, FRET should be an effective mechanism of detecting metal binding. Visually, as the metal binds, the peptide chelating unit will wrap or fold around it, decreasing the distance between the fluorophores and causing an increase in FRET. A cartoon of the proposed system is shown in Figure 1.4.

Figure 1.4 Cartoon of FRET based peptide metal ion sensor

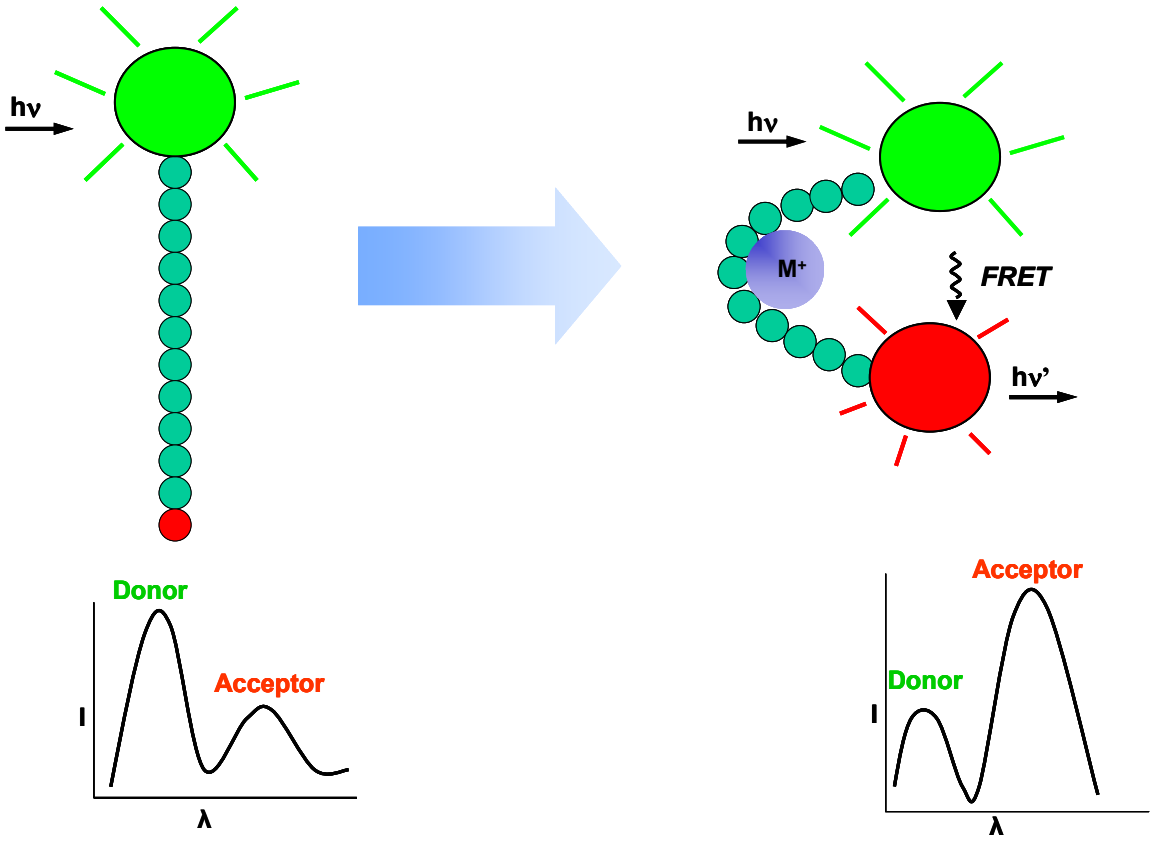

FRET based sensors would allow the concept of the metal serving as a "folding facilitator" or even an in-chain "short circuit" to enhance energy transfer from donor to acceptor, resulting in an *increase* in acceptor fluorescence. This is an improvement over conventional fluorescence sensors which utilize a quenching response. Additionally, FRET allows a larger wavelength separation between the excitation and emission wavelengths, thereby permitting the use of lower resolution wavelength isolation devices (e.g., filters) to measure emission without interference from the excitation source.

The viability of FRET as a detection mechanism in peptide based metal ion sensors has been demonstrated previously. Imperiali and coworkers developed a solution based FRET sensor built around the ACTUN motif.[53] While an enhancement response was observed for Ni^{2+}, complete metal selectivity was not achieved as a quenching response was also observed for Cu^{2+}. Similarly, Berg and coworkers developed a FRET sensor based on the zinc finger peptide motif, but no interfering ion studies were conducted leaving metal selectivity undetermined.[69] Although these sensors were not without flaws, the concept that peptide folding upon metal binding results in increased FRET was proven.

This dissertation focuses on the development of FRET based peptidyl metal ion sensors and their potential use as a portable probe for monitoring metal effluent from ion exchange columns or, in general, for *in situ* metal determinations in a remediation pond, natural waters, etc. Metal chelating units were designed based on previous polyamino acid studies as well as "hints from mother nature", i.e. metal binding proteins and their binding loops. Chapter 2 discusses the development of a selective FRET peptide sensor for Cu^{2+}. The peptide chelating unit used in this study was not based on an existing motif. Rather, aspartic acid's affinity for hard acid metals such as Cu^{2+} and Cu^{2+}'s preference for square planar coordination was used as a basis of the design. Previous

attempts at FRET based sensors for Cu^{2+} have failed due to its propensity to quench fluorescence.

Chapter 3 describes a FRET sensor based on the mercury binding protein MerP. Although MerP has been shown to bind other metals with some affinity, characterization studies have shown that the structures of the metal bound forms are very different, which can be exploited with FRET. A peptide fragment containing amino acids from MerP's metal binding loop was used as the chelating unit in hopes of achieving an enhancement response for Hg^{2+}.

In chapter 4, immobilized fluorophore labeled peptide studies are conducted and an FIA column with FRET detection is developed. While FRET has been used as a detection technique for several solution based sensors, few have utilized its enhancement properties for immobilized metal ion sensors. By coupling FRET detection to an FIA system, analyte analysis is made quicker and easier.

Chapter 5 departs from the general theme of FRET sensor development and describes the immobilization of poly-L-cysteine onto magnetic γ-Fe_2O_3 nanoparticles and the evaluation of its metal remediation potential. Magnetic nanoparticles are an attractive support because they can easily be retrieved from a remediation pond and have a larger metal binding surface area than traditional micrometer diameter supports. By immobilizing the polypeptide onto the surface of the support, metal selectivity can be achieved.

In chapter 6, a method that was developed for screening peptide combinatorial libraries using ETV-ICP-MS is described. Several techniques are available for qualitatively screening peptide combinatorial libraries for metal binding, but quantitative data is harder to obtain using existing methods. The ETV exhibits excellent metal selectivity and small sample volumes can be used, allowing metal extracts from the

library beads to be analyzed. All of the metals can be simultaneously screened by the time of flight (TOF) mass analyzer, which allows for unlimited m/z monitoring with no loss in duty cycle.

Chapter 7 wraps up the implications of this work with FRET based peptide metal ion sensors and discusses future work directed toward the development of a portable fiber optic *in situ* sensor.

1.7 REFERENCES

(1) Jarup, L. *Br. Med. Bull.* **2003**, *68*, 167-182.

(2) US EPA, http://www.epa.gov/safewater/mcl.html, 2007.

(3) Forstner, U.; Wittmann, G. T. W. *Metal pollution in the aquatic environment*; Springer-Verlag: New York, 1981.

(4) Vernet, J. P. *Impact of Heavy Metals on the Environment*; Elsevier: New York, 1992.

(5) US EPA, http://www.epa.gov, 2007.

(6) Ireland, M. P. *Biological Monitoring of Heavy Metals*; Wiley: New York, 1991.

(7) Friber, L.; Nordberg, G. F.; Vouk, B. *Handbook on the Toxicology of Metals*; Biomedical Press: Amsterdam, 1979.

(8) Krishnan, R. E. *Recovery of Metals from Sludges and Wastewaters*; Noyes Data Corp.: Park Ridge, NJ, 1993.

(9) Chen, L. H.; Chung, C. S. *Inorg. Chem.* **1988**, *27*, 1880-1883.

(10) Malamas, F.; Bengtsson, M.; Johansson, G. *Anal. Chim. Acta* **1984**, *160*, 1-10.

(11) Fang, Z.; Ruzicka, J.; Hansen, E. H. *Anal. Chim. Acta* **1984**, *164*, 23-39.

(12) Calmon, C.; Gold, H. *Ion exchange for pollution control*; CRC Press: Boca Raton, Fla, 1979.

(13) Malachowski, L.; Stair, J.; Holcombe, J. A. *Pure Appl. Chem.* **2004**, *76*, 777-787.

(14) Martell, A. E.; Hancock, R. D. *Chelating Ligands*; Plenum Press: New York, 1996.

(15) Schwarzenback, G. *Helv. Chim. Acta* **1952**, *35*, 2344.

(16) Elmahadi, H. A. M.; Greenway, G. M. *J. Anal. Atom. Spec.* **1993**, *8*.

(17) Jurbergs, H. A.; Holcombe, J. A. *Anal. Chem.* **1997**, *69*, 1893-1898.

(18) Howard, M.; Jurbergs, H. A.; Holcombe, J. A. *J. Anal. At. Spectrom.* **1999**, *14*, 1209-1214.

(19) Howard, M.; Jurbergs, H. A.; Holcombe, J. A. *Anal. Chem.* **1998**, *70*, 1604-1609.

(20) Cotton, F. A.; Wilkinson, G. *Advanced Inorganic Chemistry: A Comprehensive Text*, 4th ed. ed.; John Wiley & Sons: New York, 1980.

(21) Gutierrez, E.; Miller, T. C.; Gonzalez-Redondo, J. R.; Holcombe, J. A. *Environ. Sci. Technol.* **1999**, *33*, 1664-1670.

(22) Malachowski, L.; Holcombe, J. A. *Anal. Chim. Acta* **2004**, *517*, 187-193.

(23) Malachowski, L.; Holcombe, J. A. *Anal. Chim. Acta* **2003**, *495*, 151-163.

(24) Malachowski, L.; Stair, J. L.; Holcombe, J. A. *Pure Appl. Chem.* **2004**, *76*, 777-787.

(25) Stair, J. L.; Holcombe, J. A. *Microchem. J.* **2005**, *81*, 69-80.

(26) DeSilva, T. M.; Veglia, G.; Porcelli, F.; Prantner, A.; Opella, S. J. *Biopolymers* **2002**, *64*, 189-197.

(27) Harford, C.; Sarkar, B. *Acc. Chem. Res.* **1997**, *30*, 123-130.

(28) Kramer, R. *Angew. Chem. Int. Ed. Engl.* **1998**, *37*, 772-773.

(29) Czarnik, A. W. *Fluorescent Chemosensors for Ion and Molecule Recognition*; American Chemical Society: Washington, DC, 1993.

(30) Fabbrizzi, L.; Licchelli, M.; Pallavicini, P.; Parodi, L.; Taglietti, A. In *Transition Metals in Supramolecular Chemistry*; Sauvage, J. P., Ed.; Wiley: Chichester, 1999, pp 93-134.

(31) Desvergne, J. P.; Czarnik, A. W. *Chemosensors of Ion and Molecular Recognition*; Kluwer Academic Publishers: Dordrecht, The Netherlands, 1997.

(32) de Silva, A. P.; Nimal Gunaratne, H. Q.; Gunnlaugsson, T.; Huxley, A. J. M.; McCoy, C. P.; Rademacher, J. T.; Rice, T. E. *Chem. Rev.* **1997**, *97*, 1515-1566.

(33) Haugland, R. P. *Handbook of Fluorescent Probes and Research Chemicals, 6th ed.*, 6 ed.; Molecular Probes, Inc.: Eugene, 1996.

(34) Pina, F.; Bernardo, A.; Garcia-Espana, E. *Eur. J. Inorg. Chem.* **2000**, *20*, 2143-2157.

(35) Corradini, R.; Dossema, A.; Galaverna, G.; Marchelli, R.; Panagia, A.; Sartor, G. *J. Org. Chem.* **1997**, *62*, 6283-6289.

(36) De Santis, G.; Fabbrizzi, L.; Licchelli, M.; Mangano, C.; Sacchi, D.; Sardone, N. *Inorg. Chim. Acta* **1997**, *257*, 69-76.

(37) Yoon, J.; Ohler, N. E.; Vance, D. H.; Aumiller, W. D.; Czarnik, A. W. *Tetrahedron Lett.* **1997**, *38*, 3845-3848.

(38) Mitchell, K. A.; Brown, R. G.; Yuan, D.; Chang, S.-C.; Utecht, R. E.; Lewis, D. E. *J. Photochem. Photobiol., A* **1998**, *115*, 157-161.

(39) Prodi, L.; Bolletta, F.; Montalti, M.; Zaccheroni, N. *Eur. J. Inorg. Chem.* **1999**, 455-460.

(40) Beltramello, M.; Gatos, M.; Mancin, F.; Tecilla, P.; Tonellato, U. *Tetrahedron Lett.* **2001**, *42*, 9143-9146.

(41) Klein, G.; Kaufmann, D.; Schurch, S.; Reymond, J.-L. *Chem. Commun.* **2001**, 561-562.

(42) Prodi, L.; Montalti, M.; Zaccheroni, N.; Dallavalle, F.; Folesani, G.; Lanfranchi, M.; Corradini, R.; Pagliari, S.; Marchelli, R. *Helv. Chim. Acta* **2001**, *84*, 690-706.

(43) Bourson, J.; Badaoui, F.; Valeur, B. *J. Fluoresc.* **1994**, *4*, 275-277.

(44) Akkaya, E. U.; Turkyilmaz, S. *Tetrahedron Lett.* **1997**, *38*, 4513-4516.

(45) Kawakami, J.; Itoh, H.; Mitsuhashi, H.; Ito, S. *Anal. Sci.* **1999**, *15*, 617-618.

(46) Merrifield, R. B. *J. Am. Chem. Soc.* **1963**, *85*, 2149-2154.

(47) Atherton, E.; Sheppard, R. C. In *Solid Phase Peptide Synthesis: A Practical Approach*; IRL Press: Oxford, 1989, pp 131-148.

(48) Walkup, G. K.; Imperiali, B. *J. Am. Chem. Soc.* **1996**, *118*, 3053-3054.

(49) Zheng, Y.; Huo, Q.; Kele, P.; Andreopoulos, F. M.; Phan, S. M.; Leblanc, R. M. *Org. Lett.* **2001**, *3*, 3277-3280.

(50) Torrado, A.; Walkup, G. K.; Imperiali, B. *J. Am. Chem. Soc.* **1998**, *120*, 609-610.

(51) Zheng, Y.; Gattas-Asfura, K. M.; Konka, V.; Leblanc, R. M. *Chem. Commun.* **2002**, *20*, 2350-2351.

(52) Zheng, Y.; Cao, X.; Orbulescu, J.; Konka, V.; Andreopoulos, F. M.; Pham, S. M.; Leblanc, R. M. *Anal. Chem.* **2003**, *75*, 1706-1712.

(53) Pearce, D. A.; Walkup, G. K.; Imperiali, B. *Bioorg. Med. Chem. Lett.* **1998**, *8*, 1963-1968.

(54) Singh, A.; Yao, L.; Still, W. C.; Sames, D. *Tetrahedron Lett.* **2000**, *41*, 9601-9605.

(55) Bhattacharya, S.; Thomas, M. *Tetrahedron Lett.* **2000**, *41*, 10313-10317.

(56) Mayr, T.; Werner, T. *The Analyst* **2002**, *127*, 248-252.

(57) Jiang, P.; Guo, Z. *Coord. Chem. Rev.* **2004**, *248*, 205-229.

(58) Fabbrizzi, L.; Licchelli, M.; Pallavicini, P.; Perotti, A.; Taglietti, A.; Sacchi, D. *Chem. Eur. J.* **1996**, *2*, 75-82.

(59) Fabbrizzi, L.; Licchelli, M.; Pallavicini, P.; Perotti, A.; Sacchi, D. *Angew. Chem. Int. Ed. Engl.* **1994**, *33*, 1975-1977.

(60) Chae, M. Y.; Czarnik, A. W. *J. Am. Chem. Soc.* **1992**, *114*, 9704-9705.

(61) Selvin, P. R. *Nature Struct. Biol.* **2000**, *7*, 730-734.

(62) Cario, G.; Franck, J. *Z. Physik* **1922**, *11*, 161-166.

(63) Forster, T. *Ann. Phys.* **1948**, *2*, 55-75.

(64) Stryer, L.; Haugland, R. P. *Proc. Natl. Acad. Sci. USA* **1967**, *58*, 719-726.

(65) dos Remedios, C. G.; Moens, P. D. J. In *Resonance Energy Transfer*; Andrews, D. L., Demidov, A. A., Eds.; John Wiley and Sons: New York, 1999, pp 1-54.

(66) Demidov, A. A.; Borisov, A. Y. *Biophys. J.* **1993**, *64*, 1375-1384.

(67) van Grondelle, R.; Dekker, J.; Gillbro, T.; Sundstrom, V. *Biochim Biophys. Acta* **1994**, *1187*, 1-65.

(68) Schulten, K. In *Simplicity and Complexity in Proteins and Nucleic Acids*; Frauenfelder, H., Deisenhofer, J., Wolynes, P. G., Eds.; Dahlem University Press: Berlin, 1999, pp 227-253.

(69) Godwin, H. A.; Berg, J. M. *J. Am. Chem. Soc.* **1996**, *118*, 6514-6515.

Chapter 2: A Fluorescent Peptide Sensor for the Selective Detection of Cu^{2+}

2.1 INTRODUCTION

The significance of *in situ* determination of low level concentrations of metals such as Ca^{2+}, Cu^{2+} and Zn^{2+} in environmental and biological samples has prompted research into the development of fluorescent chemosensors.[1-7] These chemosensors are typically composed of two structural subunits intramolecularly connected through a linking bridge: a fluorophore (for signal transduction) and an ionophore (for selective recognition of the metal ion). When designing these sensors, intense effort is put into maximizing the selectivity of the metal chelating unit. Early fluorescent chemosensors focused on using chelating units composed of organic molecules, but synthesis was rigorous and binding was not always reversible.[3, 8-18] Peptide motifs from metal binding proteins proved to be a viable alternative since they often maintained the protein's metal selectivity, could be easily synthesized via fluorenylmethoxycarbonyl (Fmoc)-solid phase peptide synthesis (SPPS)[19, 20] and were useable in aqueous solutions. One of the first examples was the use of a small peptide sequence (25 residues) based on the zinc finger protein by Walkup et al.[21] Other motifs, such as the Cu^{2+} binding tripeptide growth factor[22] and the Cu^{2+} and Ni^{2+} binding ACTUN[23-26] have also been used successfully.

Typically, metal binding is detected by the quenching of a single fluorophore such as dansyl[8, 12, 15, 23-25, 27, 28], lucifer yellow [29] or anthracence.[9, 30-32] Although concentration dependent quenching mechanisms have proven successful, it is inherently less sensitive than methods that *produce* fluorescence as a result of binding.[33] Also, it is often difficult to distinguish analyte response from sensor degradation when quenching is relied upon for quantitation.

It was our initial intent to link a fluorophore to each end of the chelating unit to observe an increase in fluorescence resonance energy transfer (FRET [34-36]) with metal binding. Conceptually, if the chelating unit folds around the metal as it binds, the fluorophores are brought closer together, causing increased transfer of energy from the donor fluorophore to the acceptor fluorophore. Because it is a distance-dependent interaction, FRET can also be used as a diagnostic to understand the conformation and mechanism of metal binding to the chelating unit. In comparison to conventional fluorescence, FRET can generate a larger wavelength separation between the excitation and emission wavelengths thereby permitting lower resolution wavelength isolation devices (e.g., filters).

This chapter reports on the synthesis of a new peptide motif with FRET capabilities for the selective detection of Cu^{2+}, a trace metal that is essential to sustain life, but is toxic in excess amounts.[37-40] The 15 residue peptide (sequence: Dansyl-Gly-Gly-Asp-Gly-Gly-Asp-Gly-Gly-Asp-Gly-Gly-Asp-Gly-Gly-Trp-$CONH_2$) was not based on any metal binding proteins in an attempt to illustrate the potential of constructing a selective chelator using a short peptide without the need for a biological starting point. The FRET pair (tryptophan as donor and dansyl chloride as acceptor) were conveniently attached during SPPS, eliminating the need for labeling reactions. Each of the four aspartic acid residues, which have an affinity for hard acid metals such as Cu^{2+} [41], were separated by two glycine residues in hopes of exploiting the preference of Cu^{2+} for a square planar coordination and thus resulting in an increase in FRET. Prior to this, two examples of FRET-based fluorescent peptidyl chemosensors for Cu^{2+} have been attempted in the literature, but the addition of Cu^{2+} to the peptide solution resulted in the quenching of one or both fluorophores and no increase in FRET.[26, 42]

Unfortunately, these previous studies were unable to provide definitive evidence that a change in FRET was occurring due, in part, to the strong influence of the quenching phenomena.

2.2 EXPERIMENTAL

2.2.1 Chemicals

All chemicals were reagent grade unless noted, and deionized distilled water was used to prepare solutions. All glassware was soaked overnight in 4 mol L^{-1} HNO_3 prior to use. Peptide synthesis reagents N-Dansyl-N'-Fmoc-ethylenediamine-MPB-AM (Dansyl NovaTag®) resin (100-200 mesh; 0.38 mmol g^{-1}), Wang resin (100-200 mesh, 1.2 mmol g^{-1}), glycine (Fmoc-Gly-OH), aspartic acid (Fmoc-Asp(t. butyl ester (OtBu))-OH), tryptophan (Fmoc-Trp(Boc)-OH), 2-(1H-benzotriazole-1-yl)-1,1,3,3-tetramethylaminium hexafluorophosphate (HBTU), and 1-hydroxybenzotriazole (98%) (HOBt) were used as received from Novabiochem. All the amino acids were of L-configuration. Stock solutions of 1000 µg ml^{-1} Cd^{2+} (Anderson Laboratories), Cu^{2+} (SCP Science), Na^{+} (Sigma Aldrich), Ni^{2+} (SCP Science), and Zn^{2+} (Acros) atomic absorption standards were used to prepare metal solutions for fluorescence measurements. For Ca^{2+} and Mg^{2+} (J.T. Baker), the stock solutions were prepared from standardized solutions of the reagent grade nitrate salt in 1% (v/v) HNO_3 and 1% (v/v) HCl. A 0.05 mol L^{-1} (N-[hydroxyethyl] piperazine-N'-[2-ethanesulfonic acid]) (HEPES) (Aldrich) buffer was prepared and adjusted to pH 7.0 with ammonium hydroxide (Fisher). Other reagents used include trifluoroacetic acid (99%) (TFA), triisopropylsilane (99%) (TIPS), ethyl ether (Fisher), (ethylenedinitrilo)-tetraacetic acid (EDTA) (EM Science), N-methylmorpholine (NMM) (Fisher), N-methylpyrrolidone (NMP) (Fisher) and piperidine (99%).

2.2.2 Instrumentation

A Photon Technologies International Quanta Master Spectrofluorimeter (model QM-4/2005) was used for all fluorescence measurements.

2.2.3 Peptide Synthesis

A peptide consisting of the sequence Dansyl-Gly-Gly-Asp-Gly-Gly-Asp-Gly-Gly-Asp-Gly-Gly-Asp-Gly-Gly-Trp-$CONH_2$ (**P1**) was synthesized on Dansyl NovaTag® resin and a peptide consisting of the sequence Gly-Gly-Asp-Gly-Gly-Asp-Gly-Gly-Asp-Gly-Gly-Asp-Gly-Gly-Trp-$CONH_2$ (**P2**) was synthesized on Wang resin by Fmoc-solid phase peptide synthesis using a Ranin Symphony Quartet automated peptide synthesizer. The peptides were double coupled (each amino acid coupling reaction was performed twice) in order to increase reaction efficiency and peptide integrity. Cleavage of the peptides from the resin was conducted with TFA/ TIPS/ H_2O (95/ 2.5/ 2.5) for 2.5 hrs. The solution was then suction filtered, isolated using ether, and lyophilized. The peptide masses (1510.7 for **P1** and 1234.1 for **P2**) were confirmed using electrospray mass spectrometry and the purity of each sequence (63% for **P1** and 71% for **P2**) was determined by reverse phase-HPLC. For both **P1** and **P2**, no other single component was present in excess of 15%.

2.2.4 Fluorescence Studies

2.2.4.1 Cu^{2+} response studies

Fluorescence emission spectra were collected from 10 μmol L^{-1} solutions of **P1** and **P2** (pH 7.0, 50 mmol L^{-1} HEPES). A range of Cu^{2+} concentrations (1-20 μmol L^{-1}) were added to each peptide solution from a 0.002 mol L^{-1} stock solution. Both FRET studies (monitoring emission of Trp and dansyl) and single fluorophore studies (monitoring emission of dansyl) were conducted on **P1**. Single fluorophore studies

(monitoring emission of Trp) were conducted on **P2**. Excitation and emission wavelengths for each study are reported in Table 1. When determining signal intensity for dansyl chloride emission, an average of intensities in the wavelength region 545-550 nm was used due to the broad emission peak. For tryptophan emission, intensities at 348 nm were used.

2.2.4.2 Multi-metal response studies

A 10 μmol L^{-1} **P1** and 10 μmol L^{-1} (each) Cd^{2+}, Co^{2+}, Mn^{2+}, Ni^{2+} and Zn^{2+} solution (pH 7.0, 50 mmol L^{-1} HEPES) was prepared. A range of Cu^{2+} concentrations (1-20 μmol L^{-1}) was added to the **P1**/metal solution from a 0.002 mol L^{-1} stock solution to determine **P1**'s response to Cu^{2+} in a transition metal matrix. Excitation and emission wavelengths are reported in Table 1.

A 10 μmol L^{-1} **P1** and 5 μmol L^{-1} Cu^{2+} solution (pH 7.0, 50 mmol L^{-1} HEPES) was prepared. 400 mg L^{-1} stock solutions of Ca^{2+}, Cd^{2+}, Mg^{2+}, Na^{+}, Ni^{2+} and Zn^{2+} were prepared and 100μL aliquots were added to the **P1**/ Cu^{2+} solution. Metal interferant concentration vs. % error in Cu signal was plotted in Origin 7.0® and the polynomial fit function was used to determine the concentration of each metal that would cause a 10% error in the **P1** response to Cu^{2+}. This procedure was repeated for a 10 μmol L^{-1} **P1** and 10 μmol L^{-1} Cu^{2+} solution (pH 7.0, 50 mmol L^{-1} HEPES).

2.2.4.3 FRET measurement

In order to determine the initial distance (r) between the fluorophores before metal was added, equation 1 [34] was used.

$$E = \frac{R_0^6}{R_0^6 + r^6} \qquad (1)$$

For the measurement of the FRET efficiency (E), the emission of **P2**, which contains only tryptophan (I_D), has been compared to the emission of **P1**, which contains both tryptophan and dansyl chloride ($I_{D/A}$). Equation 2 [34] was used to calculate FRET efficiency.

$$E = 1 - \frac{I_{DA}}{I_D} \qquad (2)$$

The Forster distance, R_0, for tryptophan /dansyl chloride has been previously determined to be 21 Å [35] and their spectral overlap has been illustrated [43, 44]. The distance between the dyes is 62 Å if **P1** is completely elongated.

2.3 RESULTS AND DISCUSSION

2.3.1 Existence of FRET and Fluorescence Quenching by Cu^{2+}

The fluorescence of **P1** (λ_{ex} = 348nm) is shown in Figure 2.1a where only dansyl chloride is excited. With excitation of the Trp donor (λ_{ex} = 290 nm, Figure 2.1b), the emission spectra of dansyl chloride is again observed, thus verifying FRET.

Figure 2.1 Relationship of the fluorescence of **P1** to the concentration of Cu^{2+} (50 mmol L^{-1} HEPES, pH 7.0). Response of **P1** (10 µmol L^{-1}) to the addition of Cu^{2+} with excitation at a) 348 nm and b) 290 nm (from top to bottom 0.0, 1.0, 3.0, 5.0, 9.0, 10.0, 15.0 and 20.0 µmol L^{-1} Cu^{2+}). All spectra were smoothed using Savitzky-Golay least squares smoothing routine with a 21 point window (Origin).

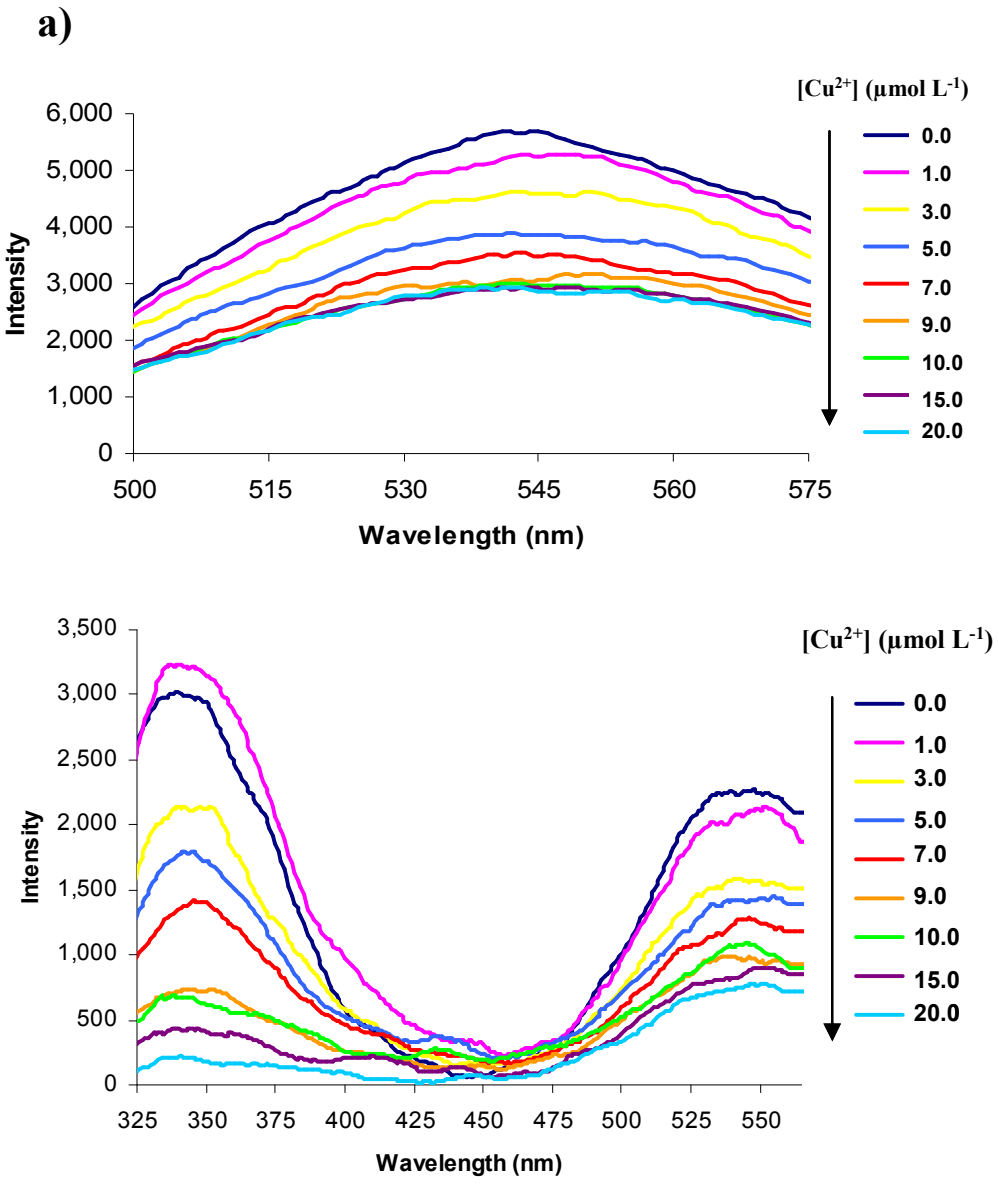

The dansyl chloride emission decreased noticeably when the pH was lowered to 3.5, but was restored to its original intensity when the pH was returned to 7.0, illustrating the robustness of the peptidyl system.

For **P1**, the fluorescence emission intensity of both fluorophores decreased with the addition of Cu^{2+} (Figure 2.1), suggesting quenching, and this quenching was easily reversed by the addition of excess EDTA to the peptide solution. Figure 2.1b suggests that dansyl chloride quenching might be a simple consequence of the reduction of FRET excitation. However, Figure 2.1a again shows Cu^{2+} quenching of dansyl at λ_{ex} = 348 nm when there is no excitation of Trp and therefore no chance of FRET. Thus, Cu^{2+} quenches both of these fluorophores. This is further supported by the more strongly dependent quenching of dansyl on Cu^{2+} when FRET is the primary excitation mode for Trp. (See Figure 2.1a and b.) This is demonstrated in a slightly different presentation in the isotherms shown in Figure 2.2.

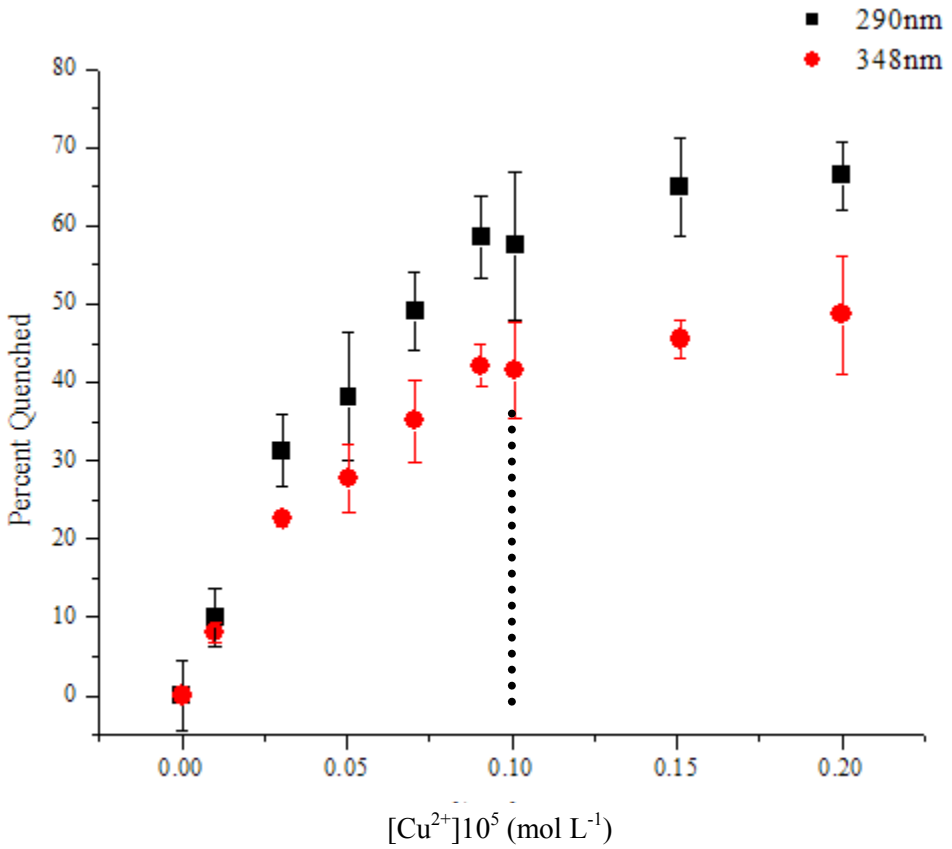

Figure 2.2 Fluorescent binding isotherms of **P1** with Cu^{2+}(excitation at 290 and 348 nm). A 1:1 copper to peptide binding ratio is observed.

Figure 2.2 also shows that the maximum Cu: peptide binding ratio is approximately one. This suggests that there is probably only one Cu binding site that is responsible for both quenching phenomena. The quenching of dansyl is likely due to Cu^{2+} complexation with the dansyl sulfonamide, which has been modeled and shown to cause quenching in other peptide systems [24, 25]. At pH 7, the Cu^{2+} coordination to the N-terminal amine of Trp may account for its quenching interaction[45].

At 1 equiv Cu^{2+}, **P1** quenched to 42.5% of its initial value when excited at 290 nm and 58.5% of its initial value when excited at 348 nm. As is seen in Figures 2.1 and 2.2, only a nominal decrease in fluorescence was observed after this point. As expected, a

larger amount of quenching occurred when excitation was at 290 nm because dansyl chloride is losing emission by both copper quenching and loss of FRET. Studies by Zheng and coworkers on short Cu^{2+} binding peptides based on the ACTUN motif showed almost 100% quenching of dansyl chloride at 1 equiv Cu^{2+} when the sulfonamide group was directly involved in Cu^{2+} binding. Incomplete quenching was seen when the dansyl chloride was located on a side chain and not close enough to the binding event to signal it completely [25]. In the case of **P1**, where dansyl chloride is located on the C-terminus, the incomplete quenching may be due to the shared Trp/ dansyl binding site. Also, as will be discussed later, **P1** exhibited excellent metal selectivity towards Cu^{2+} whereas Zheng and coworkers witnessed more nonspecific binding when dansyl chloride did not quench completely.

The log K of **P1**-Cu^{2+} was calculated by the method of Conners[46] to be 4.90. This value is much smaller than that of metal binding proteins, such as the zinc finger (log K = 9) [47] or ACTUN (log K = 17) [48], probably as a consequence of the peptide carboxylates not actually actively involved in Cu^{2+} binding in this system, as will be discussed in greater detail in section 2.3.3.

2.3.2 Cu^{2+} Determination

Calibration curves were constructed from the fluorescence spectra to illustrate the quantitative dependence of the fluorescence on Cu^{2+} concentration. Detection limits at both excitation wavelengths were calculated for **P1** complexation with Cu^{2+}. The detection limit was 129 μg L^{-1} at 290 nm and 32 μg L^{-1}at 348 nm. Due to the lower detection limit and better precision, subsequent studies using mixed-metal matrix were conducted with excitation only at 348 nm.

2.3.3 Impact of Peptide Chain's Functionalities in Cu^{2+} Binding

Using equation 1, the FRET efficiency without Cu^{2+} was determined to be 80 ± 4%, which corresponds to a distance of only 17 ± 1 Å between the fluorophores, indicating that **P1** (62 Å when completely elongated) is already tightly coiled or folded even before the addition of metal. As a result of this small separation, it again is reasonable that both the dansyl sulfonamide and the N-terminal amine may be participating in the same binding site, yielding the 1:1 binding ratio.

Even though the fluorophores are initially separated by only 17 Å, it is possible that the peptide chelating unit changes conformation when Cu^{2+} binds. Typically, an increase in FRET efficiency (*E*) denoted by an increase in the acceptor's fluorescence is used to indicate a conformational change. In the case of **P1**, both fluorophores are being quenched, making the determination of a change in *E* less straightforward. Monitoring and comparing the emission intensity of two peptide sequences, one containing both fluorophores (i.e., **P1**) and one containing just the donor (i.e., **P2**) is required. An increase in *E* due to Cu^{2+} binding should quench **P1**'s Trp emission more than **P2**'s because it is losing energy from the FRET process *and* Cu^{2+} quenching. Tryptophan quenching for both **P1** and **P2** were plotted (Figure 2.3) and found to overlap, indicating that no change in *E* occurred.

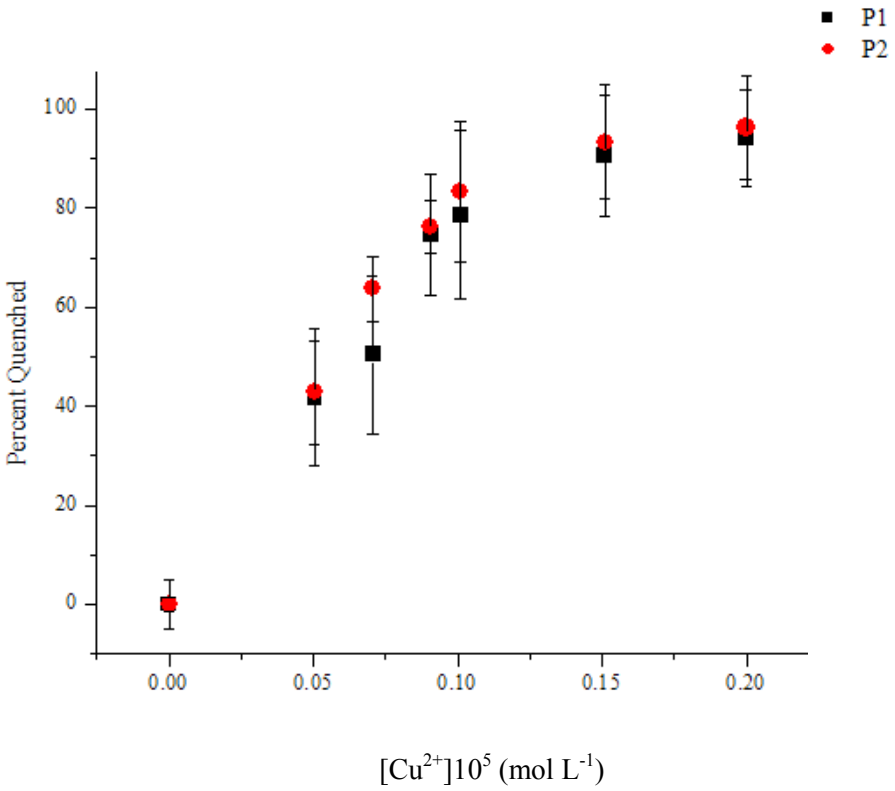

Figure 2.3 Plots of tryptophan quenching in **P1** and **P2**. The overlapping curves suggest that no change in FRET efficiency (*E*) is occurring. The fluorescence intensity has been normalized and expressed in terms of percent quenched. Excitation is at 290 nm.

It is known that Cu^{2+} has a propensity to coordinate with carboxylates[41], such as that contained within the peptide chain of **P1**. However, previous results suggest that Cu^{2+} coordination with amines is stronger than Cu^{2+} coordination with carboxylates, with Cu^{2+} able to deprotonate nitrogens on the peptide backbone[49]. The fact that a 2 fold excess of Cu^{2+} didn't significantly alter the FRET signal suggests that minimal binding to the peptide carboxylates is occurring. If binding had occurred with such an excess, then the dansyl-Trp distance would have likely changed as a result of the conformational change of the peptide unit. This should have produced an increase or decrease in the dansyl fluorescence because of an alteration in *E*. This was not observed. Because the

fluorophores are only separated by 17 Å before the addition of metal, it is likely that the peptide is significantly coiled in the absence of Cu^{2+}. Thus, the carboxyl ligands in the chain may be inaccessible or geometrically misaligned for chelation with Cu^{2+}, allowing coordination with the N-terminal amine, the dansyl sulfonamide and perhaps nitrogens located on the peptide backbone instead.

2.3.4 Evaluation of Selectivity

The selectivity of P1 towards Cu2+ was demonstrated in a pH 7.0 HEPES solution containing several transition metal ions (Figure 3.4).

Figure 3.4 Fluorescent selectivity of **P1** toward copper ions (50 mmol L^{-1} HEPES, pH 7.0). a) Free **P1** (10 µmol L^{-1}), b) **P1** and mixed metal solution containing 10 µmol L^{-1} each of Cd^{2+}, Co^{2+}, Ni^{2+}, Mn^{2+}, and Zn^{2+}, and c) **P1**, mixed metal solution and Cu^{2+} (10 µmol L^{-1}). Excitation wavelength is 348 nm.

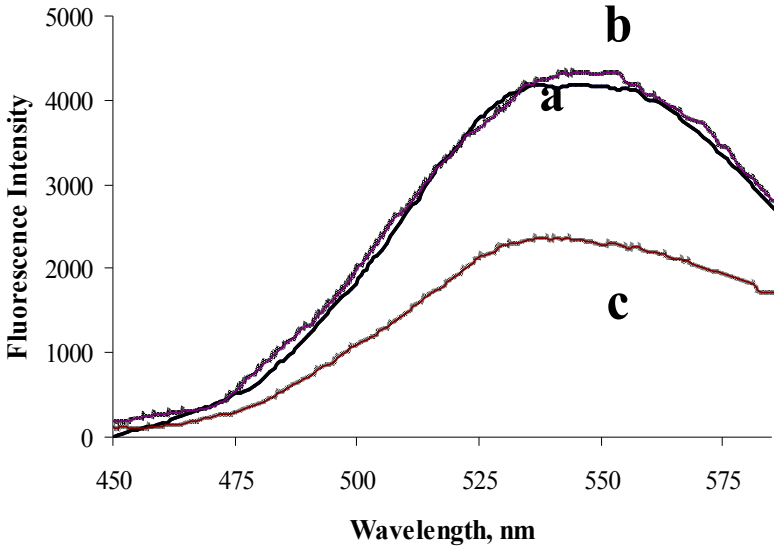

Initially, when the transition metal ions Cd^{2+}, Co^{2+}, Mn^{2+}, Ni^{2+} and Zn^{2+} (each is 1 equiv) were added to **P1**, there was no significant change in the fluorescence intensity. However, after 1 equiv of Cu^{2+} was added to the solution, the fluorescence intensity quenched to 55.1% of its initial intensity. This is a statistically similar value to what was observed for Cu^{2+} quenching of **P1** in the absence of other metal ions. It is not clear at this point how important the peptide link is in providing the proper Cu^{2+} binging geometry for dansyl and Trp, both of which appear to be involved in the complex.

The effect of six metal interferents commonly found in Cu^{2+} contaminated areas[37] on **P1**'s fluorescence signal in the presence of Cu^{2+} was determined. These metals caused an increase in **P1**'s fluorescence signal (i.e. less quenching of **P1** as a result of Cu^{2+} displacement by non-quenching metals) and Table 2 lists the concentrations required to cause a 10% error in the fluorescence signal at two different Cu^{2+} concentrations. Zn^{2+} proved to have the greatest effect on **P1**'s fluorescence signal, but needs to be present at a 22 times excess to do so.

Table 2.1 Concentration (in mg L-1) of various cations and the concentrations that produce a 10% increase in the fluorescent signal for 0.3 and 0.6 mg L-1 Cu^{2+}.

Interfering ion	0.3 mg L^{-1} Cu^{2+}	0.6 mg L^{-1} Cu^{2+}
Ca^{2+}	23	27
Cd^{2+}	15	16
Na^{+}	28	32
Mg^{2+}	37	42
Ni^{2+}	15	16
Zn^{2+}	12	13

Curiously, when the amount of Cu^{2+} in the solution doubles, the interfering metal concentration needed to cause a 10% error in signal changed very little. Several binding models with varying number of binding sites and log K values were constructed in an attempt to simulate this observation. At this time, no explanation is available.

2.4 CONCLUSION

A new fluorescent peptidyl chemosensor consisting of the amino acids glycine and aspartic acid for the detection of Cu^{2+} was designed. The amino acid sequence used was not based on any metal binding proteins, which suggests the potential utility of short peptides in designing selective detectors where a biological starting point may not be available. The sensor had a detection limit of 32 μg L^{-1} for Cu^{2+} and exhibited a statistically similar response to Cu^{2+} among other possible interfering metals in a pH 7.0 buffer. Although the sensor was designed to utilize the signal enhancement capabilities of FRET, which was observed; in this particular system fluorescence quenching of both fluorophores occurred and proved to be the most sensitive means of quantifying the results. The lack of a change in FRET efficiency indicates that the conformation of the peptide in this system is not changing as metal concentrations in the solution are altered.

2.5 REFERENCES

(1) Czarnik, A. W. *Fluorescent Chemosensors for Ion and Molecule Recognition*; American Chemical Society: Washington, DC, 1993.

(2) Fabbrizzi, L.; Licchelli, M.; Pallavicini, P.; Parodi, L.; Taglietti, A. In *Transition Metals in Supramolecular Chemistry*; Sauvage, J. P., Ed.; Wiley: Chichester, 1999, pp 93-134.

(3) Kramer, R. *Angew. Chem. Int. Ed. Engl.* **1998**, *37*, 772-773.

(4) Desvergne, J. P.; Czarnik, A. W. *Chemosensors of Ion and Molecular Recognition*; Kluwer Academic Publishers: Dordrecht, The Netherlands, 1997.

(5) de Silva, A. P.; Nimal Gunaratne, H. Q.; Gunnlaugsson, T.; Huxley, A. J. M.; McCoy, C. P.; Rademacher, J. T.; Rice, T. E. *Chem. Rev.* **1997**, *97*, 1515-1566.

(6) Haugland, R. P. *Handbook of Fluorescent Probes and Research Chemicals* 6 ed.; Molecular Probes, Inc.: Eugene, 1996.

(7) Pina, F.; Bernardo, A.; Garcia-Espana, E. *Eur. J. Inorg. Chem.* **2000**, *20*, 2143-2157.

(8) Corradini, R.; Dossema, A.; Galaverna, G.; Marchelli, R.; Panagia, A.; Sartor, G. *J. Org. Chem.* **1997**, *62*, 6283-6289.

(9) De Santis, G.; Fabbrizzi, L.; Licchelli, M.; Mangano, C.; Sacchi, D.; Sardone, N. *Inorg. Chim. Acta* **1997**, *257*, 69-76.

(10) Yoon, J.; Ohler, N. E.; Vance, D. H.; Aumiller, W. D.; Czarnik, A. W. *Tetrahedron Lett.* **1997**, *38*, 3845-3848.

(11) Mitchell, K. A.; Brown, R. G.; Yuan, D.; Chang, S.-C.; Utecht, R. E.; Lewis, D. E. *J. Photochem. Photobiol., A* **1998**, *115*, 157-161.

(12) Prodi, L.; Bolletta, F.; Montalti, M.; Zaccheroni, N. *Eur. J. Inorg. Chem.* **1999**, 455-460.

(13) Beltramello, M.; Gatos, M.; Mancin, F.; Tecilla, P.; Tonellato, U. *Tetrahedron Lett.* **2001**, *42*, 9143-9146.

(14) Klein, G.; Kaufmann, D.; Schurch, S.; Reymond, J.-L. *Chem. Commun.* **2001**, 561-562.

(15) Prodi, L.; Montalti, M.; Zaccheroni, N.; Dallavalle, F.; Folesani, G.; Lanfranchi, M.; Corradini, R.; Pagliari, S.; Marchelli, R. *Helv. Chim. Acta* **2001**, *84*, 690-706.

(16) Bourson, J.; Badaoui, F.; Valeur, B. *J. Fluoresc.* **1994**, *4*, 275-277.

(17) Akkaya, E. U.; Turkyilmaz, S. *Tetrahedron Lett.* **1997**, *38*, 4513-4516.

(18) Kawakami, J.; Itoh, H.; Mitsuhashi, H.; Ito, S. *Anal. Sci.* **1999**, *15*, 617-618.

(19) Merrifield, R. B. *J. Am. Chem. Soc.* **1963**, *85*, 2149-2154.

(20) Atherton, E.; Sheppard, R. C. In *Solid Phase Peptide Synthesis: A Practical Approach*; IRL Press: Oxford, 1989, pp 131-148.

(21) Walkup, G. K.; Imperiali, B. *J. Am. Chem. Soc.* **1996**, *118*, 3053-3054.

(22) Zheng, Y.; Huo, Q.; Kele, P.; Andreopoulos, F. M.; Phan, S. M.; Leblanc, R. M. *Org. Lett.* **2001**, *3*, 3277-3280.

(23) Torrado, A.; Walkup, G. K.; Imperiali, B. *J. Am. Chem. Soc.* **1998**, *120*, 609-610.

(24) Zheng, Y.; Gattas-Asfura, K. M.; Konka, V.; Leblanc, R. M. *Chem. Commun.* **2002**, *20*, 2350-2351.

(25) Zheng, Y.; Cao, X.; Orbulescu, J.; Konka, V.; Andreopoulos, F. M.; Pham, S. M.; Leblanc, R. M. *Anal. Chem.* **2003**, *75*, 1706-1712.

(26) Pearce, D. A.; Walkup, G. K.; Imperiali, B. *Bioorg. Med. Chem. Lett.* **1998**, *8*, 1963-1968.

(27) Bhattacharya, S.; Thomas, M. *Tetrahedron Lett.* **2000**, *41*, 10313-10317.

(28) Singh, A.; Yao, L.; Still, W. C.; Sames, D. *Tetrahedron Lett.* **2000**, *41*, 9601-9605.

(29) Mayr, T.; Werner, T. *The Analyst* **2002**, *127*, 248-252.

(30) Jiang, P.; Guo, Z. *Coord. Chem. Rev.* **2004**, *248*, 205-229.

(31) Fabbrizzi, L.; Licchelli, M.; Pallavicini, P.; Perotti, A.; Taglietti, A.; Sacchi, D. *Chem. Eur. J.* **1996**, *2*, 75-82.

(32) Fabbrizzi, L.; Licchelli, M.; Pallavicini, P.; Perotti, A.; Sacchi, D. *Angew. Chem. Int. Ed. Engl.* **1994**, *33*, 1975-1977.

(33) Chae, M. Y.; Czarnik, A. W. *J. Am. Chem. Soc.* **1992**, *114*, 9704-9705.

(34) Forster, T. *Ann. Phys.* **1948**, *2*, 55-75.

(35) Van Der Meer, B. W.; Coker III, G.; Chen, S. Y. S.; VCH Publishers, Inc.: New York, 1994, pp 157.

(36) dos Remedios, C. G.; Moens, P. D. J. In *Resonance Energy Transfer*; Andrews, D. L., Demidov, A. A., Eds.; John Wiley and Sons: New York, 1999, pp 1-54.

(37) US EPA, www.epa.gov/ost/pc/ambientwqc/copper80.pdf, 1980

(38) DiDonato, M.; Sarkar, B. *Biochim. Biophys. Acta* **1997**, *1360*, 3-16.

(39) Sarkar, B. *J. Inorg. Biochem.* **2000**, *79*, 187-191.

(40) Deibel, M. A.; Ehmann, W. D.; Markesbery, W. R. *Journal of the Neurological Sciences* **1996**, *143*, 137-142.

(41) Gutierrez, E.; Miller, T. C.; Gonzalez-Redondo, J. R.; Holcombe, J. A. *Environ. Sci. Technol.* **1999**, *33*, 1664-1670.

(42) Mokhir, A.; Kiel, A.; Herten, D.-P.; Kraemer, R. *Inorg. Chem.* **2005**, *44*, 5661-5666.

(43) Dunn, B. M.; Pham, C.; Raney, L.; Abayasekara, D.; Gillespie, W.; Hsu, A. *Biochemistry* **1981**, *20*, 7206-7211.

(44) Gustiananda, M.; Liggins, J. R.; Cummins, P. L.; Gready, J. E. *Biophys. J.* **2004**, *86*, 2467-2483.

(45) Luk, C. K. *Biopolymers* **1971**, *10*, 1229-1241.

(46) Conners, K. A. In *Binding Constants: The Measurement of Molecular Complex Stability*; John Wiley & Sons: New York, 1987, pp 339-343.

(47) Berg, J. M.; Merkle, D. L. *J. Am. Chem. Soc.* **1989**, *111*, 3759-3761.

(48) Rainer, M. J. A.; Rode, B. M. *Inorg. Chim. Acta* **1984**, *92*, 1-7.

(49) Sigel, H.; Martin, R. B. *Chem. Rev.* **1982**, *82*, 385-426.

Chapter 3: A "Turn-On" FRET Peptide Sensor Based on the Mercury Binding Protein MerP

3.1 INTRODUCTION

Determination of low level concentrations of heavy metal ions has become significant due to the severe risks they pose for human health and the environment.[1] This has prompted research into the development of fluorescent chemosensors for their detection in environmental and biological samples.[2-4] These chemosensors are typically composed of two covalently linked structural subunits: a fluorophore (for signal transduction) and an ionophore (for selective recognition of the metal ion). When designing these sensors, intense effort is put into maximizing the selectivity of the metal chelating unit. Chelating units composed of organic molecules have been used, but synthesis is rigorous and binding is not always reversible.[3, 5-15] Peptide motifs prove to be a viable alternative since they exhibit metal selectivity, can be easily synthesized via fluorenylmethoxycarbonyl (Fmoc)-solid phase peptide synthesis (SPPS)[16, 17] and are usable in aqueous solutions.

In this study a peptide fragment based on the mercury binding protein MerP was used as the metal chelating unit. MerP is a member of the bacterial mercury detoxification system[18, 19] and is responsible for binding Hg^{2+} in the periplasm and transferring it to transport protein MerT. Like other metal binding proteins, MerP contains the Cys-X-X-Cys motif and coordination to the cysteines is the dominant metal binding mechanism.[20] While the full protein is 72 amino acids in length, studies have shown that the 18 residue fragment Thr-Leu-Ala-Val-Pro-Gly-Met-Thr-Cys-Ala-Ala-Cys-Pro-Ile-Thr-Val-Lys-Lys from the metal binding loop has structural and binding characteristics similar to the full protein.[21, 22]

Typically, metal binding is detected by the quenching of a single fluorophore, e.g., dansyl chloride [5, 9, 12, 23-27], lucifer yellow [28], anthracence.[6, 29-31] Although concentration dependent quenching mechanisms have proven successful, it is inherently less sensitive than methods that *produce* fluorescence as a result of binding.[32] Also, it is often difficult to distinguish analyte response from sensor degradation when quenching is relied upon for quantitation.

The current study utilizes fluorescence resonance energy transfer (FRET) as a mechanism of detecting metal binding, allowing fluorescence *enhancement* to be monitored. Conceptually, if the chelating unit folds around the metal as it binds, the fluorophores may be brought closer together, causing increased transfer of energy from the donor fluorophore to the acceptor fluorophore. This has been successfully demonstrated by Imperiali and coworkers for Ni^{2+}[33] and Berg and coworkers for Zn^{2+}.[34] In comparison to conventional fluorescence, FRET allows a larger wavelength separation between the excitation and emission wavelengths, thereby permitting the use of lower resolution wavelength isolation devices (e.g., filters) to measure emission without interference from the excitation source.

This chapter reports on the synthesis of a new peptidyl chemosensor with FRET capabilities based on the mercury binding protein MerP that can be operated in aqueous solution at pH 7.0. The 23 residue peptide (sequence: Dansyl-Gly-Gly-Thr-Leu-Ala-Val-Pro-Gly-Met-Thr-Cys-Ala-Ala-Cys-Pro-Ile-Thr-Val-Lys-Lys-Gly-Gly-Trp-$CONH_2$) contains amino acids from MerP's metal binding loop. The FRET pair (tryptophan as donor and dansyl as acceptor) was conveniently attached during SPPS and are separated from the metal chelating unit by two glycine residues. Although MerP (and its metal binding loop fragment) has some binding affinity for other metals, the structures of the metal bound forms are very different. While the protein forms a loop around the bound

mercury, this loop is distorted or even non-existent with other metals.[22] Because FRET is a distance-dependent interaction, the structural differences are exploited by this detection mechanism. Prior to this, there have been very few examples of Hg^{2+} chemosensors utilizing fluorescence enhancement due to mercury's propensity to quench fluorescence by enhanced spin-orbit coupling.[35] Of these chemosensors, most are only usable in organic[36-42] or mixed organic-aqueous solutions[43-50]. Only four could be operated in a pure aqueous solution.[51-54] Additionally, only one example of a FRET-based chemosensor for Hg^{2+} has been attempted, but a quenching mechanism dominated.[55]

3.2 EXPERIMENTAL

3.2.1 Chemicals

All chemicals were reagent grade unless noted, and deionized distilled water was used to prepare solutions. Peptide synthesis reagents N-Dansyl-N'-Fmoc-ethylenediamine-MPB-AM (Dansyl NovaTag®) resin (100-200 mesh; 0.38 mmol g^{-1}), Wang resin (100-200 mesh, 1.2 mmol g^{-1}), glycine (Fmoc-Gly-OH), threonine (Fmoc-Thr(t. butyl ester (OtBu))-OH), leucine (Fmoc-Leu-OH), alanine (Fmoc-Ala-OH), valine (Fmoc-Val-OH), proline (Fmoc-Pro-OH), cysteine (Fmoc-Cys(Trt)-OH), isoleucine (Fmoc-Ile-OH), lysine (Fmoc-Lys(Boc)-OH, tryptophan (Fmoc-Trp(Boc)-OH) and 2-(1H-benzotriazole-1-yl)-1,1,3,3-tetramethylaminium hexafluorophosphate (HBTU) were used as received from Novabiochem. All the amino acids were of L-configuration. Metal containing solutions were prepared by dilution from 1000 μg ml^{-1} stock solutions. A 0.05 mol L^{-1} (N-[hydroxyethyl] piperazine-N'-[2-ethanesulfonic acid]) (HEPES) (Aldrich) buffer was prepared and adjusted to pH 7.0 with ammonium hydroxide (Fisher). Other reagents used include trifluoroacetic acid (99%) (TFA) (Acros),

triisopropylsilane (99%) (TIPS) (Acros), ethyl ether (Fisher), (ethylenedinitrilo)-tetraacetic acid (EDTA) (EM Science), dithiothreitol (DTT) (Acros), N-methylmorpholine (NMM) (Fisher), N-methylpyrrolidone (NMP) (Fisher) and piperidine (99%) (Fisher).

3.2.2 Instrumentation

A Photon Technologies International Quanta Master Spectrofluorimeter (model QM-4/2005) was used for all fluorescence measurements.

3.2.3 Peptide Synthesis

A peptide consisting of the sequence Dansyl-Gly-Gly-Thr-Leu-Ala-Val-Pro-Gly-Met-Thr-Cys-Ala-Ala-Cys-Pro-Ile-Thr-Val-Lys-Lys-Gly-Gly-Trp-$CONH_2$ (**P1**) was synthesized on Dansyl NovaTag® resin and the same peptide without dansyl (**P2**) was synthesized on Wang resin by Fmoc-solid phase peptide synthesis using a Ranin Symphony Quartet automated peptide synthesizer. Cleavage protocols have been described earlier.[56] The peptide masses (2494.3 for **P1** and 2217.7 for **P2**) were confirmed using electrospray mass spectrometry and the purity of each sequence (63% for **P1** and 73% for **P2**) was determined by reverse phase-HPLC. For both **P1** and **P2**, no other single component was present in excess of 15%.

3.2.4 Fluorescence Studies

3.2.4.1 Single metal response studies

Fluorescence emission spectra were collected from 10 μmol L^{-1} solutions of **P1** and **P2** (pH 7.0, 50 mmol L^{-1} HEPES, 3 μmol L^{-1} DTT). Various DTT concentrations (1-10 μmol L^{-1}) were tested due to concerns of metal-DTT complexation, but no change in fluorescence response was observed. **P1** and **P2**'s response to various metal cations (Ag^+, Ca^{2+}, Cd^{2+}, Hg^{2+}, K^+, Mg^{2+}, Na^+, Ni^{2+} and Zn^{2+}) was determined by adding a range

of metal concentrations (1-60 μmol L^{-1}) to each peptide solution from 0.002 mol L^{-1} metal stock solutions. FRET studies (monitoring emission of Trp and dansyl) were conducted on **P1** and single fluorophore studies (monitoring emission of Trp) were conducted on **P2**. For tryptophan emission, intensities at 348 nm were used. When determining signal intensity for dansyl chloride emission, an average of intensities between 545-550 nm was used except for Hg^{2+}, Cd^{2+}, Zn^{2+} and Ag^{+}, where metal binding resulted in a blue shift of emission and 498-510 nm was used.

3.2.4.2 Multi-metal response studies

A 10 μmol L^{-1} **P1** solution (pH 7.0, 50 mmol L^{-1} HEPES, 3 μmol L^{-1} DTT) was prepared. A range of Cd^{2+}, Hg^{2+} and Zn^{2+} concentrations (0.5-30 μmol L^{-1}) was added to the **P1** solution from 0.002 mol L^{-1} metal stock solutions to determine **P1**'s response to different ratios of the metals.

3.2.4.3 FRET measurement

In order to determine the distance (r) between the fluorophores, Equation 1 [57] was used:

$$E = \frac{R_0^{\,6}}{R_0^{\,6} + r^6} \qquad (1)$$

where R_0 is the Forster distance and r is the acceptor-donor distance. For the measurement of the FRET efficiency (E), the emission of **P2**, which contains only the donor tryptophan (I_D), was compared to the emission of **P1**, which contains both the donor tryptophan and the acceptor dansyl (I_{DA}). FRET efficiency was calculated by:[57]

$$E = 1 - \frac{I_{DA}}{I_D} \qquad (2)$$

The Forster distance, R_0, for tryptophan /dansyl has been previously determined to be 21 Å [58] and their spectral overlap has been illustrated.[59, 60] The distance between the fluorophores is ~ 71 Å if **P1** is completely unfolded.

3.3 RESULTS AND DISCUSSION

3.3.1 Single Metal Fluorescence Response Studies

P1, the addition of Hg^{2+} resulted in a decrease in tryptophan (donor) emission intensity and an increase in dansyl emission intensity (Figure 3.1a), indicating an increase in FRET due to Hg^{2+} binding. This response was reversible after addition of excess EDTA. A ~ 2 fold increase (ratio of **P1** in the presence of Hg^{2+} to that in the absence of Hg^{2+}) in dansyl emission was observed as well as a 35 nm blue shift in its emission to 510 nm. The blue shift in dansyl chloride's emission is not unexpected as dansyl is an environmentally sensitive fluorophore.[61] As peptide folding by metal binding occurs, the fluorophore is shielded from the polar solvent, causing a blue shift in its emission wavelength. Calibration curves were constructed from the fluorescence spectra to illustrate the quantitative dependence of the fluorescence on Hg^{2+} concentration. The detection limit for Hg^{2+} was found to be 280 μg L^{-1}. Although this is higher than the EPA's drinking water maximum contaminant level (MCL) of 2 μg L^{-1} [62], it is lower than[41, 45, 50] or comparable to[63] the detection limits of several existing Hg^{2+} fluorescent chemosensors in the literature. Additionally, this detection limit was achieved without any optimization techniques, i.e. more intense light source, longer integration time, etc. With optimization, this sensor could very well detect the level required by the EPA.

Addition of Cd^{2+}, Zn^{2+} and Ag^{+} to **P1** also resulted in a metal binding induced FRET response (Figure 3.1b-d) and this response was reversible after addition of excess EDTA.

Figure 3.1 Relationship of the fluorescence of **P1** (50 mmol L^{-1} HEPES, pH 7.0) to the concentration of a) Hg^{2+}, b) Zn^{2+}, c) Cd^{2+} and d) Ag^{+}. $\lambda_{excitation}$ = 290 nm. All spectra were smoothed using Savitzky-Golay least squares smoothing routine with a 21 point window (Origin).

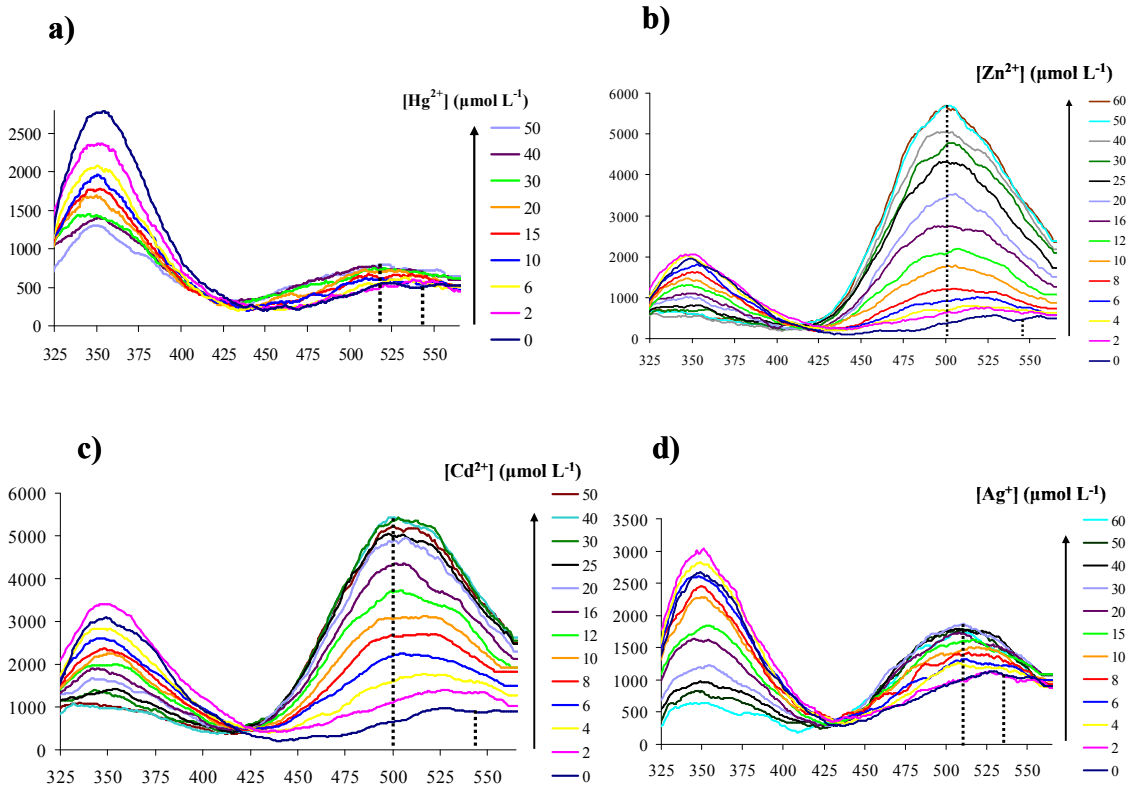

The largest FRET increase of any metal was observed for Zn^{2+}, which caused a ~ 11 fold increase in dansyl emission along with a 47 nm blue shift of the peak emission to 498 nm. The detection limit for Zn^{2+} was found to be 6 µg L^{-1}, well below the EPA's drinking water MCL of 5 mg L^{-1}.[64] Cd^{2+} addition resulted in the second largest FRET response. A ~ 6 fold increase in dansyl emission and a 45 nm blue shift to 500 nm was observed. The detection limit of Cd^{2+} was found to be 103 µg L^{-1}. While this is above the EPA drinking water MCL of 5 µg L^{-1} [64], it is only the third example of a fluorescence sensor that utilizes enhancement for the detection of Cd^{2+}. Additionally, the focus of the previous examples was not on metal detection, but rather using enhancement to monitor

protein conformational changes[65] and the synthesis of a dual receptor system for general sensing of anions and cations[66]. Similarly to Hg^{2+}, Ag^{+} addition resulted in a ~ 2 fold increase in dansyl emission intensity. A 39 nm blue shift to 506 nm was also observed. The detection for Ag^{+} was found to be 496 μg L^{-1}. A summary of these results is shown in Table 3.1.

Table 3.1 Spectroscopic data for **P1**

Metal	$\lambda_{emission}$ (nm)[a]	Enhancement Factor[b]	R (Å)[c]	Detection Limit (μg L^{-1})	LogK[d]
Hg^{2+}	510	2	19.4 ± 0.6	280	4.4
Zn^{2+}	498	11	16.6 ± 0.7	6	5.2
Cd^{2+}	500	6	17.9 ± 0.5	103	5.9
Ag^{+}	506	2	19.1 ± 0.6	496	5.4

[a] Dansyl emission peak after addition of metal. **P1's** dansyl chloride emission intensity in the absence of metal is 545 nm.
[b] Ratio of the intensity of **P1** in the presence of metal ion to that in the absence of metal ion.
[c] The distance between the fluorophores (R) before the addition of metal is 21.0 ± 0.6 Å.
[d] Metal binding constant was obtained via nonlinear fitting of the fluorescence titration data. Although **P1** contained more than one site for these metals, only one could be determined.

Although this binding motif was taken from the mercury binding protein MerP, it is not surprising that it binds other metals in addition to Hg^{2+}. The Cys-X-X-Cys motif present in MerP is also found in many other soft-metal binding proteins including cadmium transport protein CadA[67], the zinc finger domains[68] and superoxide dismutase, a yeast copper and zinc transporting protein.[69] Additionally, studies conducted by Opella and coworkers on MerP's metal binding loop fragment showed affinity for Zn^{2+} (log K = 3.5) Cd^{2+} (log K = 3.4) and Ag^{+} (log K = 3.4), which are not significantly different than that found for Hg^{2+} (log K = 4.0).[22] It is curious that this sensor does not have a larger

response to Hg^{2+}, but this may be due to the apparent quenching of the Trp donor by Hg^{2+}, which will be discussed further.

The fluorescence response of **P1** for a number of metal ions is presented in Table 3.2.

Table 3.2 Enhancement response of 10 μmol L^{-1} **P1** (50 mmol L^{-1} HEPES, pH 7.0) in the presence of various metal cations (30 μmol L^{-1}). $\lambda_{excitation}$ = 290 nm.

Metal Ion	Enhancement Factor[a]
Ag^{+}	2
Ca^{2+}	0
Cd^{2+}	6
Hg^{2+}	2
K^{+}	0
Na^{+}	0
Ni^{2+}	-1
Mg^{2+}	0
Zn^{2+}	11

[a]Ratio of the intensity of **P1** in the presence of metal ion to that in the absence of metal ion.

P1 had no response to other transition, alkali and alkaline earth metals tested, illustrating its potential use in a variety of matrices. In addition to selectivity, the robustness of the sensor was also evaluated by varying the pH. When the pH was lowered to 3.5, dansyl's emission intensity decreased noticeably by a factor of ~ 5, but was restored when the pH was returned to 7.0.

3.3.2 Evaluation of Conditional Stability Constants

Figure 3.3a-d shows that the maximum metal:peptide binding ratio is approximately three for Hg^{2+} and Zn^{2+} and two for Cd^{2+} and Ag^{+}.

Figure 3.3 Fluorescent binding curves of **P1** with a) Hg^{2+}, b) Zn^{2+}, c) Cd^{2+} and d) Ag^{+}. $\lambda_{excitation}$ = 290 nm. The metal to peptide binding ratio is 2:1 for Cd^{2+} and Ag^{+} and 3:1 for Hg^{2+} and Zn^{2+}.

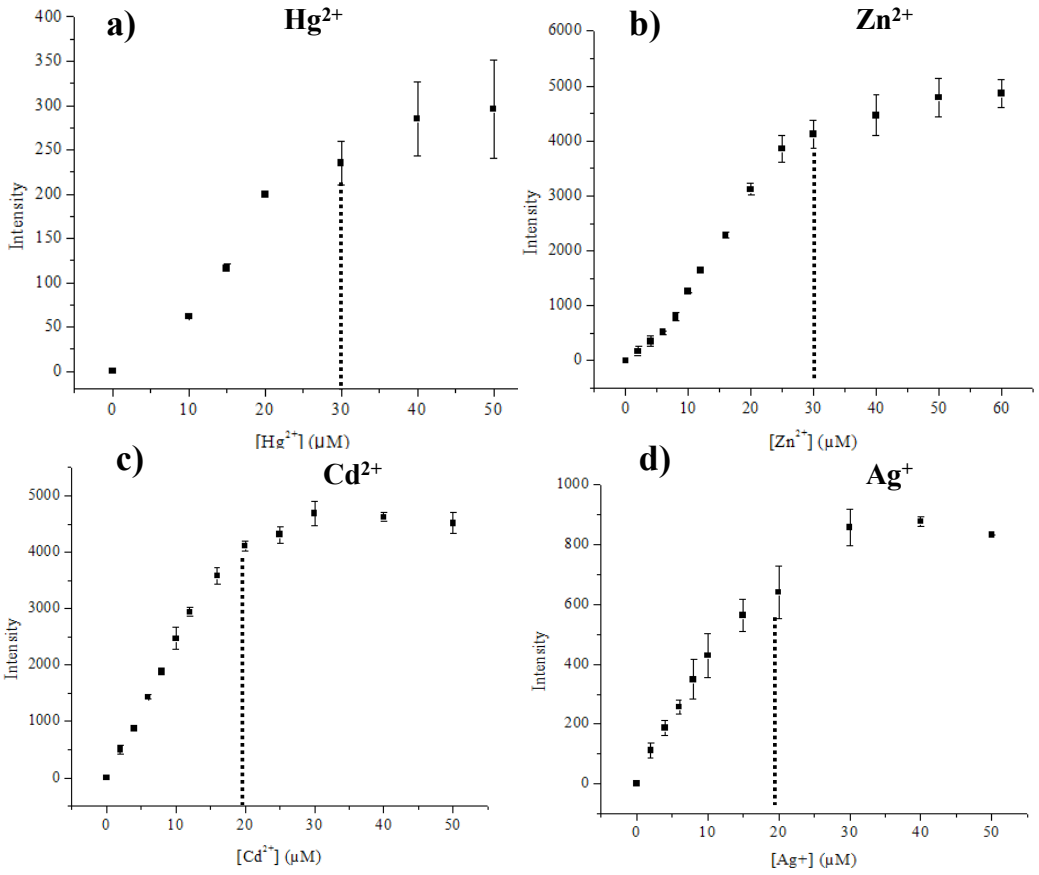

Opella and coworkers previously reported a metal:peptide binding ratio of one for all of these metals.[22] It is possible that the additional residues (four glycines and two fluorophores) in this study could allow for more binding sites or change the structure of the peptide such that other residues are available for binding.

While the FRET signal increases with metal concentration in all cases, it would not be surprising that the acceptor-to-donor distances would be different depending on whether one or two metals were bound. Hence the fluorescence sensitivity could very likely change whether **P1** is binding one, two or three cations. Thus, it is difficult to

confidently state that the proportionality constant relating the signal to the amount of metal bound has a constant value. For example, looking at the response for Zn^{2+} (Figure 3.2b), it is relatively obvious that binding the first metal (0-10 μM) produces a smaller FRET signal than when the second metal is bound (~10-20 μM). Deconvoluting the changing response is difficult but necessary if one were to attempt to develop an isotherm from which to extract logK values. In contrast to Zn^{2+}, Cd^{2+} binding (Figure 3.2c) appears to be relatively well behaved in spite of the obvious 2:1 metal:peptide ratio at saturation.

In an attempt to get some binding information, the data in Figure 3.2 were used to construct binding isotherms based on a one-site model. Using Graphpad Prism 4®, conditional stability constants were calculated for each metal. Although **P1** bound these metals in ratios greater than one, only one binding site logK was determined due, in part, to the shape of the binding curve. From a fit of the data, the estimated logK is 4.4 for Hg^{2+}, 5.2 for Zn^{2+}, 5.9 for Cd^{2+} and 5.4 for Ag^{+}. Similarly to previous reports[22], the values for Zn^{2+}, Cd^{2+} and Ag^{+} are not significantly different. While goodness of fit was poorest for Hg^{2+}, an R^2 value of 0.999 was obtained for Cd^{2+} binding.

When looking at Table 3.1, it is interesting to note that these logK values do not match the amount of FRET enhancement. For instance, Zn^{2+} binding resulted in the largest enhancement, but its logK is smaller than Cd^{2+} and Ag^{+}. This is not surprising since there is no assurance that stronger binding would necessarily bring the fluorophores in closer proximity. Additional structural studies to elucidate conformation of the peptide with and without a particular metal will be needed to make a more definitive statement.

3.3.3 Determination of FRET Efficiency

Using equation 1, the FRET efficiency without metal was determined to be 49 ± 4%, which corresponds to a distance of only 21.0 ± 0.6 Å between the fluorophores,

indicating that **P1** (71 Å when completely elongated) is coiled or folded even before the addition of metal.

Equation 1 was also used to calculate the FRET efficiency and distance between the fluorophores for **P1** after metal binding and these values are reported in Table 1. As expected, a large change in distance was seen for Zn^{2+} and Cd^{2+} which had large FRET enhancement. Hg^{2+} and Ag^{+}, which had the smallest enhancement, also had small distance changes. The small FRET efficiency increase for Hg^{2+} may be explained by its propensity to coordinate with amines.[70, 71] When monitoring **P2**, which contains just the Trp donor, its emission was quenched to 30.7% of its initial value at 30 μmol L^{-1} Hg^{2+}. It has been shown that Hg^{2+} complexes with Trp's indole ring, causing quenching.[72] If this occurs, the amount of energy Trp is able to transfer to dansyl chloride will yield an apparent reduction in the FRET signal. Additionally, Hg^{2+} binding to other amine containing sites may prevent the peptide from obtaining the loop conformation described by Opella and coworkers[22], which could also result in a lower FRET efficiency. It should be noted that no quenching of dansyl by Hg^{2+} was observed when **P1** was excited only at dansyl's absorption maximum.

3.3.4 Evaluation of mixed Hg^{2+}, Zn^{2+} and Cd^{2+} solutions

In order to determine the response of **P1** to mixed solutions of Hg^{2+}, Zn^{2+} and Cd^{2+}, various ratios of the metals were added to **P1** solutions. Initially, the enhancement and blue shift in dansyl's emission intensity for two metal solutions were monitored. Various ratios of Cd^{2+}: Zn^{2+} produced an enhancement factor and blue shift similar to what was observed for just Cd^{2+}, which is expected since Cd^{2+} had a larger logK value. Various ratios of Hg^{2+}: Zn^{2+} and Hg^{2+}: Cd^{2+} produced an enhancement factor and blue shift similar to what was observed for Hg^{2+}. Although Zn^{2+} and Cd^{2+} both individually had better FRET responses than Hg^{2+}, Hg^{2+} quenching of Trp may have the largest effect

on **P1**'s FRET response. This same result was also observed when all three metals were simultaneously monitored.

3.4 CONCLUSION

A new fluorescent peptidyl chemosensor based on the mercury binding protein MerP with FRET capabilities was designed and quantitatively characterized. To the best of our knowledge, this is the first example of a sensor with a FRET enhancement response for Hg^{2+}. Unlike many previous examples of Hg^{2+} sensors, the peptidyl chemosensor functioned in aqueous solution at pH 7.0. No FRET response to other transition, alkali and alkali earth metals tested was observed. Although it was expected that the sensor would exhibit the largest response for Hg^{2+}, FRET enhancements for Zn^{2+} and Cd^{2+} were greater. Hg^{2+} induced quenching of the Trp donor as well as Hg^{2+} binding to amine containing sites may be limiting the amount of FRET that can occur. A larger FRET enhancement for Hg^{2+} could potentially be obtained by using a different FRET pair. While two UV-excitable fluorophores were used in this study, other FRET pairs usable in the visible or infrared region could easily be implemented for *in vivo* applications.

3.5 REFERENCES

(1) Jarup, L. *Br. Med. Bull.* **2003**, *68*, 167-182.

(2) Fabbrizzi, L.; Poggi, A. *Chem. Soc. Rev.* **1995**, *24*, 197-202.

(3) Kramer, R. *Angew. Chem. Int. Ed. Engl.* **1998**, *37*, 772-773.

(4) Williams, R. E.; Peter-John, H.; Bruce, N. C.; Lowe, C. R. N. E. s. B., Ursula; Turner, Anthony P. F. In *Biosensors for Environmental Monitoring*; Bilitewski, U., Turner, A. P. F., Eds.; Harwood Academic Publishers: Amsterdam, Neth, 2000, pp 213-225.

(5) Corradini, R.; Dossema, A.; Galaverna, G.; Marchelli, R.; Panagia, A.; Sartor, G. *J. Org. Chem.* **1997**, *62*, 6283-6289.

(6) De Santis, G.; Fabbrizzi, L.; Licchelli, M.; Mangano, C.; Sacchi, D.; Sardone, N. *Inorg. Chim. Acta* **1997**, *257*, 69-76.

(7) Yoon, J.; Ohler, N. E.; Vance, D. H.; Aumiller, W. D.; Czarnik, A. W. *Tetrahedron Lett.* **1997**, *38*, 3845-3848.

(8) Mitchell, K. A.; Brown, R. G.; Yuan, D.; Chang, S.-C.; Utecht, R. E.; Lewis, D. E. *J. Photochem. Photobiol., A* **1998**, *115*, 157-161.

(9) Prodi, L.; Bolletta, F.; Montalti, M.; Zaccheroni, N. *Eur. J. Inorg. Chem.* **1999**, 455-460.

(10) Beltramello, M.; Gatos, M.; Mancin, F.; Tecilla, P.; Tonellato, U. *Tetrahedron Lett.* **2001**, *42*, 9143-9146.

(11) Klein, G.; Kaufmann, D.; Schurch, S.; Reymond, J.-L. *Chem. Commun.* **2001**, 561-562.

(12) Prodi, L.; Montalti, M.; Zaccheroni, N.; Dallavalle, F.; Folesani, G.; Lanfranchi, M.; Corradini, R.; Pagliari, S.; Marchelli, R. *Helv. Chim. Acta* **2001**, *84*, 690-706.

(13) Bourson, J.; Badaoui, F.; Valeur, B. *J. Fluoresc.* **1994**, *4*, 275-277.

(14) Akkaya, E. U.; Turkyilmaz, S. *Tetrahedron Lett.* **1997**, *38*, 4513-4516.

(15) Kawakami, J.; Itoh, H.; Mitsuhashi, H.; Ito, S. *Anal. Sci.* **1999**, *15*, 617-618.

(16) Merrifield, R. B. *J. Am. Chem. Soc.* **1963**, *85*, 2149-2154.

(17) Atherton, E.; Sheppard, R. C. In *Solid Phase Peptide Synthesis: A Practical Approach*; IRL Press: Oxford, 1989, pp 131-148.

(18) Brown, N. L. *Trends Biol. Sci.* **1985**, *10*, 400-403.

(19) Foster, T. J. *CRC Crit. Rev. Microbiol.* **1987**, *15*, 117-140.

(20) Opella, S. J.; DeSilva, T. M.; Veglia, G. *Curr. Opinion Chem. Biol.* **2002**, *6*, 217-223.

(21) Veglia, G.; Porcelli, F.; DeSilva, T.; Prantner, A.; Opella, S. J. *J. Am. Chem. Soc.* **2000**, *122*, 2389-2390.

(22) DeSilva, T. M.; Veglia, G.; Porcelli, F.; Prantner, A.; Opella, S. J. *Biopolymers* **2002**, *64*, 189-197.

(23) Torrado, A.; Walkup, G. K.; Imperiali, B. *J. Am. Chem. Soc.* **1998**, *120*, 609-610.

(24) Bhattacharya, S.; Thomas, M. *Tetrahedron Lett.* **2000**, *41*, 10313-10317.

(25) Singh, A.; Yao, L.; Still, W. C.; Sames, D. *Tetrahedron Lett.* **2000**, *41*, 9601-9605.

(26) Zheng, Y.; Gattas-Asfura, K. M.; Konka, V.; Leblanc, R. M. *Chem. Commun.* **2002**, *20*, 2350-2351.

(27) Zheng, Y.; Cao, X.; Orbulescu, J.; Konka, V.; Andreopoulos, F. M.; Pham, S. M.; Leblanc, R. M. *Anal. Chem.* **2003**, *75*, 1706-1712.

(28) Mayr, T.; Werner, T. *The Analyst* **2002**, *127*, 248-252.

(29) Jiang, P.; Guo, Z. *Coord. Chem. Rev.* **2004**, *248*, 205-229.

(30) Fabbrizzi, L.; Licchelli, M.; Pallavicini, P.; Perotti, A.; Taglietti, A.; Sacchi, D. *Chem. Eur. J.* **1996**, *2*, 75-82.

(31) Fabbrizzi, L.; Licchelli, M.; Pallavicini, P.; Perotti, A.; Sacchi, D. *Angew. Chem. Int. Ed. Engl.* **1994**, *33*, 1975-1977.

(32) Chae, M. Y.; Czarnik, A. W. *J. Am. Chem. Soc.* **1992**, *114*, 9704-9705.

(33) Pearce, D. A.; Walkup, G. K.; Imperiali, B. *Bioorg. Med. Chem. Lett.* **1998**, *8*, 1963-1968.

(34) Godwin, H. A.; Berg, J. M. *J. Am. Chem. Soc.* **1996**, *118*, 6514-6515.

(35) McClure, D. S. *J. Chem. Phys.* **1952**, *20*, 682-686.

(36) Hennrich, G.; Sonnenschein, H.; Resch-Genger, U. *J. Am. Chem. Soc.* **1999**, *121*, 5073-5074.

(37) Rurack, K.; Kollmannsberger, M.; Resch-Genger, U.; Daub, J. *J. Am. Chem. Soc.* **2000**, *122*, 968-969.

(38) Rurack, K.; Resch-Genger, U.; Bricks, J. L.; Spieles, M. *Chem. Commun.* **2000**, 2103-2104.

(39) Hennrich, G.; Walther, W.; Resch-Genger, U.; Sonnenschein, H. *Inorg. Chem.* **2001**, *40*, 641-644.

(40) Mello, J. V.; Finney, N. S. *J. Am. Chem. Soc.* **2005**, *127*, 10124-10125.

(41) Martinez, R.; Espinosa, A.; Tarraga, A.; Molina, P. *Org. Lett.* **2005**, *7*, 5869-5872.

(42) Zhang, H.; Han, L.; Zachariasse, K. A.; Jiang, Y. *Org. Lett.* **2005**, *7*, 4217-4220.

(43) Prodi, L.; Bargossi, C.; Montalti, M.; Zaccheroni, N.; Su, N.; Bradshaw, J. S.; Izatt, R. M.; Savage, P. B. *J. Am. Chem. Soc.* **2000**, *122*, 6769-6770.

(44) Guo, X.; Qian, X.; Jia, L. *J. Am. Chem. Soc.* **2004**, *126*, 2272-2273.

(45) Caballero, A.; Martinez, R.; Lloveras, V.; Ratera, I.; Vidal-Gancedo, J.; Wurst, K.; Tarraga, A.; Molina, P.; Veciana, J. *J. Am. Chem. Soc.* **2005**, *127*, 15666-15667.

(46) Zhang, G.; Zhang, D.; Yin, S.; Yang, X.; Shuai, Z.; Zhu, D. *Chem. Commun.* **2005**.

(47) Yang, Y.; Yook, K.; Tae, J. *J. Am. Chem. Soc.* **2005**, *127*, 16760-16761.

(48) Zhao, Y.; Lin, Z.; He, C.; Wu, H.; Duan, C. *Inorg. Chem.* **2006**, *45*, 10013-10015.

(49) Zheng, H.; Qian, Z.; Xu, L.; Yuan, F.; Lan, L.; Xu, J. *Org. Lett.* **2006**, *8*, 859-861.

(50) Kim, S. H.; Kim, J. S.; Park, S. M.; Chang, S. *Org. Lett.* **2006**, *8*, 371-374.

(51) Nolan, E. M.; Lippard, S. J. *J. Am. Chem. Soc.* **2003**, *125*, 14270-14271.

(52) Nolan, E. M.; Racine, M. E.; Lippard, S. J. *Inorg. Chem.* **2006**, *45*, 2742-2749.

(53) Ko, S.-K.; Yang, Y.-J.; Tae, J.; Shin, I. *J. Am. Chem. Soc.* **2006**, *128*, 14150-14155.

(54) Yoon, S.; Albers, A.; Wong, A. P.; Chang, C. J. *J. Am. Chem. Soc.* **2005**, *127*, 16030-16031.

(55) Ono, A.; Togashi, H. *Angew. Chem. Int. Ed.* **2004**, *43*, 4300-4302.

(56) White, B. R.; Holcombe, J. A. *Talanta* **2007**, *71,* 2015-2020.

(57) Forster, T. *Ann. Phys.* **1948**, *2*, 55-75.

(58) Van Der Meer, B. W.; Coker III, G.; Chen, S. Y. S.; VCH Publishers, Inc.: New York, 1994, pp 157.

(59) Dunn, B. M.; Pham, C.; Raney, L.; Abayasekara, D.; Gillespie, W.; Hsu, A. *Biochemistry* **1981**, *20*, 7206-7211.

(60) Gustiananda, M.; Liggins, J. R.; Cummins, P. L.; Gready, J. E. *Biophys. J.* **2004**, *86*, 2467-2483.

(61) Lakowicz, J. R. In *Principles of Fluorescence Spectroscopy*; Plenum Press: New York, 1983, pp 189-218.

(62) US EPA, Office of Water: Washington, DC, 2001.

(63) Descalzo, A. B.; Martinez-Manez, R.; Radeglia, R.; Rurack, K.; Soto, J. *J. Am. Chem. Soc.* **2003**, *125*.

(64) US EPA, http://www.epa.gov/safewater/mcl.html, 2007.

(65) Hong, S.-H.; Maret, W. *Proc. Natl. Acad. Sci.* **2003**, *100*, 2255-2260.

(66) Oton, F.; Tarraga, A.; Molina, P. *Org. Lett.* **2006**, *8*, 2107-2110.

(67) Nucifora, G.; Chu, L.; Misra, T. K.; Silver, S. *Proc. Natl. Acad. Sci. USA* **1989**, *86*, 3544-3548.

(68) Berg, J. M. *Acc. Chem. Res.* **1995**, *28*, 14-19.

(69) Culotta, V. P.; Klomp, L. W. J.; Strain, J.; Casareno, R. L. B.; Krems, B.; Gitlin, J. D. *J. Biol. Chem.* **1997**, *272*, 23469-23472.

(70) Lehn, J.-M.; Montavon, F. *Helv. Chim. Acta* **1978**, *61*, 67-82.

(71) Cha, N. R.; Kim, M. Y.; Kim, Y. H.; Choe, J.-I.; Chang, S.-K. *J. Chem. Soc., Perkin Trans. 2* **2002**, 1193-1196.

(72) Chen, R. F. *Arch. Biochem. Biophys.* **1971**, *142*, 552-564.

Chapter 4: A FRET Peptide Sensor Immobilized onto a Solid Support for Determination of Heavy Metals Using a Column-FIA System

4.1 INTRODUCTION

This chapter details the attempts to develop a column based flow injection analysis system using FRET detection. Traditionally, atomic spectrometric techniques such as flame atomic absorption and inductively coupled plasma emission or mass spectrometry are used for metal detection. Although these techniques are extremely sensitive with sub-nanomolar or picomolar detection limits, they are all usually laboratory based, difficult to use in the field and not adaptable to *in situ* analysis. The system describe herein was developed as a more portable and less costly alternative to traditional techniques.

An immobilized fluorophore labeled peptide based on the mercury binding protein MerP was used as the ion exchange material. The 14 residue peptide (sequence: LRB-Gly-Gly-Gly-Pro-Cys-Ala-Ala-Cys-Thr-Met-Gly-Gly-Gly-Cys-6-IAF) contains amino acids from MerP's metal binding loop. In the previous chapter, a similar 23 residue fragment showed a FRET enhancement response in the presence of Hg^{2+}, Cd^{2+}, Zn^{2+} or Ag^{+}.[1] The peptide fragment used in this study only contained amino acids that are directly involved in metal binding.[2]

This system might be used as a means of detecting breakthrough for a chelation column for water purification or in a prototype fiber optic based sensor. Thus, a high quantum efficiency acceptor and donor fluorophores with excitation and emission wavelength in the visible were desired for purposes of sensitivity and in the use of simple, visible excitation sources. Therefore, the FRET pair (6-iodoacetamidofluorescein (6-IAF) as donor and lissamine rhodamine B (LRB) as acceptor) was employed to replace dansyl chloride and tryptophan used in the previous chapter. These fluorophores

were attached to the peptide chain via simple labeling reactions and are separated from the metal chelating unit by two glycine residues.

Tentagel was used as solid support resin because it has a high loading capacity, swells minimally in various solvents and has good transport through its cross-linked interior. Additionally, Tentagel is a non-cleavable resin, allowing the peptide to be built directly within the solid support during SPPS. To the best of our knowledge, this would be the first example of a column-based flow injection analysis system that uses FRET for the detection of metal ions.

4.2 EXPERIMENTAL

4.2.1 Chemicals

All chemicals were reagent grade unless noted, and deionized distilled water was used to prepare solutions. All glassware was soaked overnight in 4 mol L^{-1} HNO_3 prior to use. Peptide synthesis reagents NovaSyn TG (Tentagel) resin (170 mesh; 0.25 mmol g^{-1}), NovaSyn TGR (cleavable Tentagel) resin (170 mesh; 0.25 mmol g^{-1}) , glycine (Fmoc-Gly-OH), threonine (Fmoc-Thr(t. butyl ester (OtBu))-OH), alanine (Fmoc-Ala-OH), proline (Fmoc-Pro-OH), cysteine (Fmoc-Cys(Trt)-OH), cysteine (Fmoc-Cys(Mmt)-OH), methionine (Fmoc-Met-OH) 2-(1H-benzotriazole-1-yl)-1,1,3,3-tetramethylaminium hexafluorophosphate (HBTU), and 1-hydroxybenzotriazole (98%) (HOBt) were used as received from Novabiochem. Cd^{2+}, Zn^{2+} and Hg^{2+} solutions were prepared by dilution from 1000 µg ml^{-1} stock solutions. A 0.05 mol L^{-1} (N-[hydroxyethyl] piperazine-N'-[2-ethanesulfonic acid]) (HEPES) (Aldrich) buffer was prepared and adjusted to pH 7.0 with ammonium hydroxide (Fisher). Other reagents used include lissamine rhodamine B sulfonyl chloride (LRB) (99%) (Acros), 6-iodoacetamidofluorescein (6-IAF) (Invitrogen), trifluoroacetic acid (99%) (TFA), triisopropylsilane (99%) (TIPS), ethyl

ether (Fisher), (ethylenedinitrilo)-tetraacetic acid (EDTA) (EM Science), dithiothreitol (DTT) (Acros), N-methylmorpholine (NMM) (Fisher), methanol, dichloromethane (DCM), dimethyl formamide (DMF), N-methylpyrrolidone (NMP) (Fisher) and piperidine (99%).

4.2.2 Instrumentation

A Photon Technologies International Quanta Master Spectrofluorimeter (model QM-4/2005) was used for all fluorescence measurements.

A 40 mm long quartz column was constructed from 7 mm diameter quartz tubing and the spectrofluorimeter's cuvette holder was modified so the in-house quartz column could be used in place of the conventional cuvette. The quartz column was held in place using a compression fit Teflon holder and an aluminum cap was constructed to fit over the top of column to hold it in place during analysis. A diagram of this system is shown in Figure 4.1a and a picture is shown in 4.1b.

Figure 4.1 a) Compression fit quartz column holder system. The column is placed into the bottom piece, which is threaded for FIA fittings. An O-ring is placed around the column and the top piece is screwed into the bottom piece to obtain the compression fit. Both the top and bottom piece are made of Teflon. The aluminum cap is placed over the column and into the cuvette holder to maintain the column's position during analysis. b) A picture of the system.

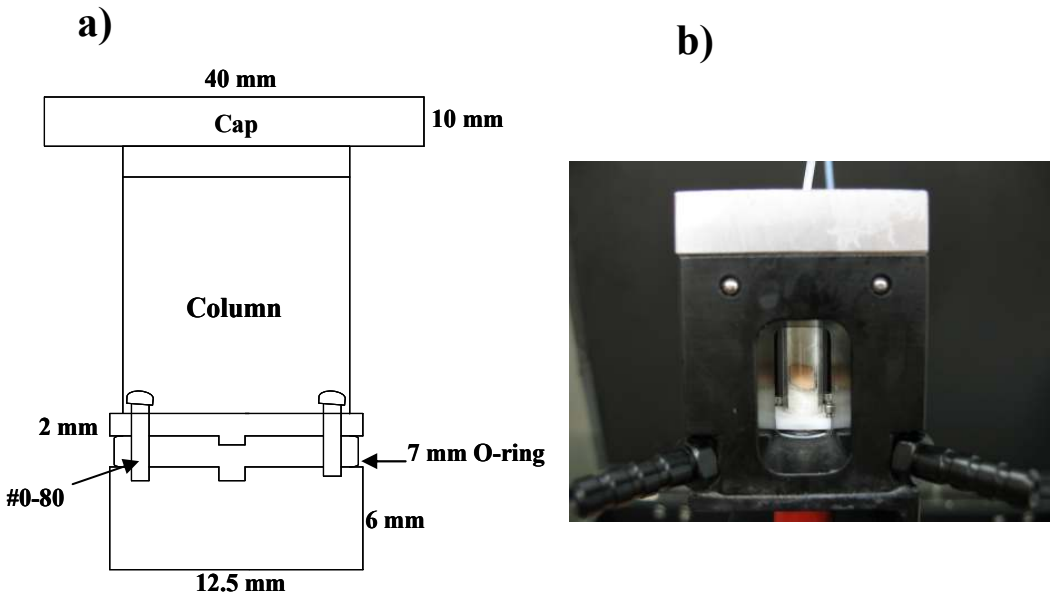

The solution reached the quartz column using an eight-roller peristaltic pump (Manostat Carter 4/8 cassette pump) and 0.76 mm i.d. PTFE tubing and connectors. Approximately 0.05 g of dry resin was packed into the column, filling approximately 20% of the column. The resin was held into place using (100 μm pore size) PTFE frits and the remaining dead space was filled with glass wool. The glass wool has no discernable metal binding metal binding capacity for the metals used in this study. The experimental set-up is shown in Figure 4.2

Figure 4.2 Flow-injection manifold for the determination of heavy metals

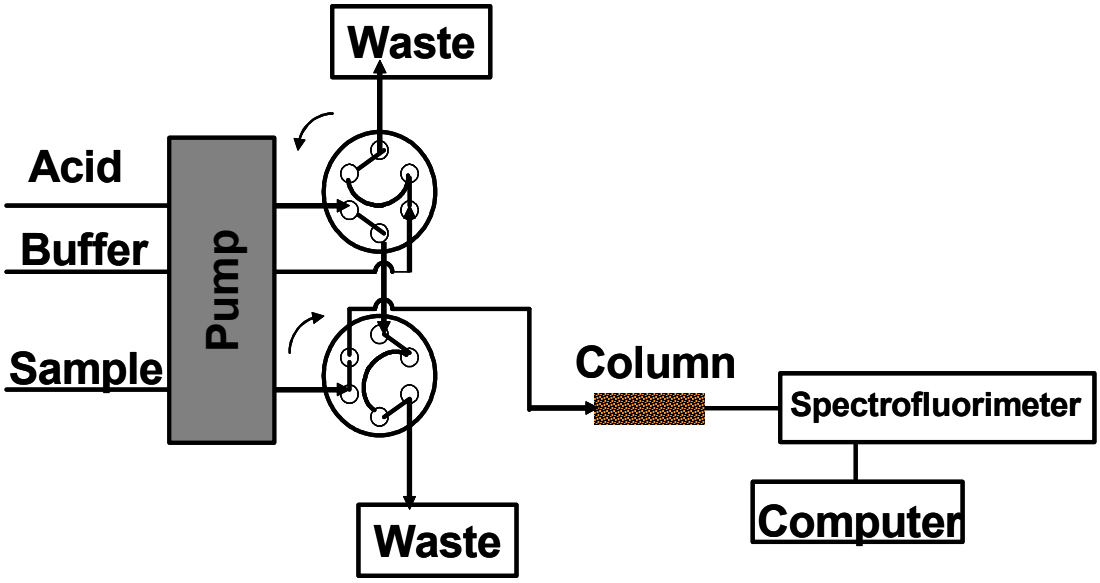

4.2.3 Peptide Synthesis

A peptide consisting of the sequence Gly-Gly-Gly-Pro-Cys-Ala-Ala-Cys-Thr-Met-Gly-Gly-Gly-Cys-$CONH_2$ (**P1**) was synthesized on Tentagel resin consisting of 94% Tentagel TG and 6% Tentagel TGR (which contains a cleavable Rink linker) by Fmoc-solid phase peptide synthesis using a Ranin Symphony Quartet automated peptide synthesizer. The peptides were double coupled (each amino acid coupling reaction was performed twice) in order to increase reaction efficiency and peptide integrity.

At the end of the synthesis, the resin was rinsed in methanol and DCM. Fluorophore labeling reactions were then conducted, which is described below. Resin deprotection and cleavage (of the 6% cleavable peptide) was conducted with TFA/ TIPS/ H_2O (95/ 2.5/ 2.5) for 2.5 hrs. The solution was then suction filtered, isolated using ether, and lyophilized. The 6% of cleavable peptide was then analyzed for purity using

electrospray mass spectrometry and reverse phase-HPLC. A peptide mass of 1140.3 for **P1** was confirmed using electrospray mass spectrometry and its purity was determined to be 71%. No other single component was present in excess of 15%.

4.2.4 Fluorophore Labeling

Fluorophores were attached to the peptide sequence prior to deprotection using standard protocols.[3] LRB, an amine reactive probe, was attached to the amine terminus of the peptide sequence. 6-IAF, a thiol reactive probe, was then attached to Cys residue 3 (Cys closest to the carboxylate terminus), which had been selectively deprotected from other Cys(Trt) groups using 1% TFA in DCM.[4] Various 6-IAF/LRB labeling ratios were tested by limiting the amount of fluorophore reagent used in the labeling reactions. After each set of reactions, the FRET signal of the immobilized peptides was determined using the quartz column.

4.2.5 Fluorescence Studies

The previously described analysis system was utilized in the metal binding studies after a 15 min warm-up of pumps, tubing and lamp. Before binding experiments were performed, the column was conditioned by passing 20 ml of 0.1 mol L^{-1} HNO_3 followed 40 mL of 0.02 mol L^{-1} DTT and then 4 mL of 0.05 mol L^{-1} HEPES buffer (pH 7.0). Because the resin contained Cys residues, all solutions were deaerated with N_2 gas for 20 min. DTT was passed through the column to ensure the reduction of disulfide groups. Metal solutions were then passed through the column and monitored using fluorescence. Specifically, 40μg L^{-1}, 200 μg L^{-1}, and 1 mg L^{-1} metal solutions (Cd^{2+}, Zn^{2+} or Hg^{2+}) in 0.05 mol L^{-1} HEPES buffer (pH 7.0) were passed through the column at 1 mL/min until breakthrough was reached (i.e. when the fluorescence signal became constant and indicated that the effluent concentration had reached the influent concentration). The

fluorescence intensity was monitored at LRB's emission maximum of 588 nm (excitation 492 nm) and recorded vs. time.

After breakthrough, HEPES buffer was passed through the column at 1 mL/min for ~ 1 min to remove metal-containing solution from the column dead volume and line tubing. A 0.1 mol/L HNO_3 solution was then passed through the column to strip the metal from the column. The solution was collected in an appropriate volumetric flask for subsequent "strip analysis" via ICP-MS.

4.2.6 ICP-MS Analysis of Acid Strips

Determinations of strip concentrations were carried out on an Optimass 8000 inductively coupled plasma time-of-flight mass spectrometer (GBC Scientific; Hampshire, IL).

4.3 RESULTS AND DISCUSSION

4.3.1 Fluorophore Labeling

Tentagel resin has one of the highest loading capacities of any commercially available resin and as a result, a lot of interactions between peptide chains likely occur.[5] If every peptide were labeled with a donor and acceptor fluorophore, maximized FRET would occur before the introduction of metal due to energy transfer between chains, i.e., both inter- and intra-chain donor-acceptor energy transfer. Because of this, a degree of fluorophore labeling that resulted in fluorescence signal, but a low probability of inter-chain interaction had to be determined. Due to the high quantum yield of 6-IAF (Q~1), it was felt that a low density coverage would still provide a measurable signal and a labeling of 0.01% was used. Beginning with 0.01%, increasing amounts of LRB were added until both a 6-IAF peak and a small LRB peak were observed in the emission spectrum, indicating that the fluorophores are close enough together for a small amount

of energy transfer to occur, but far enough away that peptide folding caused by metal binding result in a signal. An optimal LRB labeling was determined to be 0.05%. This translates into a peptide to fluorophore labeled peptide ratio of 10,000:1 for 6-IAF and 2,000:1 for LRB. It should be noted that because every peptide chain is not labeled with both fluorophores, FRET distances determined in this study cannot be used to say anything definitive about peptide conformation.

4.3.2 Fluorescence Studies

When running solutions for all three metals through the column for up to 2 h, no change in FRET was observed. This is shown in Figure 4.3 for a 1 mg L^{-1} solution of Cd^{2+}.

Figure 4.3 Emission spectra before (blue) and after (pink) the addition of Cd^{2+}. No change in FRET is observed.

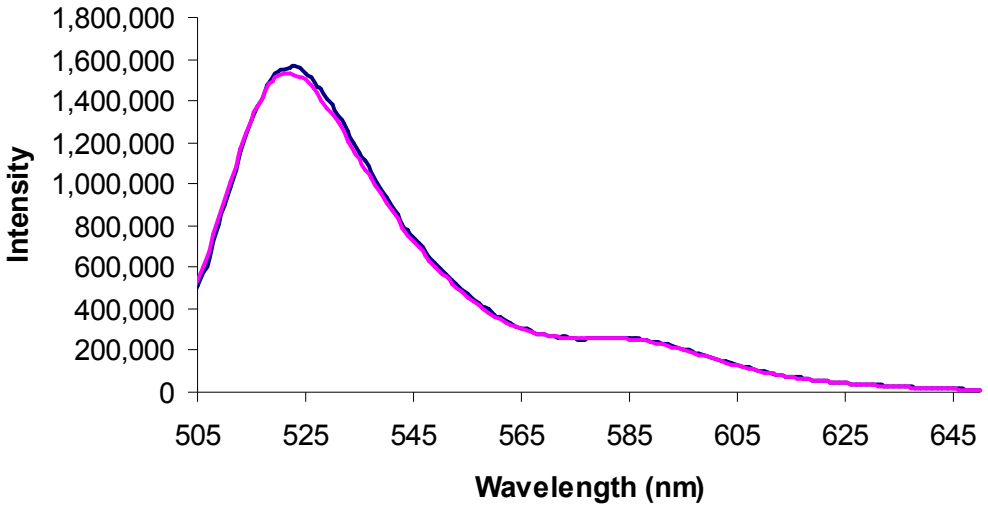

In order to confirm that absence of a signal was not a result of no metal chelation, strips from three replicates of 1 mg L^{-1} Cd^{2+} solution were analyzed by ICP-MS. From

the strips, a capacity of 3.6 ± 0.1 μmol Cd^{2+}/g resin was calculated, indicating that metal binding has taken place. The lack of a change in FRET could be explained by the high loading capacity of the Tentagel resin combined with the short length of the peptide chain. Studies by Stair and Holcombe[5] showed that the immobilization of short peptides (7 residues) onto Tentagel resin resulted in binding capacities over an order of magnitude better than results previously obtained with homopolymers (~ 50 residues) on lower loading control pore glass. It was postulated that this was due to the high capacity of the Tentagel resin along with the rigidity of the short peptides which allows more residues available for metal binding. If the peptide is rigid because of immobilization in this study, it may not be able to take on the metal bound conformations that were observed in previous solution studies.[1, 2, 6] Further characterization studies such as solid state NMR need to be conducted to determine the peptide conformation while immobilized and in solution. Additionally, the low percentage of donor and acceptor present might never allow for an increased FRET signal, even if the peptide is changing conformation upon metal binding. A lower loading support where every peptide can be labeled with both a donor and acceptor may be a better system.

4.4 CONCLUSION

In this study, an inexpensive column based flow injection analysis system was developed. The new system allows for the simple evaluation of fluorescence signals from ion exchange materials immobilized onto particulate supports. Unfortunately, the immobilized MerP peptide fragment used in this initial evaluation did not yield the sought after FRET response to added metal ions. This could be due to the high loading capacity of the Tentagel resin as well as the rigid character of the peptide chain when immobilized. A FRET response may be achieved by using a resin with a lower loading capacity. This would limit peptide chain interaction and allow every chain to be labeled

with both a donor and acceptor fluorophore. A planar support such as glass would be ideal starting point for these studies, as it serves as a good prototype to a fiber optic. Additionally, characterization studies such as solid state NMR could be carried out on immobilized peptides to determine if a change in conformation occurs upon the addition of metal. Structural studies conducted in solution are not always a good indicator, as the peptide loses an entire degree of freedom when immobilized.

4.5 REFERENCES

(1) White, B. R.; Liljestrand, H.; Holcombe, J. A. *submitted* 2007.

(2) DeSilva, T. M.; Veglia, G.; Porcelli, F.; Prantner, A.; Opella, S. J. *Biopolymers* 2002, *64*, 189-197.

(3) Haugland, R. P. *Handbook of Fluorescent Probes and Research Chemicals, 6th ed.*, 6 ed.; Molecular Probes, Inc.: Eugene, 1996.

(4) Galande, A. K.; Weissleder, R. *J. Comb. Chem.* 2005, *9*, 174-177.

(5) Stair, J. L.; Holcombe, J. A. *Microchem. J.* 2005, *81*, 69-80.

(6) Veglia, G.; Porcelli, F.; DeSilva, T.; Prantner, A.; Opella, S. J. *J. Am. Chem. Soc.* 2000, *122*, 2389-2390.

Chapter 5: Magnetic γ-Fe_2O_3 Nanoparticles Coated with Poly-L-Cysteine for Chelation of As(III), Cu(II), Cd(II), Ni(II), Pb(II) and Zn(II)

5.1 INTRODUCTION

Remediation of heavy metal ions from contaminated areas has become a significant area of research due to the severe risks they pose for human health and the environment.[1] The development of novel systems for remediation and preconcentration is required because unlike organic pollutants, metals can be a recirculating contaminant[2,3] and cannot be metabolized and decomposed. A recent advancement in metal remediation and extraction has been the exploration of peptides immobilized onto solid supports.[4] In biological systems, the tertiary structure of metal binding proteins is responsible for the formation of size selective cavities, but this tertiary structure is frequently lost once the proteins are removed from their pristine cellular environment.[5] Short chain synthetic peptides are more durable than natural proteins due to the *absence of a preformed structure*, allowing the peptide backbone to "wrap" around a metal as it binds. This allows for fast binding kinetics, which is an improvement over common metal chelators such as crown ethers.[6] Additionally, the metal can be released “on demand” by simply lowering the pH, which alters the peptide’s structure.[7]

These immobilized peptides have also demonstrated high metal binding capacities and frequently exhibit metal selectivity, which is due to the side group functionality of the amino acid(s).[4] In particular, the biohomopolymer poly-L-cysteine, PLCys, (Figure 1) has been shown to be an effective metal chelator in aqueous solution.[8] It preferentially and strongly (log $K_f > 12$) binds soft metal acids such as Cd^{2+} and Pb^{2+} through its soft donor ligand thiol side groups.[9] As a result, PLCys has successfully been used as an ion-exchange system for the remediation of soft acid metals while

immobilized on a variety of supports such as glassy carbon electrodes[10], control pore glass[8, 11, 12], membranes[13, 14] and graphite powder[15].

Figure 5.1 Structure of poly-L-cysteine.

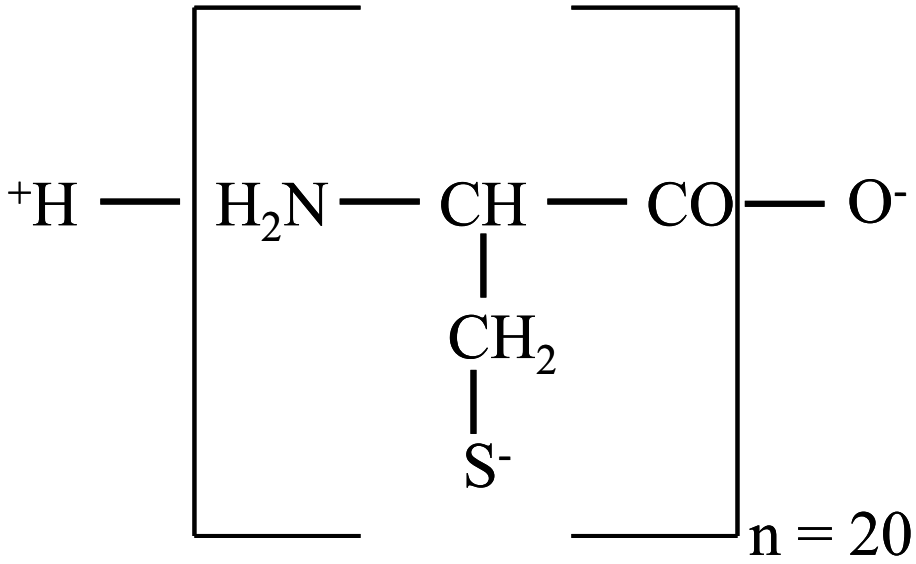

While many functionalized resin materials and support media with immobilized chelators are used in flow through, column applications; bulk remediation through the addition of an adsorbing media to a solution to be remediated is another alternative. The removal of metal chelating particles from an aqueous waste stream needs to be done effectively and efficiently. This research considers the incorporation of ferromagnetic, Fe_2O_3 nanoparticles as the support media. Most other support materials used for PLCys or other immobilized chelators have to be removed from solution by filtration or centrifugation. Studies have shown these methods are not as selective, efficient or rapid as using a magnetic field to collect particles.[16-18] Furthermore, common supports such as resin beads, porous glasses and carbon-based powders have diameters in the μm-mm regime. While this may allow them to settle or be filtered from bulk solutions more easily, transport to the particles' interior where a vast majority of the binding sites are

located can be slow. To maximize the fraction of sites on the surface of the support, smaller particles should be employed. For example, simply decreasing the size of the magnetic particle from micrometers to nanometers increases the amount of available metal binding surface area by 100 to 1000 times.[19]

Unfunctionalized iron oxide has been used as a metal adsorber[19-22], but control of metal selectivity is limited and the interactions between the iron oxide and metal are often irreversible.[22, 23] Additionally, other species such as phosphates also adsorb well and can out-compete metals for sorption sites due to their high concentrations in ground water.[24]

In this study, we have immobilized PLCys onto the surface of commercially available magnetic γ-Fe_2O_3 nanoparticles. Attaching PLCys to the surface of the nanoparticle may allow the metal chelating system to benefit from the selectivity of the peptide motif. Also, the PLCys surface coverage may protect the nanoparticles from acid attack and thus permit acid stripping of the loaded particles so that they can be reused after the target metals are reclamated. The binding affinity of the PLCys Fe_2O_3 nanoparticles (PLCys-Nano) to the metals Cu(II), Cd(II), Ni(II), Pb(II) and Zn(II) were tested due to their known affinities for PLCys from previous studies.[8, 11, 12] As(III) binding was also investigated because of its extreme toxicity[25, 26] mobility, and its propensity to bind sulfur groups in essential proteins.[27, 28]

5.2 EXPERIMENTAL

5.2.1 Chemicals

All chemicals were reagent grade unless noted, and deionized distilled water was used to prepare solutions. All glassware and plasticware were soaked overnight in 4 mol L^{-1} HNO3 prior to use. Peptide synthesis reagents Wang resin (100-200 mesh, 1.2 mmol g-1), cysteine (Fmoc-Cys(Trt)-OH) and 2-(1H-benzotriazole-1-yl)-1,1,3,3-

tetramethylaminium hexafluorophosphate (HBTU) were used as received from Novabiochem. Metal containing solutions were prepared by dilution from 1000 μg ml^{-1} stock solutions. A 0.05 mol L^{-1} (N-[hydroxyethyl] piperazine-N'-[2-ethanesulfonic acid]) (HEPES) (Aldrich) buffer was prepared and adjusted to pH 7.0 with ammonium hydroxide (Fisher). Other reagents used include toluene (99.8%) (Acros), (3-amino-propyl) triethoxysilane (98%), trifluoroacetic acid (99%) (TFA) (Acros), triisopropylsilane (99%) (TIPS) (Acros), ethyl ether (Fisher), dithiothreitol (DTT) (Acros), potassium hydroxide (KOH) (EM Science), L-cysteine hydrochloride monohydrate, (MP Biomedicals), N-methylmorpholine (NMM) (Fisher), N-methylpyrrolidone (NMP) (Fisher), gluteraldehyde (25%) (Sigma), concentrated HNO_3 (Sigma), concentrated HCl (Sigma) and piperidine (99%) (Fisher).

5.2.2 Instrumentation

The introduction of 3-amino-propyl triethoxysilane (3-APS) groups to the surface of the γ-Fe_2O_3 nanoparticles and the linking of PLCys were investigated using a Fourier transform infrared (FTIR) spectrometer (JEOL JIR-WINSPEC 50). A KBr pellet containing the sample was used for the FTIR spectroscopic measurements and the spectra were collected between 400 and 4200 cm^{-1}.

Determinations of metal concentrations were carried out on an Optimass 8000 inductively coupled plasma time-of-flight mass spectrometer (GBC Scientific; Hampshire, IL).

5.2.3 Peptide Synthesis

A peptide consisting of PLCys (n = 20) was synthesized on Wang resin by Fmoc-solid phase peptide synthesis using a Ranin Symphony Quartet automated peptide synthesizer. Cleavage protocols have been described earlier.[29] The purity of the

sequence was found to be 87% as determined by reverse phase-HPLC. No other single component was in excess of 5%.

5.2.4 Immobilization of PLCys onto γ-Fe_2O_3 nanoparticles

γ-Fe_2O_3 nanoparticles with diameters of 5-25 nm (surface area 50-245 m^2 g^{-1}) were purchased from Aldrich (Iron(III) oxide nanopowder). Modification of 0.1 g γ-Fe_2O_3 nanoparticles with 3-aminopropyltriethoxysilane (3-APS) was carried out according to a procedure by Iida and coworkers **(I)**.[30] After modification, the particles were rinsed with copious amounts of water and dried under N_2. PLCys attachment was then carried out using a gluteraldehyde linkage. Following a modified procedure by Masoom and Townshend[31], the 3-APS modified particles were allowed to react with 5% gluteraldehyde in a 0.01 M phosphate buffer (pH 8.0) under nitrogen for 90 min at room temperature **(II)**. The gluteraldehyde serves as a linker between the amine terminus on the 3-APS and the amine terminus of the PLCys. Once the gluteraldehyde was attached, the nanoparticles were rinsed with water. PLCys was dissolved in 0.01 M phosphate buffer (pH 8.5) and allowed to react with ~ 10 mg of gluteraldehyde modified γ-Fe_2O_3 nanoparticles for 2 h at room temperature under N_2 **(III)**. Equations 1-3 show the steps leading to the immobilization of PLCys on γ-Fe_2O_3 nanoparticles.

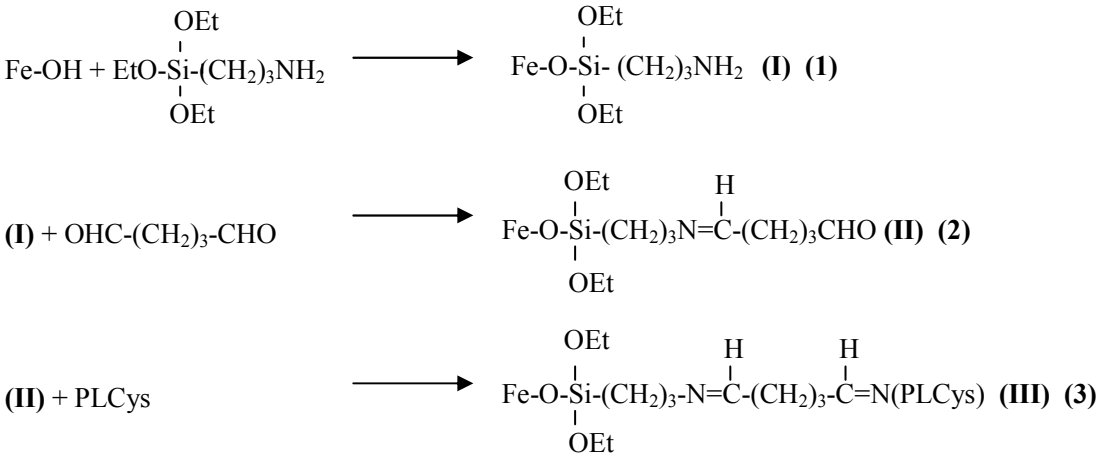

5.2.5 Metal binding characteristics of PLCys-Nano and unfunctionalized γ-Fe_2O_3

Prior to metal binding, the PLCys-Nano were rinsed in 0.02 mol L^{-1} DTT in 0.02 mol L^{-1} of HEPES buffer (pH 8.0) in order to reduce disulfide bonds that may have formed between cysteine groups. The DTT solution was deaerated with N_2 prior to use and the reaction was allowed to proceed under constant mixing for 1 h. The PLCys-Nano were then collected using a neodymium-boron (Nd-B) magnet (3 mm x 3 mm x 3 mm) that produced an inhomogeneous magnetic field (0.37 T on the surface of the magnet). For all experiments, 0.5 mg PLCys-Nano were added to 100 mL of a deaerated metal solution consisting of 1000 μg L^{-1} metal(s) in 0.02 mol L^{-1} HEPES buffer (pH 7.0). The metals examined were As^{3+}, Cd^{2+}, Cu^{2+}, Ni^{2+}, Pb^{2+} and Zn^{2+}. The PLCys-Nano were dispersed in solution using sonication and allowed to react in the metal solution. After collection using the Nd-B magnet, the final metal concentration of the reaction solution was determined using ICP-MS. All metal standards were prepared in 0.02 mol L^{-1} HEPES. All studies were repeated with the unfunctionalized γ-Fe_2O_3 nanoparticles as a comparison.

The efficiency of metal extraction was also evaluated. After exposure to metal solution, PLCys-Nano were rinsed with 5 mL 0.02 mol L^{-1} HEPES in order to remove

any non-specifically bound metal and the rinse was analyzed by ICP-MS. The particles were then dispersed in a 0.1 mol L^{-1} HNO_3 solution, allowed to react for 5 min, and the subsequent metal extract was analyzed by ICP-MS. Metal standards for the extraction experiments were prepared in both 0.02 mol L^{-1} HEPES and 0.1 mol L^{-1} HNO_3.

5.3 RESULTS AND DISCUSSION

5.3.1 Immobilization of PLCys onto γ-Fe_2O_3 nanoparticles

FTIR spectra of unfunctionalized γ-Fe_2O_3 nanoparticles, 3-APS modified γ-Fe_2O_3 nanoparticles and PLCys-Nano are shown in Figure 2. A broad absorption band in the range from 900 to 1100 cm^{-1} observed in the FTIR spectrum (b) of the 3-APS modified γ-Fe_2O_3 nanoparticles can be attributed to Si-O stretching.[32] The 3-APS modified γ-Fe_2O_3 nanoparticles also possess absorption bands in 1096.9 cm^{-1} and 1010.1 cm^{-1} due to Si-O-Si and Si-O-Fe bonds[33-35], bands at 2918.6 and 2960.8 cm^{-1} due to stretching vibration of C-H bond and 799.3 cm^{-1} due to the bending vibration of $–NH_2$ group[32]. All these confirm that 3-APS was chemically bound to the surface of the nanoparticles. The immobilization of PLCys on the surface of the γ-Fe_2O_3 nanoparticles is also suggested in spectrum (c) by the presence of an absorption band in 2575 cm^{-1} due to the S-H bond.[32]

Figure 5.2 FTIR spectra for: (a) as- received unfunctionalized γ-Fe_2O_3 nanoparticles; (b) 3-APS modified γ-Fe2O3 nanoparticles; (c) functionalized PLCys-Nano

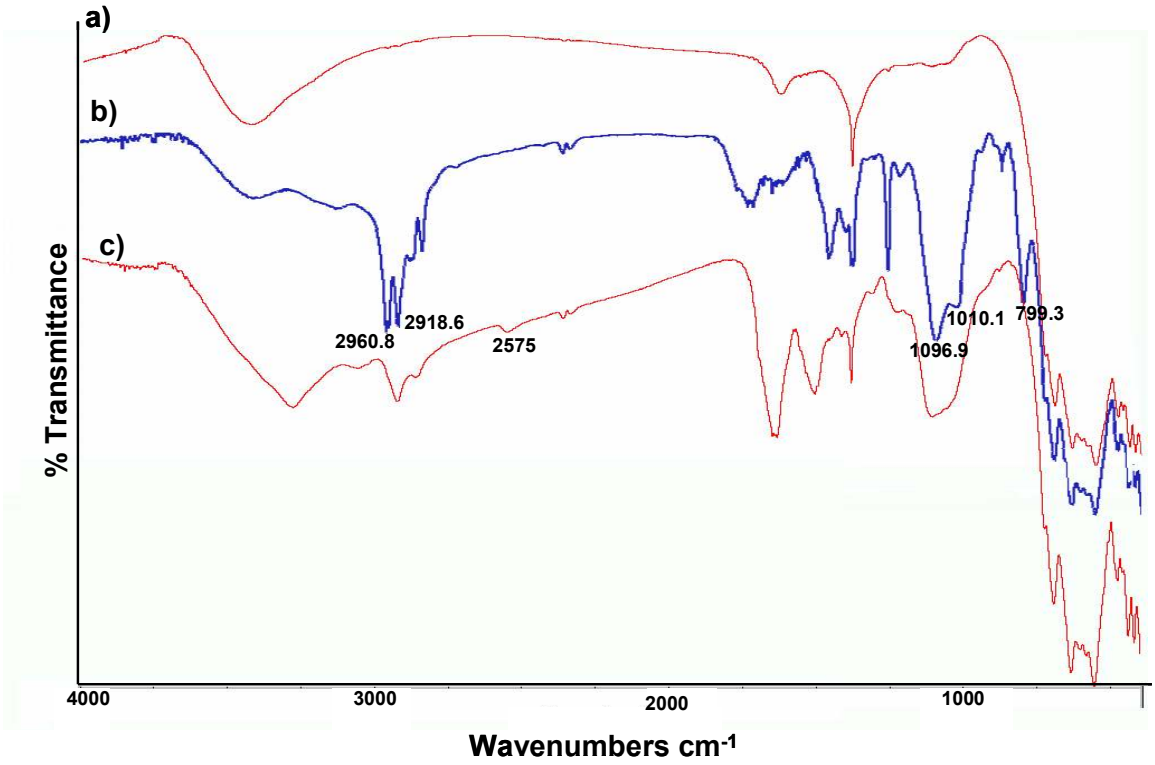

Both PLCys-Nano and the unfunctionalized γ-Fe_2O_3 nanoparticles were exposed to a solution of 4 mol L^{-1} HCl in order to examine whether the PLCys coverage was sufficient to protect the base ferric oxide particle. The solution containing the unfunctionalized γ-Fe_2O_3 nanoparticles turned bright yellow immediately, indicating that the nanoparticles had dissolved resulting in the formation of iron(III) chloride. The PLCys-Nano never dissolved, even after 48 h of exposure. Thus, the coverage of the immobilized of PLCys must be sufficient to prevent the solvent interaction and might even suggest near monolayer coverage. This experiment also suggests the possible use of the modified nanoparticles in harsher chemical environments than might have been possible with the uncoated particle. The use of acid rinse reclamation of metals from the

particles is feasible, giving the functionalized particles a longer lifetime and greater cost effectiveness if the media can be fully recovered.

5.3.2 Metal binding studies of PLCys-Nano

5.3.2.1 Determination of reaction time

The length of time PLCys-Nano was exposed to metal solution was varied from 2.5 min to 10 min in order to determine appropriate reaction times. The amounts of metal uptake for all exposure times were found to be statistically similar, indicating that binding occurs in $\leq$ 2.5 min. This result is not unexpected as earlier studies conducted by Stair and Holcombe suggested rapid metal-peptide binding kinetics.[37] Additionally, metal diffusion was expected to be fast as it is only limited by the amount of time it takes to reach the nanoparticles, which are present in relatively high density (ca. 5 g/cc[30]). This is an advantage over other common porous solid supports such as modified polymer resin beads, porous glass, etc. where metal solution has to diffuse relatively long distances into the media to gain full access to the binding sites. The improved particle (or bead) density facilitates mass transport also.

5.3.2.2 Binding of metals to PLCys-Nano

The PLCys-Nano and unfunctionalized γ-Fe_2O_3 nanoparticles binding/adsorption capacities were obtained for As(III), Cu(II), Cd(II), Ni(II), Pb(II) and Zn(II) and the results are shown in Table 5.1.

Table 5.1 Metal-Binding capacities on PLCys-Nano and unfunctionalized γ-Fe_2O_3 nanoparticles as determined by ICP-MS.

Metal Ion	Capacity(μmol metal/g Fe_2O_3) on PLCys-Nano	Capacity (μmol metal/g Fe_2O_3) on unfunctionalized γ-Fe_2O_3	Enhancement Factor[a]
As(III)	341 ± 58	164 ± 35	2
Cd(II)	385 ± 36	491 ± 15	0.8
Cu(II)	681 ± 19	522 ± 39	1.3
Ni(II)	559 ± 34	316 ± 32	1.8
Pb(II)	71 ± 12	90 ± 8	0.8
Zn(II)	368 ± 22	317 ± 15	1.2

50 mmol L^{-1} HEPES, pH 7.0, triplicate measurements. Uncertainties expressed as sample standard deviations, reflect measurement uncertainties only.
[a] Ratio of metal capacity of PLCys-Nano to metal capacity of unfunctionalized γ-Fe_2O_3.

PLCys-Nano displays large binding capacities for all of the metal tested, and in the case of As(III), Cu(II), Ni(II) and Zn(II), these capacities are larger than adsorption capacities obtained for the unfunctionalized γ-Fe_2O_3 nanoparticles. Additionally, the uptake of all the metals tested based on a per gram basis is over an order of magnitude greater than previous results with PLCys immobilized onto control pore glass and glassy carbon electrodes[8, 10-12], probably due to the larger surface area of the γ-Fe_2O_3 nanoparticles. Metal adsorption capacities over an order of magnitude greater than those observed in this study have been obtained for unfunctionalized iron oxide nanoparticles in other studies[23, 38-40], but metal exposure times were longer (up to 24 hrs) and different iron oxide forms and crystal structures were used. It is not known if the unfunctionalized γ-Fe_2O_3 nanoparticles have rapid metal absorption kinetics as the exposure times for both the functionalized and unfunctionalized particles were kept the same in this study in order to make a fair comparison.

Assuming monolayer coverage of PLCys on the surface of the γ-Fe_2O_3 nanoparticles, metal to PLCys ratios were calculated for each metal. Previously, monolayer coverage of the γ-Fe_2O_3 nanoparticles with 3-APS has been observed[30] as well as monolayer coverage of control pore glass with polyamino acids using the same procedure employed in this study[36], making this a fair assumption. The ratios were 2.8 ± 0.5 As(III)/chain, 3.2 ± 0.3 Cd(II)/chain, 5.7 ± 0.2 Cu(II)/chain, 4.7 ± 0.3 Ni(II)/chain, 0.6 ± 0.1 Pb(II)/chain and 3.1 ± 0.2 Zn(II)/chain. These ratios are very similar to those obtained in previous studies with PLCys immobilized onto glass and glassy carbon electrodes.[8, 10-12]

The functionalized and unfunctionalized nanoparticles also exhibit different metal affinities, which is to be expected due to the metal selectivity of PLCys. PLCys-Nano had a binding trend of Cu(II) > Ni(II) > Cd(II) = Zn(II) = As(III) > Pb(II). This trend, with the exception of Pb(II) and Ni(II), closely corresponds with typical soft acid metal binding preferences that are expected of a soft acid base such as a thiol.[9] The unfunctionalized γ-Fe_2O_3 nanoparticles, on the other hand, had an adsorption trend of Cu(II) > Cd(II) > Ni(II) = Zn(II) > As(III) > Pb(II). This trend is surprising since both As(III) and Pb(II) are known to adsorb well to iron oxide. As was previously mentioned, a longer metal exposure time may result in better adsorption for some metals and therefore change the current observed trend.

Previous studies conducted with PLCys have shown that metals can be quantitatively recovered by simply lowering the pH, which induces a tertiary structure change in the peptide. Metal recoveries obtained after sonicating PLCys-Nano in 5 mL of a 0.1 mol L^{-1} HNO_3 solution for 5 min are shown in Table 5.2.

Table 5.2 Metal recovery for PLCys-Nano

Metal Ion	Recovery (%)
As(III)	22 ± 8
Cd(II)	71 ± 9
Cu(II)	60 ± 20
Ni(II)	89 ± 15
Pb(II)	67 ± 4
Zn(II)	50 ± 10

Good metal recoveries were observed for Ni(II), while poorer recoveries were seen for the other metals (Cd(II), Cu(II), Pb(II) and Zn(II)). Very poor recoveries were observed for As(III). In a study by Howard et al., it was determined that PLCys contains both strong and weak sites for Cd(II), Cu(II) and Pb(II), while almost no strong sites were observed for Ni(II).[12] It is reasonable to believe that the Cd(II), Cu(II) and Pb(II) that were not recovered are bound to strong binding sites within the PLCys. As(III) has been shown to bind strongly (log K > 16) and irreversibly to cysteine containing proteins[41, 42], which may explain why very little recovery was observed. Additionally, Compton and coworkers also experienced irreversible As(III) binding to immobilized PLCys on glassy carbon micorspheres.[43]

5.4 CONCLUSIONS

We have successfully immobilized PLCys onto magnetic γ-Fe_2O_3 nanoparticles and demonstrated its use as an inexpensive and novel heavy metal chelator. The use of magnetic particles with a chelator "coating" is attractive since such a system can potentially provide fast, efficient and selective recovery of the metal chelating system following their use in bulk extractions from solutions. Furthermore, the PLCys-Nano exhibited metal binding capacities over an order of magnitude larger than traditional supports perhaps due to the high density of particles in solution and the larger number of

metal binding sites on the *surface* of the support. PLCys-Nano also exhibited rapid metal uptake (< 3 min) and had larger metal capacities than unfunctionalized γ-Fe_2O_3 nanoparticles for several metals. Using a simple acid solution, metal recoveries of > 50% were obtained for all of the metals except As(III).

PLCys, which has a general metal selectivity towards soft metals acids, was chosen to demonstrate the proof of concept. Greater metal selectivity can be achieved through the use of a combinatorial peptide library or by using peptide fragments based on metal binding proteins.

5.5 REFERENCES

(1) Jarup, L. *Br Med Bull.* **2003**, *68*, 167-182.

(2) Ireland, M. P. *Biological Monitoring of Heavy Metals*; Wiley: New York, 1991.

(3) Vernet, J. P. *Impact of Heavy Metals on the Environment*; Elsevier: New York, 1992.

(4) Malachowski, L.; Stair, J. L.; Holcombe, J. A. *Pure Appl. Chem.* **2004**, *76*, 777-787.

(5) Anderson, B. PhD, The University of Texas at Austin, Austin, TX, 1994.

(6) Chen, L. H.; Chung, C. S. *Inorg. Chem.* **1988**, *27*, 1880.

(7) Miller, T. C.; Kwak, E.-S.; Howard, M. E.; Vanden Bout, D. A.; Holcombe, J. A. *Anal. Chem.* **2001**, *73*, 4087-4095.

(8) Jurbergs, H. A.; Holcombe, J. A. *Anal. Chem.* **1997**, *69*, 1893-1898.

(9) Cotton, F. A.; Wilkinson, G. *Advanced Inorganic Chemistry: A Comprehensive Text*, 4th ed. ed.; John Wiley & Sons: New York, 1980.

(10) Johnson, A. M.; Holcombe, J. A. *Anal. Chem.* **2005**, *77*, 30-35.

(11) Howard, M.; Jurbergs, H. A.; Holcombe, J. A. *Anal. Chem.* **1998**, *70*, 1604-1609.

(12) Howard, M.; Jurbergs, H. A.; Holcombe, J. A. *J. Anal. At. Spectrom.* **1999**, *14*, 1209-1214.

(13) Ritchie, S. M. C.; Bhattacharyya, D. *J. Hazard. Mater.* **2002**, *92*, 21-32.

(14) Ritchie, S. M. C.; Kissick, K. E.; Bachas, L. G.; Sikdar, S. K.; Parikh, C.; Bhattacharyya, D. *Environ. Sci. Technol.* **2001**, *35*, 3252-3258.

(15) Wildgoose, G. G.; Leventis, H. C.; Davies, I. J.; Crossley, A.; Lawrence, N. S.; Jiang, L.; Jones, T. G. J.; Compton, R. G. *J. Mater. Chem.* **2005**, *15*, 2375-2382.

(16) Chang, S. C.; Anderson, T. I.; Bahrman, S. E.; Gruden, C. L.; Khijiniak, A. I.; Adriaens, P. *J. Ind. Microbiol. Biotechnol.* **2005**, *32*, 629-638.

(17) Hubbuch, J. J.; Matthiesen, D. B.; Hobley, T. J.; Thomas, O. R. T. *Bioseparation* **2001**, *10*, 99-112.

(18) Hirschbein, B. L.; Brown, D. W.; Whitesides, G. M. *Chemtech* **1982**, *12*, 172-179.

(19) Tamura, H.; Furrichi, R. *J. Colloid Interface Sci.* **1997**, *195*, 241-249.

(20) Ziemniak, S. E.; Anovitz, L. M.; Machesky, M. L.; Benezeth, P.; Palmer, D. A. In *Aqueous Systems at Elevated Temepratures and Pressures*; Palmer, D. A., Fernandez-Prini, R., Harvey, A. H., Eds.; Elsevier: London, 2004, pp 493-595.

(21) McKenzie, R. M. *Aust. J. Soil Res.* **1980**, *18*, 61-73.

(22) Clifford, D. A.; Ghurye, G. L. In *Environmental Chemistry of Arsenic*; Frankenberger, W. T., Jr., Ed.; Marcel Dekker, Inc.: New York, 2002, pp 217-245.

(23) Yavuz, C. T.; Mayo, J. T.; Yu, W. W.; Prakash, A.; Falkner, J. C.; Yean, S.; Cong, L.; Shipley, H. J.; Kan, A.; Tomson, M.; Natelson, D.; Colvin, V. L. *Science* **2006**, *314*, 964-967.

(24) Dixit, S.; Hering, J. G. *Environ. Sci. Technol.* **2003**, *37*, 4182-4189.

(25) Ferguson, J. F.; Gavis, J. *Wat. Res.* **1972**, *6*, 1259-1274.

(26) Jain, C. K.; Ali, I. *Wat. Res.* **2000**, *34*, 4304-4312.

(27) Li, S.; Chen, Y.; Rosen, B. P. *Mol. Microbiol.* **2001**, *41*, 687-696.

(28) Shi, W.; Dong, J.; Scott, R. A.; Ksenzenko, M. Y.; Rosen, B. P. *J. Biol. Chem.* **1996**, *271*, 9291-9297.

(29) White, B. R.; Holcombe, J. A. *Talanta* **2007**, *71*, 2015-2020.

(30) Iida, H.; Nakanishi, T.; Osaka, T. *Electrochim. Acta* **2005**, *51*, 855-859.

(31) Masoom, M.; Townshend, A. *Anal. Chim. Acta* **1985**, *166*, 111-118.

(32) Lide, D. R., Ed. *CRC Handbook of Chemistry and Physics*, 83 ed.; CRC Press, 2002.

(33) Mikhailik, O. M.; Fedorenko, O. M.; Mikhailova, S. S.; Povstugar, V. I.; Lyakhovich, A. M.; Kurbatova, G. T.; Shklovskaya, N. I.; Chuiko, A. A. *Colloids Surf.* **1991**, *52*, 331-338.

(34) Wapner, K.; Grundmeier, G. *Surf. Coat. Technol.* **2005**, *200*, 100-103.

(35) Xu, Z.; Liu, Q.; Finch, J. A. *Appl. Surf. Sci.* **1997**, *120*, 269-278.

(36) Malachowski, L.; Holcombe, J. A. *Anal. Chim. Acta* **2004**, *517*, 187-193.

(37) Stair, J. L.; Holcombe, J. A. *Microchem. J.* **2005**, *81*, 69-80.

(38) Kanel, S. R.; Manning, B.; Charlet, L.; Choi, H. *Environ. Sci. Technol.* **2005**, *39*, 1291-1298.

(39) Yean, S.; Cong, L.; Yavuz, C. T.; Mayo, J. T.; Yu, W. W.; Kan, A.; Colvin, V. L.; Tomson, M. *J. Mater. Res.* **2005**, *20*, 3255-3264.

(40) Gadde, R. R.; Laitinen, H. A. *Anal. Chem.* **1974**, *46*, 2022-2026.

(41) Silver, S.; Ji, G.; Broer, S.; Dey, S.; Dou, D.; Rosen, B. P. *Mol. Microbiol.* **q1993**, *8*, 637-642.

(42) Rey, N. A.; Howarth, O. W.; Pereira-Maria, E. C. *J. Inorg. Biochem.* **2004**, *98*, 1151-1159.

(43) Wildgoose, G. G.; Leventis, H. C.; Simm, A. O.; Jones, J. H.; Compton, R. G. *Chem Commun.* **2005**.

Chapter 6: Quantitative Determination of Single Bead Metal Content from a Peptide Combinatorial Library Using ETV-ICP-MS

6.1 INTRODUCTION

The use of combinatorial libraries has allowed the evaluation of numerous variations to a chemical system in a shortened amount of time. Combinatorial approaches have been utilized in many fields including catalysis,[1,2] chiral separations,[3] drug discovery,[4,5] and inorganic material synthesis.[6,7] In all approaches, one challenge is finding suitable ways to screen thousands of beads to obtain the desired information.

One recent area of growth is the use of peptide combinatorial libraries for identifying selective metal chelators.[8] In these libraries, one approach is to design or optimize the composition of a short, metal binding peptide based on information from a larger protein (such as a metallothionein[9]). One objective is to simplify the chelator without losing metal binding capacity or specificity, and in some instances perhaps even increasing selectivity. This is done using libraries where specific amino acid positions along the peptide chain can be varied to increase and tune metal binding capacity and specificity. There are many advantages to this approach,[10,11] including the design flexibility provided by 26 naturally occurring amino acid building blocks as well as the ease of peptide library synthesis. Beads with the desired metal binding properties can then be sequenced using methods such as Edman degradation and mass spectrometry.

Screening beads from a combinatorial library for metal content has previously been achieved through colorimetric or fluorescent dyes complexing with the metal of interest[12,13] or by observing color changes due to metal-peptide complexation itself[14,15]. Although non-destructive, these approaches are largely qualitative and are usually limited to the analysis of one metal at a time. Non-destructive techniques are mandatory for later determination of peptide sequences. For metal remediation and reclamation, determining

how well a chelator selects for or discriminates against particular species is often important and obtained through examining the binding of multiple metals simultaneously. Energy-dispersive X-ray spectroscopy (EDS) on a scanning electron microscope (SEM) has been previously used for multi-elemental analysis on single beads; however, beads must be initially flattened and then coated with a conductive material before analysis.[16] Recently, Havrilla and coworkers have used micro x-ray fluorescence (MXRF) for both bulk and selective metal screening of beads exposed to metal solutions.[17,18] This approach involves minimal sample preparation, is non-destructive, and also capable of simultaneous multi-elemental screening of single beads. The relative metal composition is determined from point scans and/or elemental imaging on the surface of the bead. Although this technique provides relative metal content at particular points within the bead, absolute metal content is more difficult to obtain.[17]

In the current study, electrothermal vaporization inductively coupled plasma mass spectrometry (ETV-ICP-MS) is used for the simultaneous quantitative determination of several metals extracted into solution from a single bead for purposes of characterizing binding properties of the peptide immobilized on the bead. The ETV exhibits excellent sensitivity (e.g., sub-picogram or part per trillion detection limits) and is ideally suited for use with very small sample volumes (≤10 μL). The mass analyzer used was a time-of-flight (TOF) system. The TOF mass analyzer allows for multi-elemental analysis with no loss in analytical duty cycle as the number of monitored masses increases.[19]

6.2 EXPERIMENTAL

6.2.1 Chemicals

All chemicals were reagent grade unless otherwise noted, and deionized distilled water was used to prepare solutions. All glassware and plasticware were soaked

overnight in 4 mol L^{-1} HNO_3 prior to use. The synthesis procedure for polyaspartic acid (PLAsp; n = 20) was similar to that previously described[20] and characterization using mass spectrometry showed the peptide was composed of 40% 20 residue form, 40% 19 residue form, and 20% 18 residue. The combinatorial library (CPC Scientific) was composed of the sequence Gly-X-X-Gly-X-X-Gly-X-X-Gly-X-X (X = cysteine, aspartic acid, or glutamic acid; Gly = glycine) and synthesized onto Tentagel Macrobeads (Rapp-Polymere MB 250 002) resin (60 mesh; 0.25 mmol g^{-1}). Microwell plates (96 wells; 300 μL) were purchased from Fisher Scientific (21-377-203), adhesive sheets used to cover the wells were purchased from Nunc (236366), and Tacky Dot slides (glass slides with arrays of adhesive spots used to easily array microbeads) were purchased from SPI supplies (2388). Stock solutions of 1000 μg mL^{-1} Cd^{2+} , Ni^{2+}, and Eu^{2+} (Acros) and Pb^{2+}, In^{2+}, Cu^{2+}, and Mn^{2+} (SCP Science) standards in 2 and 4% HNO_3 were used to prepare both the multi-metal binding solution and the multi-metal standards. For Mg^{2+}, the metal solutions were prepared from a standardized solution of the reagent grade nitrate salt (J.T. Baker) in 1% (v/v) HNO_3 and 1% (v/v) HCl. A 0.2 mol L^{-1} ammonium acetate (Aldrich) and 0.2 mol L^{-1} (N-[Hydroxyethyl]piperazine-N'-[2-ethanesulfonic acid]) (HEPES) (Acros) buffer were prepared and purified by passing the buffer through a 100-200 mesh Chelex 100 (Bio-Rad) ion exchange column. These metals were selected to demonstrate the multi-metal capability of this technique. Previous studies have shown that many of these metals should preferentially bind while others have no affinity for the amino acids selected.[21] Ar was used for the ICP and sweep gas (Praxair, Austin, TX). Other reagents used included nitric acid (70%, redistilled 99.999%) (Sigma); and DL-1,4-dithiothreitol (99%) (DTT) (Acros).

6.2.2 Metal Binding and Extraction

Prior to metal binding, the combinatorial library beads were exposed to 0.02 mol L^{-1} DTT in 0.02 mol L^{-1} of HEPES buffer (pH 8.0) in order to reduce disulfide bonds that may have formed between cysteine groups. The DTT solution was deaerated with N_2 prior to use and the reaction was allowed to proceed under constant mixing for 1 h. For both bead sets, approximately 50 beads were added to 20 mL of a deaerated multi-metal solution composed of 20 μg mL^{-1} Mg^{2+}, Mn^{2+}, Ni^{2+}, Cu^{2+}, Cd^{2+}, Eu^{2+}, and Pb^{2+} in 0.02 mol L^{-1} ammonium acetate buffer (pH 7.0). The reaction solution was allowed to react under constant mixing for 2 h. The beads were suction filtered (no rinse) and dried under N_2(g) overnight. The beads were then shaken onto a Tacky Dot slide for stereoscope measurements. Using microtweezers, individual beads were selected randomly from the Tacky Dot slide and placed into individual wells containing 100 ng μL^{-1} In in 250 μL of 0.1 mol L^{-1} of nitric acid. Indium was used as an internal standard in the ETV-ICP-MS to correct for solvent evaporation as well as autosampler variation. The acid solution from wells exposed only to the microtweezers which were placed in the sticky substance of the Tacky Dot slide was used for blank measurements. Once all the beads were placed into the wells, the wells were covered with a sealing adhesive sheet. The beads were soaked in acid for 2 h with 15 min on/off sonication cycling. After 2 h, 100 μL of the metal extract was transferred from the well into autosampler cups for elemental analysis. Multi-metal standards were prepared with 100 ng μL^{-1} In in 250 μL of 0.1 mol L^{-1} of nitric acid. For oxygen ashing experiments, the standards were rerun under the new ETV parameters (described under ETV-ICP-MS). After removing the nitric acid solution, water (150 μL) was added to each well containing a bead and each bead was pipetted up with ~100 μL of water and deposited into the ETV for elemental analysis.

6.2.3 Stereoscope Measurements

An Olympus (SZX12) Stereoscope was used to obtain images of the beads arrayed on a Tacky Dot slide. Slide sections were labeled for easy identification of the bead regions. Immediately after a bead image was saved, an image of a stage micrometer (1 mm long with and subdivided into 10 μm increments) was taken at the same magnification. These images were used to determine the diameter of each bead prior to acid extraction for adjusting the metal capacities with respect to the bead volume.

6.2.4 ETV-ICP-MS

Measurements were carried out on a Optimass 8000 inductively coupled plasma orthogonal acceleration time-of-flight mass spectrometer (GBC Scientific; Hampshire, IL). Operating parameters for the ICP-MS are described in Table 6.1.

Table 6.1 ICP operating parameters

Sample Gas Flow	1.15 L min^{-1}
Plasma Gas Flow	10.0 L min^{-1}
Auxiliary Gas Flow	0.90 L min^{-1}
RF Generator Forward Power	700 W
Torch Position (x)	8.0 mm
Torch Position (y)	0.3 mm
Torch Position (z)	-0.2 mm
Skimmer Potential	-1,000 V
Extraction Lens	-1,400 V
Pushout Plate	510 V
Pushout Grid	-540 V
Reflectron	580 V
Detector	3,200 V
Analytes (primary isotopes used)	^{24}Mg, ^{55}Mn, ^{58}Ni, ^{63}Cu, ^{114}Cd, ^{208}Pb, ^{153}Eu
Confirmation isotope (where applicable)	^{25}Mg, ^{60}Ni, ^{65}Cu, ^{112}Cd, ^{206}Pb, ^{151}Eu

Calibration was performed with the ETV prior to bead analysis using standard solutions containing the ions of interest. Calibrations were retaken before oxygen ashing experiments to account for changes in sensitivity due to the altered ETV parameters.

The ICP-MS was coupled to the ETV, a modified electrothermal atomizer and autosampler (Varian model GTA-95 ; Walnut Creek, CA) that has been previously described.[22]. Each sample was measured in triplicate using 10 µL injections. Pyrolytically coated graphite tubes were used as the vaporizer (Varian, part no. 6310001200). A valve system was utilized to separate the ETV from the ICP when material was not being vaporized (i.e., during drying and ashing cycles). During these steps, the instrument's sample gas flow was diverted directly into the torch. During analyte vaporization, the valves were toggled so Ar gas flow was directed through the graphite tube to sweep analyte into the mass spectrometer. During this cycle, the dosing hole of the graphite furnace was plugged by means of a pneumatically-activated graphite-tipped plunger. This also triggered data collection in the Optimass 8000. Analyte was carried to the ICP torch by 1 m of 6 mm i.d. Tygon® tubing. The ETV heating program is described in Table 6.2.

Table 6.2 ETV heating program

Step	**Temperature (ºC)**	**Ramp Time (s)**	**Hold Time (s)**	**Dosing Hole Closed**
Dry	100	5	10	No
Char	300	20	20	No
Pause	50	3	15	Yes
Vaporize	2,800	3	5	Yes *
Cool	50	14	0	Yes *
Clean	2,800	1.3	3	No
Cool	50	14	0	No

*Denotes mass spectrometry data collection.

For oxygen ashing studies, the drying step was increased to 60 s to accommodate the increased sample volume of 100 μL. During the oxygen ash step, air was used in place of Ar, passing through the furnace at a rate of approximately 1.2 mL/min and the ash temperature was set to 800 ºC (viz., dull red furnace appearance looking through dosing hole) for 20 s. After ashing, the furnace was cooled to room temperature with air still flowing through the furnace. After a 10 s Ar flush, the ETV was heated to a vaporization temperature of 2,800 ºC and the signal collected.

6.3 RESULTS AND DISCUSSION

6.3.1 Metal determination from beads with immobilized PLAsp

In order to determine the precision of the ETV-ICP-MS method, beads containing the same peptide sequence were analyzed. The bead set used for this study was immobilized PLAsp (n = 20) which was reacted with a multi-metal solution for 2 h as described earlier. Depending on the peptide sequence and resin material used for the analysis, careful determination of reaction times must be considered for equilibrium conditions to be met. Based on the diffusion of large dye molecules through Tentagel,[23,24] metal diffusion through Tentagel beads should occur in 15 min, and earlier studies suggested rapid metal-peptide binding kinetics[20]. After metal exposure and drying, a light image of the beads was taken using a stereoscope. All beads were medium blue in color after metal binding indicating that each bead possessed the PLAsp and some complexed metal(s). A set of 9 beads was taken from the slide after the diameters were measured. The beads ranged in size from 85 to 105 μm (± 2 μm).

The concentration of metal in the extract solution from each bead is shown in Figure 6.1 along with the bead volumes calculated from the bead diameters.

Figure 6.1 Concentration of metal extracted from single Tentagel-PLAsp beads and calculated bead volumes (right axis). The error bars represent ± 1 σ (n=3) based on error propagated using the analysis error of the sample, blank, and calibration solutions. (Two beads were present in Well #5.)

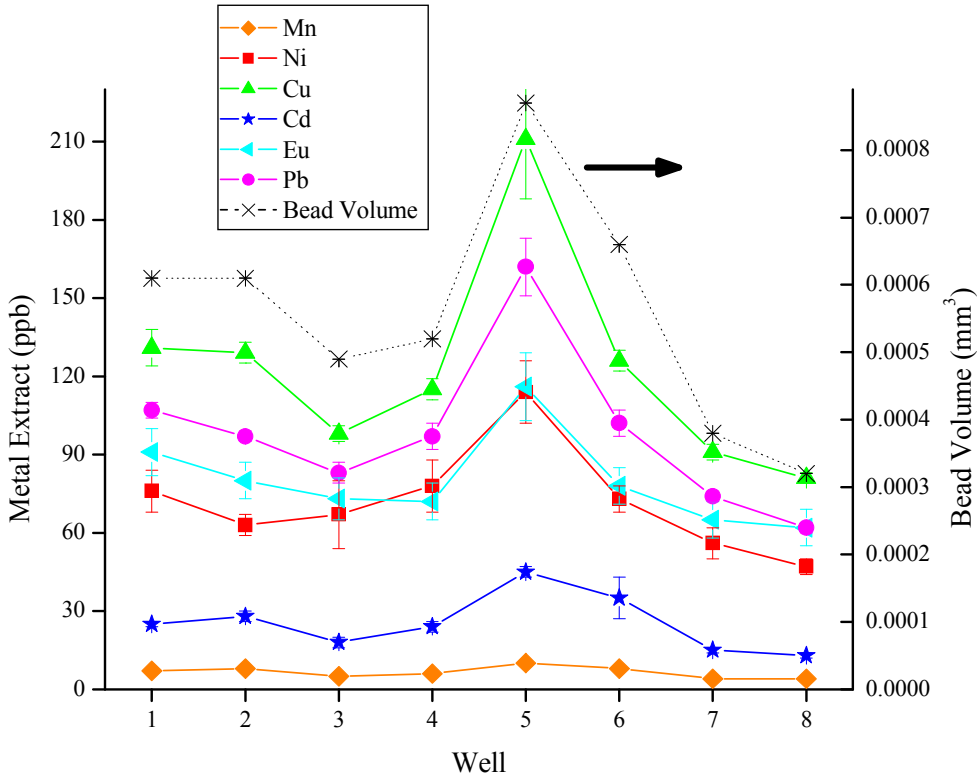

Well #5 mistakenly contained two beads (d = 90 and 98, ± 2 µm), and thus the overall concentration is close to double that of the values in the other seven wells. The figure shows bead extract concentrations as low as 4 ng mL^{-1} for Mn^{2+} and as high as 130 ng mL^{-1} for Cu^{2+}, excluding well #5; Mg values were omitted from this figure because they were not significantly detectable above the blank levels. Acid introduced into wells containing no bead were used as controls and showed metal signals near the detection limits, indicating that metal contamination from the microwell plate, well cover adhesive and tweezers was negligible. A small amount of Ni was observed, possibly from the

tweezers, but was only slightly above the limit of detection. The bead-to-bead variation in the average metal content was relatively consistent (also see Table 6.3), but there was an obvious binding selectivity for certain metals. As might be expected, much of the metal concentration variation in Figure 6.1 follows that of the bead size.

Table 6.3 Bead-to-bead variation in metal extract before and after adjusting for bead volume. Poly-L-aspartate (n=20) was immobilized on the beads.

Element	Mn^{2+}	Ni^{2+}	Cu^{2+}	Cd^{2+}	Pb^{2+}	Eu^{2+}
Metal Extracted (bead-to-bead RSD[a])	29%	17%	18%	34%	18%	13%
Metal Extracted/ Bead Volume (bead-to-bead RSD[a])	9%	14%	10%	13%	9%	16%

[a] %RSD values were calculated from the average extract concentrations from seven beads. The metal extract from Well #5 was not included due to the presence of two beads giving a larger overall concentration.

Due to the variations in bead diameter, the metal extract values from Figure 1 were divided by the volume of the respective beads to calculate metal capacities. The standard deviation in the bead diameters was 7% (n = 35), which resulted in a 21% RSD in the volumes. When the metal capacities for each bead are normalized by the individual bead volume, a reduction in the bead-to-bead capacity variation (9-16% RSD) is observed. (Figure 6.2 and Table 6.3)

Figure 6.2 Single bead metal extract concentrations of Tentagel-PLAsp normalized to the individual bead volumes. The error bars represent ± 1 σ (n = 3) based on error propagated using the analysis error of the sample, blank, and calibration solutions. (Two beads were present in Well #5.)

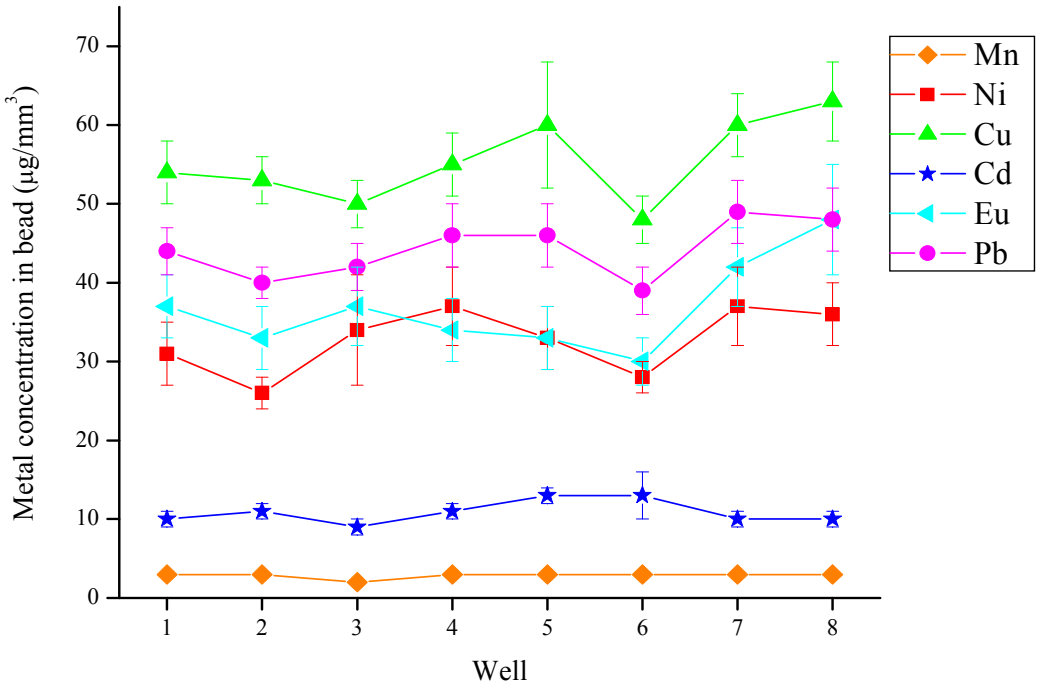

The more refractory nature of Ni and Eu may account for the somewhat poorer precision between beads for these particular metals even after volume adjustment. The remaining error between capacity values is likely the result of measurement uncertainties in the determination of individual bead capacities.

An attempt was made to identify the possible sources of uncertainty when determining the volume corrected metal capacity of a single bead. The sources of indeterminate errors (i.e., precision) were: analysis error, variation in bead-to-bead binding site density, and error in measuring the bead diameter. The "analysis error" included contributions from the bead extract measurement, blank measurement, and calibration curve slope error; and excluded particle diameter measurement and bead-to-

bead variations in active site density. An internal standard was used to minimize errors caused by evaporation and sample introduction into the ETV**.** After volume normalization of the bead set, the relative precision in the capacity (i.e., $\mu g/mm^3$) can be represented by Eq. 1.

$$RSD_{capacity} = \sqrt{RSD^2_{analysis} + RSD^2_{site\,density} + 9RSD^2_{micrometer}} \qquad (1)$$

It should be noted that propagating the measurement error of the radius (or diameter) to the bead volume yields a volume uncertainty of $3*RSD_{micrometer}$. Error propagation in Eq. 1 requires summing the squares of the relative error, hence $9\ RSD^2_{micrometer}$. Variations in the site density cannot be measured directly; however, Eq. 1 can be used to determine if the $RSD_{site\ density}$ is significant relative to the other RSDs since they are known. Using 2 μm as σ for the micrometer stage error for a 98 μm bead yields 6.1% for $3*RSD_{micrometer}$. Using pooled data for each element, $RSD_{analysis}$ was determined to be Mn (3%), Ni (11%), Cu (4%), Cd (12%), Pb (4%) and Eu (10%). Finally, the $RSD_{capacity}$ was arrived at from the experimental data for Mn (7%), Ni (13%), Cu (7%), Cd (14%), Pb (7%) and Eu (12%). Using these data, it is obvious that major uncertainties in site density are not required to account for the observed deviations in capacity measurements. Additionally, it can be deduced that analysis precision dominates the uncertainty in the Ni, Cd, and Eu capacities and that analysis *and* particle diameter imprecision contribute significantly to the uncertainty in the Mn, Cu, and Pb capacities for these beads. The F-test (95% CI) confirmed this conclusion, i.e., only small error contributions arise from errors in determining the bead diameters and negligible contribution comes from binding site density variations. Since no significant error was caused by variation in bead-to-bead differences in site density, all of the beads observed had nearly the same density of active sites. This observation is in agreement with a

previous study using confocal Raman microscopy,[24] but in disagreement with diffusion studies of Rhodamine 6G through Tentagel[23].

To determine the amount of metal extracted by the acid soaking procedure, a selection from the PLAsp beads whose acid extract had been previously analyzed were separately analyzed directly in the ETV. In this study, total consumption of the beads was used to ensure that metal was extracted from the beads with acid. Total bead consumption is not necessary if peptide sequencing is desired. After inserting the bead and a small amount of solution into the ETV, the resin material was removed by O_2 ashing in the ETV at about 900^{o}C, and the remaining metal was then vaporized and determined via ICP-MS. Total metal exposure was calculated by combining the metal amount extracted from the bead with the metal amount remaining on the bead to calculate the total metal on the bead after multi-metal exposure. The results for wells 1-4 and 6-7 showed approximately 97, 99, 100, 98, 100, and 100% of Mn, Ni, Cu, Cd, Eu and Pb were released upon acid exposure, which indicates quantitative release of the metals bound to this particular peptide.

6.3.2 Metal determination from the combinatorial library beads

A combinatorial peptide library was then used as an example for determination of selective metal binding peptides by this method. In order to minimize analysis error by increasing the signal magnitude, Tentagel Macrobeads were used for the combinatorial library. They were twice the diameter (i.e., 8 times the volume) of those used with the PLAsp but otherwise had the same nominal specification. Measurements of 35 beads showed an average diameter of 251 μm ± 5.4% (i.e., ± 16% in volume). After exposing the beads to a mixed metal solution, the library beads were noticeably different in color, ranging from dark red to light blue.

Figure 6.3 shows the resulting volume-normalized capacities determined for the small set of peptide library beads.

Figure 6.3 Single bead metal extract concentrations of the peptide combinatorial library normalized to the individual bead volumes. The error bars represent ± 1 σ (n = 3) based on error propagated using the analysis error of the sample, blank, and calibration solutions. Mg concentration in well B, C, E, and J were negligible. (<0.6 ug/mm^3)

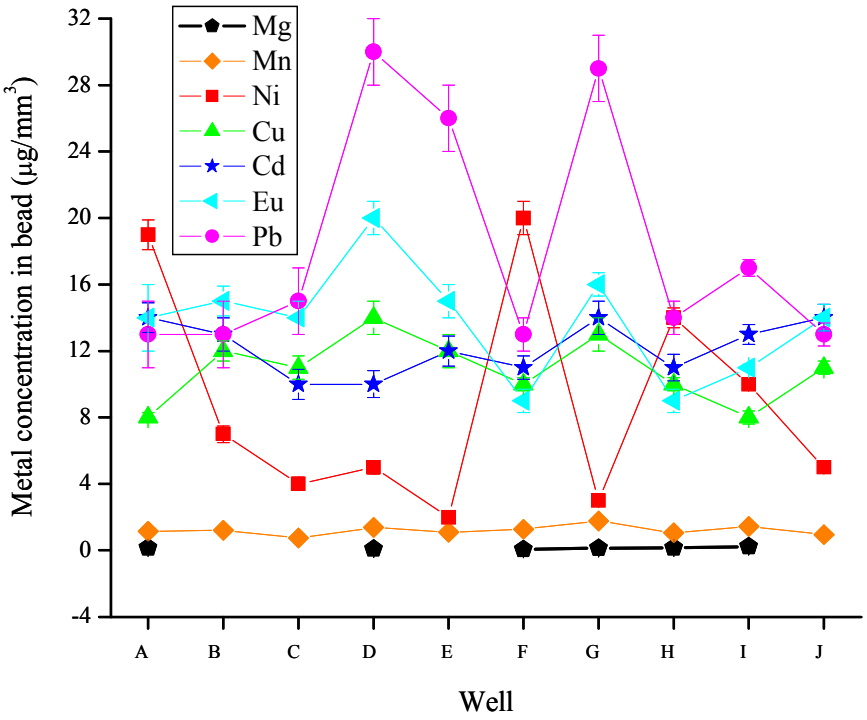

Mg values for wells B, C, E, and J were omitted from this figure because they were not significantly detectable above the blank levels. As expected, there are distinct differences in capacities for each element as well as in the relative capacities of one element to another for each bead. For example, beads from wells A and I had the highest capacity for Mg; beads from wells A and F had the highest capacities for Ni; beads from wells D and G had the highest capacities for Cu, Pb, and Eu; and beads from wells G and I had the highest capacities for Mn and Cd. Similarly, if one were in search of a bead that

provided good Pb binding capacity with maximum rejection of Ni, bead G from this small set of the library would be the optimal choice.

Since these beads were also measured with the stage micrometer and were manufactured in a similar manner (i.e., similar variation in bead composition), the remaining error after bead volume adjustment can be ascribed primarily to analysis error since the relative error from the particle diameter uncertainty is smaller for these larger beads. In addition, the precision in these calculated capacities was slightly improved as a result of the higher concentrations extracted from the larger beads as a result of improved measurement precision and less error in measuring the bead diameter: Mg (10%), Mn (3%), Ni (5%), Cu (5%), Cd (6%), Pb (9%) and Eu (7%). In cases where measuring individual beads diameters would be difficult and/or excessively time consuming, larger bead sizes provide a means to decrease the overall concentration uncertainty from bead-to-bead by decreasing the relative analysis error. Obviously, bead sets with better monodispersity could also be used to increase precision if the diameters of individual beads were not measured.

A sample of 5 library beads were also analyzed directly using ETV after they had been soaked and rinsed in HNO_3 to see if the acid extraction was complete. While the beads released Mn, Cd, Eu, and Pb with 99-100% efficiency and Mg with 95-100% efficiency; Cu^{2+} showed a more varied retention (75, 100, 90, and 91, and 97% metal extracted). Since each of these particular beads likely had a unique peptide sequence, it is not unexpected that strong binding sites on any given bead may not release the metal using this particular stripping solution. The beads were not sequenced in this study since the scope of the work was intended only to demonstrate the viability of using ETV-ICP-MS as a metal screening technique using a small bead set. While 95+% extraction is probably adequate for screening purposes, perhaps one might be concerned with <80%

efficiency depending on the level of screening being sought. Clearly, total consumption of the bead via oxygen ashing and ETV-ICP-MS is not the answer if the peptide sequence is to be determined. It was only used in this study to illustrate that most metal is released by acid extraction. If the peptide is intended to be used as a *reusable* chelating media for metal remediation, one could argue that sites that cannot be reclaimed do not effectively "exist" and thus should not be counted in the binding capacity of the material. In these cases, beads with inadequate release should be preferentially *selected against* if the target metal concentration in the extract was low, regardless of how much metal was actually bound to the bead.

6.4 CONCLUSIONS

With the exception of metals that are bound tightly to the peptide, acid stripping of the metals in a single bead into a small volume is demonstrated to be a viable quantitative analytical approach when using determination by ETV-ICP-MS. Precisions of better than ±10% were achieved for all metals when the larger polymer beads were employed. While acid was used in this study, other reclamation (stripping) solutions could be employed, such as a competitive chelator like EDTA. Obviously, the use of different extraction solutions may also yield additional information on the relative strength of binding sites and other characteristics of the peptide sequence. The high sensitivity and low volume requirements of the ETV allow for single beads to be easily analyzed, and the TOF allows for unlimited m/z monitoring analysis with no sensitivity loss for multi-elemental analysis since there is no loss in the mass analyzer duty cycle. Though the method presented here could be performed on other types of mass spectromemters (i.e. quadrupoles), the large number of isotopes observed might result in duty cycle related losses in sensitivity. For this study, the PLAsp beads and library beads had 21% and 17% variation in the volumes, respectively. This bead-to-bead variability

associated with the metal extracted can be corrected for by normalization to the bead volume with the remaining error primarily ascribed to analysis error and for the smaller beads to the particle measurement error. Such volume correction may not be necessary, depending on the monodispersity of the bead set and the acceptable precision limit set by the analyst for the screen. Interestingly, this study does show that bead-to-bead site density variability was not a major contributor to the uncertainty in the overall capacity values for the Tentagel bead sets used.

The 2-3 min analysis time needed for each sample per replicate presently makes this technique suited for quantitative analysis of *selected* beads after an initial bulk screening method. Use of this approach for rapid, quantitative screening may be viable with automation of bead manipulation and an increase in throughput for the ETV-ICP-MS, such has been suggested by work with a multiplexed ETV system[25,26] where >100 analyses/h were reported.

6.5 REFERENCES

(1) Breit, B. *Angew. Chem. Int. Ed.* **2005**, *44*, 6816-6825.

(2) Qi, S.; Yang, B.; Zhuo, Y. *Xiandai Huagong* **2003**, *23*, 58-60.

(3) Bluhm, L.; Huang, J.; Li, T. *Anal. Bioanal. Chem.* **2005**, *382*, 592-598.

(4) Kellam, B. *Smith and Williams' Introduction to the Principles of Drug Design and Action (4th Edition)* **2006**, 355-376.

(5) Weber, L. *QSAR Comb. Sci.* **2005**, *24*, 809-823.

(6) Koinuma, H.; Takeuchi, I. *Nat. Mater.* **2004**, *3*, 429-438.

(7) Woo, S. I.; Kim, K. W.; Cho, H. Y.; Oh, K. S.; Jeon, M. K.; Tarte, N. H.; Kim, T. S.; Mahmood, A. *QSAR Comb. Sci.* **2005**, *24*, 138-154.

(8) Francis, M. B.; Jamison, T. F.; Jacobsen, E. N. *Curr. Opin. Chem. Biol.* **1998**, *2*, 422-428.

(9) Stillman, M. J.; Shaw, C. F., III; Suzuki, K. T.; Editors *Metallothioneins: Synthesis, Structure and Properties of Metallothioneins, Phytochelatins and Metal-Thiolate Complexes*, 1992.

(10) Atherton, E.; Sheppard, R. C. *Solid Phase Peptide Synthesis: A Practical Approach*, 1989.

(11) Merrifield, R. B. *J. Am. Chem. Soc.* **1963**, *85*, 2149-2154.

(12) Francis, M. B.; Finney, N. S.; Jacobsen, E. N. *J. Am. Chem. Soc.* **1996**, *118*, 8983-8984.

(13) Franz, K. J.; Nitz, M.; Imperiali, B. *ChemBioChem* **2003**, *4*, 265-271.

(14) Shibata, N.; Baldwin, J. E.; Wood, M. E. *Bioorg. Med. Chem. Lett.* **1997**, *7*, 413-416.

(15) Pirrung, M. C.; Park, K.; Tumey, L. N. *J. Comb. Chem.* **2002**, *4*, 329-344.

(16) Neilly, J. P.; Hochlowski, J. E. *J. Appl. Spectrosc.* **1999**, *53*, 74-81.

(17) Miller, T. C.; Mann, G.; Havrilla, G. J.; Wells, C. A.; Warner, B. P.; Baker, R. T. *J. Comb. Chem.* **2003**, *5*, 245-252.

(18) Minogue, E. M.; Havrilla, G. J.; Taylor, T. P.; Burrell, A. K.; Warner, B. P. *Proceedings of SPIE-The International Society for Optical Engineering* **2005**, *5699*, 526-530.

(19) Vazquez Pelaez, M.; Costa-Fernandez, J. M.; Sanz-Medel, A. *J. Anal. At. Spectrom.* **2002**, *17*, 950-957.

(20) Stair, J. L.; Holcombe, J. A. *Microchem. J.* **2005**, *81*, 69-80.

(21) Malachowski, L.; Stair, J. L.; Holcombe, J. A. *Pure Appl. Chem.* **2004**, *76*, 777-787.

(22) Langer, D.; Holcombe, J. A. *Anal. Chem.* **1999**, *71*, 582-588.

(23) Taniguchi, M. M.; Farrer, R. A.; Fourkas, J. T. *J. Comb. Chem.* **2005**, *7*, 54-57.

(24) Kress, J.; Zanaletti, R.; Rose, A.; Frey, J. G.; Brocklesby, W. S.; Ladlow, M.; Bradley, M. *J. Comb. Chem.* **2003**, *5*, 28-32.

(25) Venable, J. D.; Detwiler, M.; Holcombe, J. A. *Spectrochim. Acta B* **2001**, *56B*, 1697-1706.

(26) Kreschollek, T.; Holcombe, J. A., *32nd meeting of the Federation of Analytical Chemistry & Spectroscopy Societies (FACSS)*, Quebec City, Canada, October 9-13 2005; 204.

Chapter 7: Conclusions and Future Work

7.1 CONCLUSIONS

This work has involved the development of fluorescence resonance energy transfer (FRET) based peptide chelators for the sensitive and selective detection of metal ions. FRET has been used for many years as a spectroscopic ruler for distance determinations and recently has been established as a metal binding detector in DNA, RNA and proteins.[1] A few examples of FRET based peptide metal ion sensors exist in the literature[2, 3], but only solution studies were conducted and selectivity was not optimized. In the current studies, other peptide motifs have been designed in an attempt to improve metal selectivity and target other metal ions. The distance-dependent interaction also allowed FRET to be used as a diagnostic to help understand the conformation and mechanism of the metal binding chelating unit. Both solution and immobilization studies were conducted.

The application of FRET provides a tool well suited to the goal of an optimal fluorescent metal ion sensor because it utilizes signal *enhancement* rather than quenching. Although quenching sensors have been successfully used, this mode of detection is inherently less sensitive than methods that produce fluorescence as a result of metal binding. In addition, analyte response can often not be distinguished from sensor molecule degradation. FRET also benefits from the nanomolar sensitivity of conventional fluorescence, but is able to generate a longer wavelength separation between the excitation and emission wavelengths thereby permitting lower resolution wavelength isolation devices (e.g., filters). By using solid phase peptide synthesis to create peptides, FRET fluorophore pairs can be easily incorporated into the chain without any additional labeling reactions.[4]

Conventionally, organic molecules have been used as the fluorescent sensor's metal chelating unit. Unfortunately, several problems are associated with their use such as rigorous synthesis, irreversible metal binding and the need for organic co-solvents. [5-16] Peptide motifs are a viable alternative as they exhibit metal selectivity, are easily synthesized using Fmoc-SPPS[17, 18], are environmentally innocuous and are useable in aqueous solution. The combination of FRET detection's enhancement capabilities and sensitivity with the selectivity of the peptide metal chelating unit results in an improvement over current fluorescent metal ion sensor technology.

Initially, a fluorescent peptidyl sensor for Cu^{2+} ions with FRET capabilities was developed. The amino acid sequence was designed in hopes of exploiting Cu^{2+}'s preference for square planar coordination and aspartic acid's affinity for hard acid metals such as Cu^{2+}.[19] Although the sensor was designed to utilize the signal enhancement capabilities of FRET, which was observed; in this particular system fluorescence quenching of both fluorophores occurred and proved to be the most sensitive means of quantifying Cu^{2+} binding. Additionally, no change in FRET efficiency was observed, indicating that the conformation of the peptide is not changing as metal concentrations are altered. This was not surprising as it was determined that the peptide was quite coiled prior to metal exposure. Nonetheless, the sensor provided a selective and sensitive response to Cu^{2+}.

Another FRET peptide metal ion sensor was designed with the help of a biological starting point, the mercury binding protein MerP. A sensitive FRET enhancement or "turn on" response was observed for Hg^{2+}, as well as Zn^{2+}, Cd^{2+} and Ag^{2+} in homogeneous pH 7.0 solution. While a selective response for only Hg^{2+} was the ultimate goal of this study, this sensor is still an improvement over current systems. Very few fluorescence sensors for Hg^{2+} utilize enhancement because this metal ion is prone to

quench fluorescence by enhanced spin-orbit coupling.[20] Additionally, this is the first example of a sensor with a FRET enhancement response for Hg^{2+}.

While the previous studies investigated these chelators in homogeneous aqueous solutions, the end goal was to devise a sensor based on an immobilized peptide chelator with FRET capabilities. To this end, immobilized, fluorophore labeled peptide studies were then conducted on Tentagel resin in order to determine the correct labeling efficiency to achieve FRET. Due to the success of the MerP peptide fragment in solution studies, a similar fragment was used. The FRET pair 6-iodoacetamidofluorescein (donor) and lissamine rhodamine B (acceptor) were employed because they are excitable in the visible region and exhibit high quantum efficiencies. Since tight packing of the peptide within the Tentagel could produce efficient intermolecular energy transfer even in the absence of a chelated metal ion, the molecular density or density of peptides with acceptor and donor fluorophores had to be limited. A labeling degree of 0.01% for 6-IAF and 0.05% for LRB was found to be optimal, since a donor and acceptor peak was observed in the emission spectrum, indicating a small amount of energy transfer is occurring before the addition of metal.

A flow injection fluorescence analysis system was then designed using the immobilized fluorophore labeled peptide as the ion exchange material. In order to use quartz tubing as the column, a cuvette adapter was fabricated so that the quartz column could sit in the path of the spectrofluorimeter's light source. The results of this study yielded the development of a relatively simple means of evaluating fluorescence signals from systems immobilized on particulate support materials. Unfortunately, the material used in the initial evaluation did not yield the sought after FRET response to added metal ions. This may be due to the behavior of the peptide when immobilized. Although the MerP peptide fragment changes conformation in solution, studies have shown that

freedom to alter conformation for some short peptides may actually be reduced when immobilized on Tentagel.[21] Further characterization studies, such as solid state NMR, could be conducted on immobilized peptides before use. Additionally, the low percentage of donor and acceptor present might never allow for an increased FRET signal, even if the peptide is changing conformation upon metal binding. Success may be achieved by reducing the coverage of the peptide so that every chain can be labeled with a donor and acceptor fluorophore. While this is difficult to do with a resin such as Tentagel, a planar support such as glass could be used. Glass also serves as a better prototype to a fiber optic tip, which is one possible end product for a portable device.

In addition to the work conducted with FRET based peptide metal ion sensors, studies were also conducted using magnetic γ-Fe_2O_3 nanoparticles with PLCys immobilized onto the surface. Many of the existing supports that have been used for PLCys would have to be used in a column-based flow system or removed by filtration or centrifugation if beads were mixed or added to solutions. Additionally, current resin beads are relatively large, and when used in batch extractions become mass transport limited with respect to overall metal uptake rates. A more practical approach would be the use of much smaller particles to improve extraction rates as well as some other means of removing the metal-loaded particles besides filtration or centrifugation.

The γ-Fe_2O_3 nanoparticles may satisfy both of these requirements since they can be magnetically collected and have a very large surface area to mass ratio. In this study, immobilization of PLCys onto the surface of the nanoparticles resulted in binding capacities over an order of magnitude larger than those obtained in previous studies using traditional micrometer diameter supports.[22-24] Furthermore, all of the metals (Cu(II), Cd(II), Ni(II), Pb(II) and Zn(II)) except As(III) could be reclaimed via stripping with 0.1M HNO_3. This is an improvement over unfunctionalized γ-Fe_2O_3 nanoparticles,

where metal adsorption is often irreversible[25, 26], relatively unselective and the use of strong acids can cause dissolution of the ferric oxide particles.

Finally, a method was developed to quantitatively screen metals bound to single polystyrene (Tentagel) beads with immobilized peptides using electrothermal vaporizer inductively coupled plasma mass spectrometer (ETV-ICP-MS). Screening of a PLAsp control set as well as a combinatorial library showed excellent precision of capacity measurements in a single bead (7-14%) as well as between beads (3-10%). Additionally, analysis of the metal extract proved viable as 97-100% of all metals except Cu^{2+} were found to be released. This method is an improvement over existing methods because it is nondestructive and provides the absolute content of all metals bound simultaneously. The 2-3 min analysis time needed for each sample per replicate presently makes this technique suited for quantitative analysis of *selected* beads after an initial bulk screening method. A multiplexed ETV system that is currently being developed[27, 28] could be used to speed up analysis time.

7.2 FUTURE WORK

7.2.1. Continuous Monitoring in situ FRET sensor

Environmental trace metal analysis frequently requires grab samples and subsequent transport back to the laboratory for quantitation by one of the traditional atomic spectroscopic techniques (i.e., AA, ICP-OES, ICP-MS, etc.). The development of a FRET-based sensor for use in a continuous, *in situ* monitoring mode would be a much more practical approach. The requirements include good sensitivity, good selectivity (or ability to account for interferents), low power requirements and (ideally) extremely low cost.

As has been noted, the development of FRET acceptor/donor pairs linked with an ion selective chelating peptide provides selectivity and sensitivity, with nanomolar detection limits. Enzymes are routinely immobilized using covalent binding mechanisms on optical fibers without loss in activity.[29-32] Additionally, proteins and biocatalysts have also been successfully immobilized onto fiber optic surfaces for spectroscopic sensing applications.[33] Thus, it is reasonable to postulate that it would also be possible to immobilize the FRET-peptide moiety onto the surface of a fiber optic. Using the end of the fiber optic as the active area, fluorescence measurements would be made using a moderately intense light source and dichroic mirror configuration with appropriate filters as shown in Figure 7.1.

Figure 7.1 One possible embodiment of battery operated in situ monitoring device based on FRET system with metal-selective peptide chelator.

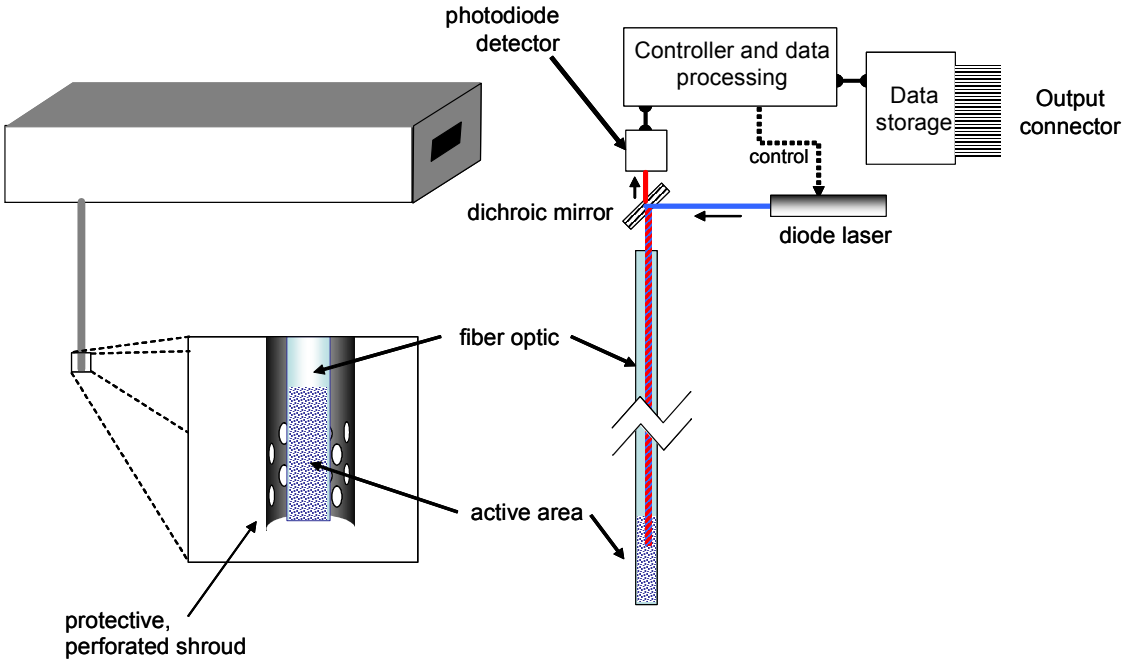

Unlike regular fluorescence, FRET offers the advantage of relatively large wavelength displacement between donor excitation and acceptor emission. This should enhance S/N by minimizing background radiation from any scattering of the excitation beam and place less stringent bandpass requirements on the emission filter. Additionally, there are a number of donor/acceptor pairs that can be used since the change in the FRET signal is dependent on the tertiary structure change of peptide when it chelates the metal and not on an interaction between the metal and the fluorophores.

Choosing a FRET pair that is excitable in the visible region would allow an LED or diode laser light source to be used. One could envision, for example, the use an inexpensive laser pointer of a suitable wavelength as the light source. Several sensitive and inexpensive solid state detectors exist for the 550-700 nm spectral region, including avalanche photodiodes. While analog signal detection is possible, it is equally possible that photon counting could be employed for optimal sensitivity.

Since it is the intent that this device be left unattended, battery or solar cell operation would be ideal. Feasibility of such a design is reasonable since both the diode laser and detection circuitry have low power requirements. As importantly, the expected use of this devise is for continuous, periodic measurements rather than continuous data collection. Thus, for example, a 1-10 s measurement period every hour represents a duty cycle of only 0.03-0.3%. With inexpensive static memory, it is also reasonable to save the collected data in memory within the device for subsequent retrieval. One could also envision even more sophisticate device where RF transmission of the collected data is done on a regular basis. If the device were “throw away cheap” one could float such a device down a river, for example while recording the concentrations with regard to geographical position and not have a great deal of concern if the device gets lost or destroyed en route.

The first step, however, in realizing this end goal lies in the chemistry: developing an immobilization media and immobilization protocol that permits a FRET based response for the immobilized chelators that are similar to observations in homogeneous solution. It also follows that selectivity and sensitivity need to be achieved.

7.2.2 *De novo* design of FRET based peptide metal ion sensors

Heavy metal peptide binding has been studied using a variety of techniques such as NMR spectroscopy, circular dichromism (CD), and UV/Vis spectroscopy. Although a lot of information is available from these techniques, it is still very difficult to predict how a peptide will behave once a metal is introduced and binds. Many studies have recently focused on the interplay between the metal and peptide conformation, and success has been achieved by introducing metal binding sites into *de novo* designed peptide structures. *De novo* design works by taking a molecular framework, such as a peptide backbone or helix, and adding functional groups computationally to obtain a biological or physical property of interest. Therefore, a primary peptide sequence can be designed that can fold into a predetermined secondary and tertiary structure.[34, 35] A schematic of *de novo* design is shown in Figure 7.2

Figure 7.2 Schematic of *de novo* design[36]

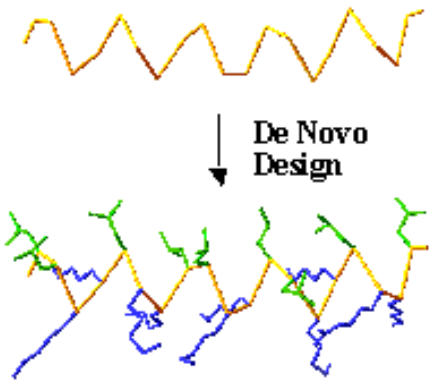

Because of the preliminary success achieved using *de novo* design to create chelators for the removal of target heavy metal ions, it is reasonable to believe that this method could be used to construct new and selective FRET based peptide metal ion sensors. A few *de novo* software packages are now available such as HostDesigner[37], which was created specifically for determining metal ion receptors or EPDA.[38] The user only needs to input a file for each fragment (i.e. amino acids of interest) that specifies coordinates for all the atoms, atom connectivity and attachment vectors such as C (sp^3)-H or C (sp^2)-H. The software then behaves like a high throughput screening combinatorial library by building structures and comparing them against a library of known structural fragments. Peptide binding energies, folding free energies, and Van der Waals interactions are taken into account. While not always perfect, preliminary work suggests that optimal structures are frequently obtained.

7.3 REFERENCES

(1) dos Remedios, C. G.; Moens, P. D. J. In *Resonance Energy Transfer*; Andrews, D. L., Demidov, A. A., Eds.; John Wiley and Sons: New York, 1999, pp 1-54.

(2) Pearce, D. A.; Walkup, G. K.; Imperiali, B. *Bioorg. Med. Chem. Lett.* **1998**, *8*, 1963-1968.

(3) Godwin, H. A.; Berg, J. M. *J Am Chem Soc* **1996**, *118*, 6514-6515.

(4) Haugland, R. P. *Handbook of Fluorescent Probes and Research Chemicals, 6th ed.*, 6 ed.; Molecular Probes, Inc.: Eugene, **1996**.

(5) Corradini, R.; Dossema, A.; Galaverna, G.; Marchelli, R.; Panagia, A.; Sartor, G. *J. Org. Chem.* **1997**, *62*, 6283-6289.

(6) De Santis, G.; Fabbrizzi, L.; Licchelli, M.; Mangano, C.; Sacchi, D.; Sardone, N. *Inorg. Chim. Acta* **1997**, *257*, 69-76.

(7) Yoon, J.; Ohler, N. E.; Vance, D. H.; Aumiller, W. D.; Czarnik, A. W. *Tetrahedron Lett.* **1997**, *38*, 3845-3848.

(8) Kramer, R. *Angew. Chem. Int. Ed. Engl.* **1998**, *37*, 772-773.

(9) Mitchell, K. A.; Brown, R. G.; Yuan, D.; Chang, S.-C.; Utecht, R. E.; Lewis, D. E. *J. Photochem. Photobiol., A* **1998**, *115*, 157-161.

(10) Prodi, L.; Bolletta, F.; Montalti, M.; Zaccheroni, N. *Eur. J. Inorg. Chem.* **1999**, 455-460.

(11) Beltramello, M.; Gatos, M.; Mancin, F.; Tecilla, P.; Tonellato, U. *Tetrahedron Lett.* **2001**, *42*, 9143-9146.

(12) Klein, G.; Kaufmann, D.; Schurch, S.; Reymond, J.-L. *Chem. Commun.* **2001**, 561-562.

(13) Prodi, L.; Montalti, M.; Zaccheroni, N.; Dallavalle, F.; Folesani, G.; Lanfranchi, M.; Corradini, R.; Pagliari, S.; Marchelli, R. *Helv. Chim. Acta* **2001**, *84*, 690-706.

(14) Bourson, J.; Badaoui, F.; Valeur, B. *J. Fluoresc.* **1994**, *4*, 275-277.

(15) Akkaya, E. U.; Turkyilmaz, S. *Tetrahedron Lett.* **1997**, *38*, 4513-4516.

(16) Kawakami, J.; Itoh, H.; Mitsuhashi, H.; Ito, S. *Anal. Sci.* **1999**, *15*, 617-618.

(17) Merrifield, R. B. *J. Am. Chem. Soc.* **1963**, *85*, 2149-2154.

(18) Atherton, E.; Sheppard, R. C. In *Solid Phase Peptide Synthesis: A Practical Approach*; IRL Press: Oxford, 1989, pp 131-148.

(19) Gutierrez, E.; Miller, T. C.; Gonzalez-Redondo, J. R.; Holcombe, J. A. *Environ. Sci. Technol.* **1999**, *33*, 1664-1670.

(20) McClure, D. S. *J. Chem. Phys.* **1952**, *20*, 682-686.

(21) Stair, J. L.; Holcombe, J. A. *Microchem. J.* **2005**, *81*, 69-80.

(22) Jurbergs, H. A.; Holcombe, J. A. *Anal. Chem.* **1997**, *69*, 1893-1898.

(23) Howard, M.; Jurbergs, H. A.; Holcombe, J. A. *Anal. Chem.* **1998**, *70*, 1604-1609.

(24) Howard, M.; Jurbergs, H. A.; Holcombe, J. A. *J. Anal. At. Spectrom.* **1999**, *14*, 1209-1214.

(25) Clifford, D. A.; Ghurye, G. L. In *Environmental Chemistry of Arsenic*; Frankenberger, W. T., Jr., Ed.; Marcel Dekker, Inc.: New York, 2002, pp 217-245.

(26) Yavuz, C. T.; Mayo, J. T.; Yu, W. W.; Prakash, A.; Falkner, J. C.; Yean, S.; Cong, L.; Shipley, H. J.; Kan, A.; Tomson, M.; Natelson, D.; Colvin, V. L. *Science* **2006**, *314*, 964-967.

(27) Venable, J. D.; Detwiler, M.; Holcombe, J. A. *Spectrochim. Acta, B* **2001**, *56B*, 1697-1706.

(28) Kreschollek, T.; Holcombe, J. A., Quebec City, Canada, October 9-13 2005; 204.

(29) Abdel-Latif, M. S.; Guilbault, G. G. In *Biosensor technology : fundamentals and applications*; Buck, R. P., Ed.; Dekker: New York, 1990, pp 285-298.

(30) Cordek, J.; Wang, X.; Tan, W. *Anal. Chem.* **1999**, *71*, 1529-1533.

(31) Liu, X.; Tan, W. *Mikrochim. Acta* **1999**, *131*, 129-135.

(32) Marazuela, M. D.; Moreno-Bondi, M. C. *Anal. Chim. Acta* **1998**, *374*, 19-29.

(33) Arnold, M. A. *Anal. Chem.* **1992**, *64*, 1015A.

(34) Farrer, B. T.; Pecoraro, V. L. *Curr. Opin. Drug Discov. Devel.* **2002**, *5*, 937-943.

(35) Doerr, A. J.; McLendon, G. L. *Inorg. Chem.* **2004**, *43*, 7916-7925.

(36) PolyMedix Technology, www.polymedix.com, 2007.

(37) Hay, B. P.; Firman, T. K. *Inorg. Chem.* **2002**, *41*, 5502-5512.

(38) Belda, I.; Madurga, S.; Llora, X.; Martinell, M.; Tarrago, T.; Piqueras, M. G.; Nicolas, E.; Giralt, E. *J. Comput. Aided Mol. Des.* **2005**, *19*, 585-601.

Bibliography

See REFERENCES sections of each individual chapter for references cited in each chapter

Vita

Brianna Rose White was born May 20, 1981 in Kalamazoo, Michigan to James and Sydonie White. She attended Comstock High School in Kalamazoo and later graduated as valedictorian in 1999. She then attended Saginaw Valley State University in University Center, MI where she received both academic and volleyball scholarships. While at SVSU, she pursued research with derivatized fullerenes under the direction of Dr. Deborah Huntley. Following her junior year, she received an ERULF fellowship and worked at Oak Ridge National Laboratory with Dr. Phillip Britt pursuing new purification methods for single-walled carbon nanotubes. She graduated summa cum laude from SVSU in 2003 with a Bachelors of Science in Chemistry. She started pursuing a PhD at The University of Texas at Austin in 2003, working for James A. Holcombe.

Permanent address: 1727 Sandy Cove Dr., Kalamazoo, MI 49048

This dissertation was typed by the author.